THE UNIVERSITY
of EDINBURGH

The role of the lactate receptor, GPR81, in renal haemodynamic physiology

Natalie Kathryn Jones

Doctor of Philosophy (PhD)

The University of Edinburgh

2020

Declaration

I hereby declare that all work carried out during this PhD was performed by myself, unless otherwise stated, under the supervision of Prof. Matthew Bailey and Prof. John Mullins. This thesis has not previously been submitted for any other degree of qualification

Signed: Date:

Natalie Kathryn Jones

Acknowledgements

First and foremost, an unmeasurable amount of thanks goes to my supervisor Prof. Matt Bailey. I could not have imagined a more supportive or understanding supervisor with the ability to change my attitude in a matter of minutes with one of your famous pep talks. You have played a huge role in my desire to continue with academic research and I can't express my gratitude enough. Secondly, to Prof. John Mullins for playing such supportive role throughout my MSc and PhD.

A huge thanks to the whole BDD lab group, a wonderful group of scientists that it is a pleasure to work with. In particular thank you to Morag for being my unofficial 'women in academia' mentor, your advice is second to none and I hope I can be half the scientist you are. Thank you to Hannah for being the most hardworking member of the group who still can't do enough to help the rest of us.

I am so grateful to my parents for their unwavering support and sympathy when they knew I needed it. To Teo, for making sure we both stayed (almost) sane in the final stages of the PhD. All of the other CVS PhD students have made these the most enjoyable 3 years and I am forever thankful for that.

For technical support throughout my PhD I would like to acknowledge Kevin Stewart for the many weeks of surgery he has undertaken with me. Thank you to the whole LF1 and LF2 staff for their animal husbandry assistance. A final acknowledgement to our collaborators at AstraZeneca for providing us with both the GPR81 agonist and the knockout mouse line.

Abstract

G protein-coupled receptor 81 (GPR81) is abundantly expressed in adipocytes where activation by the endogenous ligand lactate inhibits lipolysis. GPR81 is also found in non-adipose tissue but the receptor's function here is currently not fully understood. *In vivo* infusion of specific GPR81 agonist, AZ'5538, has been shown to increase blood pressure (BP). We therefore hypothesised a role for GPR81 in the cardiovascular and renal systems with the aim to examine the *in vivo* effects of AZ'5538 on renal haemodynamics and to localise expression of the receptor within the kidney and vasculature. Initially, we found expression of *Gpr81* mRNA in the whole aorta, mesenteric and renal arteries of C57Bl/6JCrl mice using end point PCR. Then, using RNAscope *in situ* hybridisation in *Gpr81*$^{-/-}$ mice and wildtype (WT) littermates we found expression in the kidney medulla, arterioles of the glomerulus and smooth muscle cells of the vasculature. WT and *Gpr81*$^{-/-}$ mice were terminally anaesthetised, the carotid artery cannulated and renal blood flow (RBF) or perfusion measured by a Doppler ultrasound probes during IV infusion of either AZ'5538 or vehicle. Infusion of AZ'5538 significantly increased BP and reduced HR, RBF and cortical and medullary perfusion. Activation of GPR81 *in vivo* also decreased glomerular filtration rate with no change in ion excretion. All of these effects were absent in *Gpr81* null mice. Plasma endothelin-1 (ET-1) was increased in mice treated with AZ'5538 with no change in whole kidney and aorta homogenate levels, suggesting release of ET-1 into the circulation. Prior treatment with BQ-123 (endothelin-A receptor antagonist) prevented the AZ'5538 mediated blood pressure increase whereas BQ-788 (endothelin-B receptor antagonist) had no effect. We showed *Gpr81* expression in vascular smooth muscle, glomerulus and medulla of the mouse kidney. *In vivo*, GPR81 activation influences cardiorenal haemodynamics in an endothelin-A receptor mediated manner by stimulating circulating ET-1. The sensitivity of the renal circulation to GPR81 activation may become physiologically significant when circulating lactate, the endogenous ligand of GPR81, concentration rises, as can occur in ischemic renal disease.

Lay summary

High blood pressure, also known as hypertension, affects 1 in 4 adults worldwide and is the largest single known risk factor for cardiovascular disease and related disability. Understanding what causes hypertension and finding potential targets is important for treating the disease in the future. Lactate is a molecule which is formed when the body does not have enough oxygen. Lactate can bind to the receptor GPR81 which is found mainly in fat but also throughout the body. We currently do not know what the function of GPR81 is in the heart and kidney. A drug which is similar to lactate, AZ'5538, has been designed to bind to GPR81. This drug has been found to increase blood pressure, but it is not understood why. In my thesis I found that AZ'5538 not only increases blood pressure but also prevents the flow of blood to the kidney by causing blood vessels to constrict. We found that GPR81 is found in blood vessels throughout the body as well as in the small arteries in the kidney. This receptor could be important in controlling blood pressure as well as in diseases where lactate levels are high.

List of achievements

- Vice president of the Little France Postgraduate Society 2016-2018
- Head of the Edinburgh University BHF Fundraising Group 2016-2018 and a keen member 2016-2019
- STEM Ambassador throughout my PhD
- Edinburgh University BHF Fundraising Group were winners of 'The best new fundraising group' 2017

Conference presentations

- Experimental Biology 2017, Chicago, USA – Poster presentation
- BHF Student Conference, 2018, Edinburgh UK – Poster presentation
- Europhysiology 2018, London, UK – Poster presentation
- Bristol-Cardiff-Edinburgh Renal Symposium 2018, Edinburgh, UK – Poster presentation
- Experimental Biology 2019, Orlando, USA – Poster presentation
- Renal physiology: Recent advances and emerging concepts 2019, Aberdeen, UK – Oral and poster presentation
- Physiology 2019, Aberdeen, UK – Oral Presentation

Awards and funding

- Deanery of Clinical Sciences Funding Challenge 2017 - Awarded £1,389 for a homeothermic monitoring system for rodents.
- BHF CoRE Travel award - £800 to attend EB2017
- Bristol-Cardiff-Edinburgh Renal Symposium 2018 - Best poster presentation prize awarded by Prof Peter Mathieson (University Principal)

Abbreviations

3-HBA	3-Hydroxybutyric acid
3,5-DHBA	3,5-Dihydroxybenzoic acid
ACH	Acetylcholine
AKI	Acute kidney injury
ANG II	Angiotensin II
ANOVA	Analysis of variance
ATP	Adenosine triphosphate
BP	Blood pressure
bw	Body weight
cAMP	Cyclic adenosine monophosphate
CHBA	3-Chloro-5-hydroxybenzoic acid
CKD	Chronic kidney disease
DBP	Diastolic blood pressure
DMSO	Dimethyl sulfoxide
DNA	Deoxyribonucleic acid
EC50	Half maximal effective concentration
ECE	Endothelin converting enzyme
ET	Endothelin
ETRA	Endothelin A receptor
ETRB	Endothelin B receptor
FACS	Fluorescence-activated cell sorting
Fe	Fractional excretion
FFA	Free fatty acid
FITC	Fluorescein isothiocyanate
GFR	Glomerular filtration rate
GI	Gastrointestinal
GK5	Glycerol Kinase 5
GPCR	G protein coupled receptor
GPR	G protein receptor
HCA	Hydroxycarboxylic acid
HDL	High density lipoprotein
HET	Heterozygote

HR	Heart rate
IC50	Half maximal inhibitory concentration
IP	Intraperitoneal
IRI	Ischemia reperfusion injury
IV	Intravenous
KO	Knock out
KPSS	High potassium physiological salt solution
LDL	Low density lipoprotein
MABP	Mean arterial blood pressure
MPC	Mitochondrial pyruvate carrier
mRNA	Messenger ribonucleic acid
NLRP3	NACHT, LRR, and pyrin domain-containing protein 3
NO	Nitric oxide
PAH	Pulmonary artery hypertension
PCR	Polymerase chain reaction
PE	Phenylephrine
PLC	Phospholipase C
PSS	Physiological salt solution
qPCR	Quantitative real time polymerase chain reaction
RAS	Renin-angiotensin system
RBF	Renal blood flow
RNA	Ribonucleic acid
RVR	Renal vascular resistance
SBP	Systolic blood pressure
SD	Standard deviation
SEM	Standard error of the mean
SH	Spontaneously hypertensive
SNP	Sodium nitroprusside
TCA	Tricarboxylic acid
TG	Triglyceride
UPL	Universal probe library
VEGF	Vascular endothelial growth factor
VSMC	Vascular smooth muscle cells
WT	Wildtype

Contents

List of figures

List of tables

Chapter 1 - Introduction

1.1 Renal control of blood pressure

Currently, 25% of the worldwide population suffer from high blood pressure (hypertension)[1], which is classified as pressures over 140/90 mmHg. Hypertension is also the major modifiable risk factor for the majority of cardiovascular diseases including cardiomyopathy, stroke, atherosclerotic vascular disease, congestive heart failure and chronic kidney disease (CKD)[2–4]. Control of blood pressure is complex and involves integration of multiple regulatory pathways (e.g. neural, hormonal, immune and paracrine) throughout many key cardiovascular control systems of the body[5]. Although controversial, the Guyton hypothesis places renal control of salt and extracellular fluid volume at the centre of long-term blood pressure homeostasis[6]. The mechanism known as pressure natriuresis relates to changes in renal perfusion pressure which alters sodium reabsorption by the proximal tubule to regulate blood pressure homeostasis[7]. Although the mechanisms of the acute pressure natriuresis response are still not fully understood, pressure natriuresis is abnormal in almost every model of hypertension[7], confirming the importance of this response in blood pressure stabilisation.

1.2 Renal haemodynamics

Renal blood flow (RBF) is tightly autoregulated in the kidneys by mechanisms of vasoconstriction and dilation by the large arteries and smaller arterioles of the kidneys to allow a relatively constant flow rate of blood and GFR in the face of fluctuations in arterial pressure. An overview of the renal vasculature is shown in Figure 1.1. Autoregulation is essential to stabilise GFR, and therefore the filtered load of different solutes to keep concentrations of electrolytes stable even with changes in blood pressure. It is also important to prevent glomerular capillaries from barotrauma by stopping increases in blood pressure reaching these delicate renal vessels. Damage to these capillaries can lead to glomerulosclerosis due to hypertrophy and the thickening of arteriole walls and results in an inability of the kidneys to properly filter[8,9].

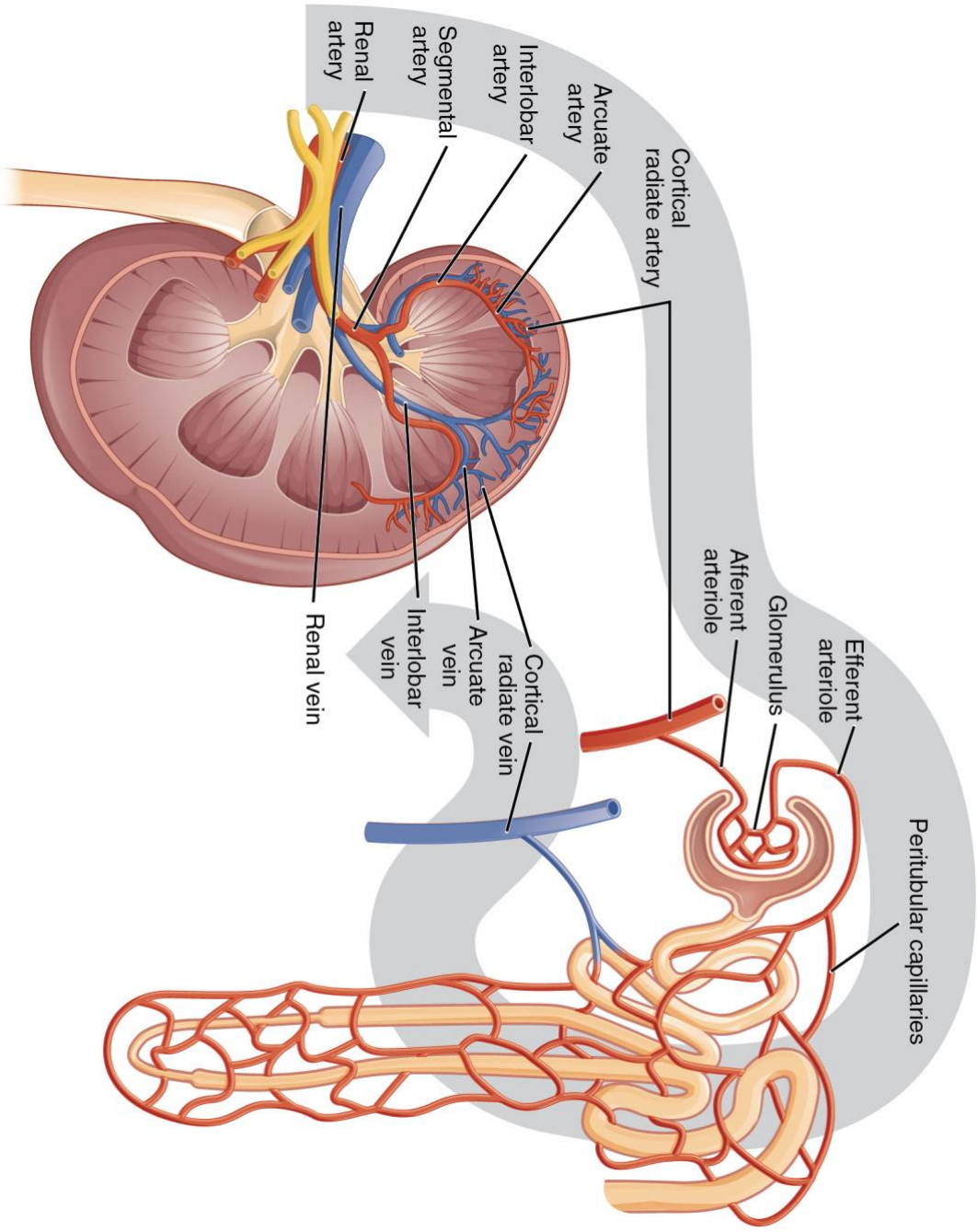

Figure 1.1 An overview of the renal vasculature

Adapted from Openstax Anatomy and Physiology textbook[10] under the license https://creativecommons.org/licenses/by/4.0/ to redistribute. Blood enters the kidney through the renal artery which divides into the segmental arteries and further branches to form the interlobar arteries which pass through the renal columns into the cortex. The interlobar arteries branch into arcuate arteries, cortical radiate arteries and finally into afferent arterioles. After passing through the renal corpuscle, the capillaries exit as efferent arterioles which then form a network around the nephron as peritubular capillaries before returning to the venous system.

There are two main mechanisms of renal haemodynamic autoregulation which are responsible for controlling RBF and GFR with either rapid or slower increases in systemic blood pressure. The first mechanism, which responds with rapid compensation in a matter of seconds, is the myogenic response[9]. Here, the preglomerular afferent arterioles constrict in response to an increase in transmural pressure[11]. Vasoconstriction of these arterioles is due to an influx of intracellular calcium initiating depolarisation of vascular smooth muscle cells (VSMC)[12]. In response to slower increases in blood pressure or for increases which are not fully compensated by the myogenic response, tubuloglomerular feedback takes place. In this state there is increased glomerular capillary pressure, increased GFR and inhibition of sodium reabsorption in the proximal tubule. The macula densa cells of the distal tubule sense increases in sodium chloride concentration (which indicates increase flow) which causes release of adenosine to initiate contraction of the VSMC of afferent arterioles by A_1 receptor activation[13,14]. Both of these mechanisms are in place to stabilise GFR and prevent injury to the glomerulus by increased load. In healthy humans, as long as mean arterial blood pressure (MABP) is within a normal range (70-130 mmHg), RBF is able to autoregulate and remain stable even with changes in BP (Figure 1.2). In certain disease states however, including diabetes, salt-sensitive hypertension and CKD, we see impaired autoregulation[11] while patients with essential hypertension retain their ability to autoregulate. Impaired renal autoregulation increases the susceptibility to glomerulosclerosis and proteinuria leading to renal disease even with modest changes in MABP, although the mechanisms behind alterations in autoregulatory sensitivity is still not understood. Although perfusion of the renal artery and kidney cortex are effective in their ability to autoregulate, the vasculature of the deep medulla is poorly autoregulated[15], therefore the regulation of salt balance, fluid volume and blood pressure is determined by the renal artery and cortical vasculature[16].

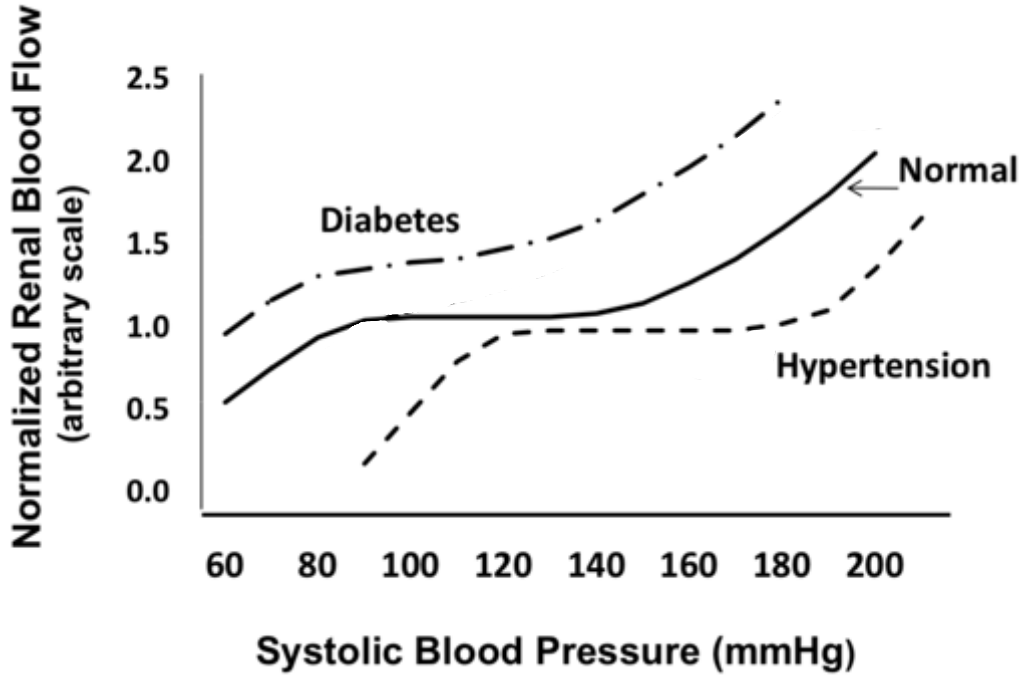

Figure 1.2 Autoregulation of renal blood flow in health and disease

In healthy individuals, renal blood flow is maintained over a range of arterial pressures from around 70 to 130 mmHg by autoregulatory mechanisms. In humans with mild to moderate hypertension, the autoregulatory range is shifted to higher pressures due to elevations in preglomerular vascular tone and structural changes in the microcirculation. This is also seen in rodent models of hypertension such as SH or angiotensin II infused animals. In diabetic individuals, renal vascular resistance is reduced due to impaired efficiency of autoregulation. Figure adapted from Burke *et al.*[17]

Autoregulation of perfusion is an intrinsic properly of both arteries and arterioles, in particular in tissues with protected circulations, including the heart, brain and kidneys. This tight regulation can, however, be modulated by extrinsic factors including nerves, hormones and vasoactive peptides[18]. Particularly potent in altering renal perfusion are endothelin-1 (ET-1) and ATP ET-1 causes a prolonged vasoconstriction of both the afferent and efferent arterioles and associated reduction in RBF and GFR[19]. When in the renal extracellular space, ATP can act in a paracrine manner by activating the P2 family of receptors to cause vasoconstriction of juxtaglomerular afferent arterioles causing decreased renal perfusion[20]. More recently, complex Krebs cycle intermediates have been implicated in renal haemodynamics and the

control of blood pressure. For example, succinate, formed from fumarate, has been shown to activate GPR91 on the macula densa cells of the kidney to release prostaglandin E(2), a potent vasodilator and paracrine mediator of renin release, ultimately resulting in Ang II production, vasoconstriction of peripheral arteries, and an increase in blood pressure[21]. GPR91 activation has also been shown to cause initial vasodilation by prostaglandin E(2) of the afferent arterioles to control glomerular hyperfiltration[22]. Both of these findings present renal vasoactive mechanisms of GPR91 activation. My thesis focusses on the regulation of renal haemodynamics by GPR81, introduced below.

1.3 HCA receptor family

G protein coupled receptors (GPCR's) are one of the largest protein families within mammals[23]. The hydroxy-carboxylic acid (HCA) subfamily of GPRC's has 3 members, HCA_1, HCA_2 and HCA_3 which are also referred to as GPR81, GPR109A and GPR109B, respectively. These receptors all have a single exon and high sequence homology with GPR81 being the most different; GPR109A/B share 96% sequence homology at a protein level while GPR81 shares 55% of the amino acid sequence identity with the other two members[24,25]. It is therefore unsurprising that these receptors have been found to have similar endogenous ligands which are all intermediates of metabolic pathways. Nicotinic acid (Figure 1.3(D)) was first found to activate GPR109A[26] however endogenous plasma concentrations were shown to be too low for physiological receptor activation which lead to the discovery that the free fatty acid derived ketone body 3-hydroxybutyric acid (Figure 1.3(B)) could physiologically activate GPR109A but not GPR109B or GPR81[27]. Other endogenous carboxylic acids are also able to activate the receptor, but these have much lower plasma concentrations and are therefore not physiologically as relevant. Although GPR109A and B have only 16 amino acids difference in their sequence, these differences are essential for ligand binding and agonists of GPR109A do not activate GPR109B. In contrast, this receptor is activated by intermediates of mitochondrial β-oxidation of fatty acids, specifically 2- and

3-hydroxyoctanoic acid[28]. While plasma levels of 3-hydroxyoctanoic acid (Figure 1.3(C)) are increased sufficiently to activate the receptor in conditions which increase β-oxidation[29] (e.g. starvation or ketogenic diet), currently the physiological relevance of 2-hydroxyoctanoic acid is unknown. Finally, GPR81 is activated by its endogenous ligand lactate[30,31] (Figure 1.3(A)). It has also been shown that other hydroxy-carboxylic acids, for example 2-hydroxy and 4-hydroxybutyrate have some activity toward GPR81 however these have much reduced potencies in comparison to lactate and the physiological concentrations of these are much too low to be physiologically relevant[30]. Although single nucleotide polymorphisms have been identified in the HCA receptors, they have so far not been associated with any disease states and their physiological or pharmacological relevance are unknown[32,33].

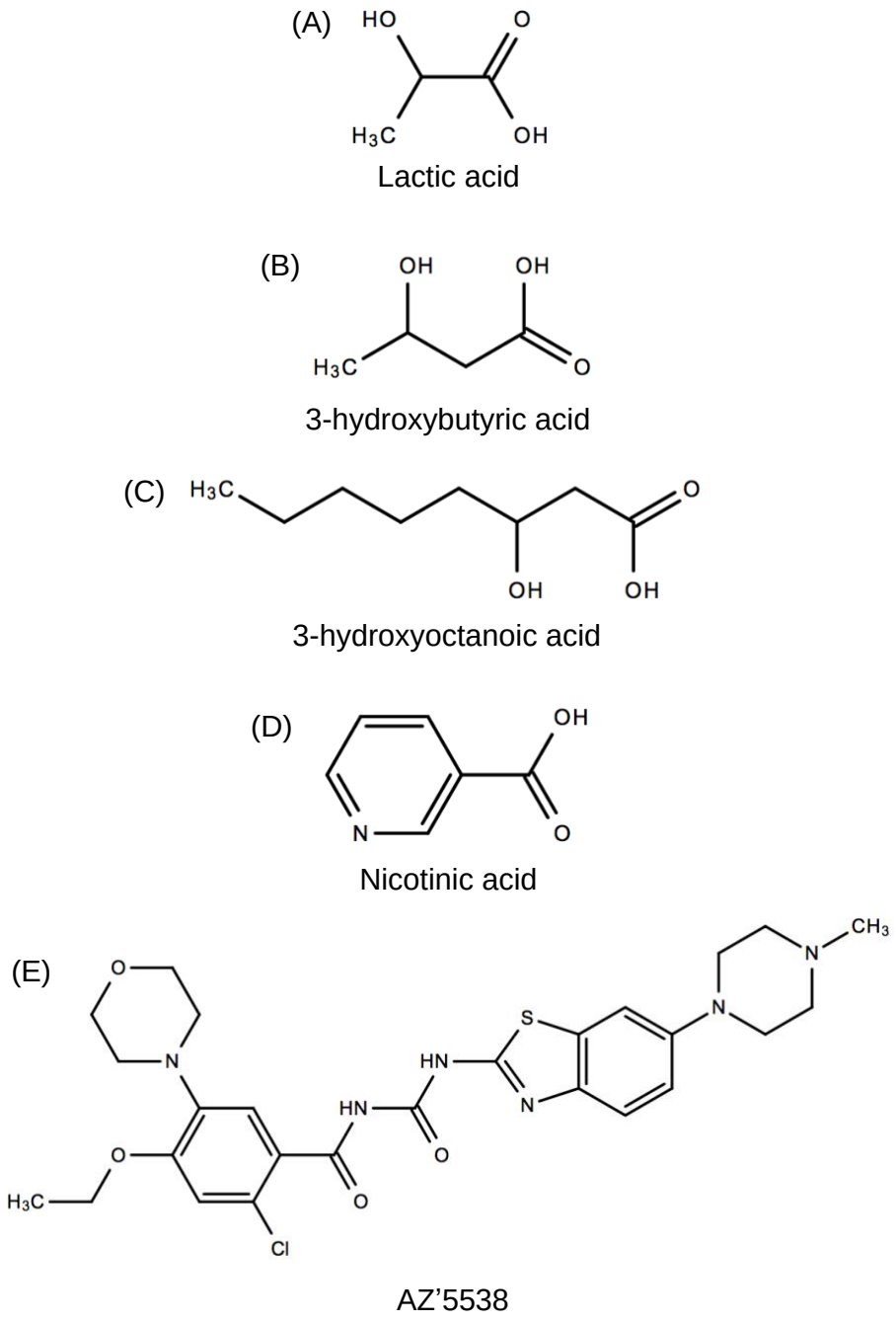

Figure 1.3 Agonists of the hydroxy-carboxylic acid receptors

Hydroxy-carboxylic acid (HCA) receptors are activated by metabolic intermediates. (A) Lactic acid is the endogenous ligand for GPR81, (B) GPR109A is primarily activated by the ketone body 3-hydoxybutyric acid formed from fatty acids, (C) GPR109B is activated with the highest potency by 3-hydroxybutyric acid. (D) Nicotinic acid is able to exogenously activate GPR109A however plasma levels are too low. (E) AstraZeneca compound AZ'5538 was designed as a therapeutic compound which activates GPR81. Structures created using Chemspider, Royal Society of Chemistry.

Both GPR81 and GPR109A are found in most mammalian species, including humans and rodents, however GPR109B is limited to humans and higher primates[28]. The majority of expression of the three receptors in this subfamily is found within adipose tissue, both brown and white[30,34,35] although they are seen throughout many tissue depots throughout the body at much lower levels. All three of the receptors have been shown to be expressed on a number of immune cells including macrophages, monocytes and neutrophils[28,36–39]. It has been suggested that both GPR109A/B are expressed in colonic epithelium as well as the skin[40,41] although the function here is unclear. GPR81 has been shown to be expressed in the cardiovascular system including the heart and kidney[30] as well as within certain regions of the brain with expression in both rodents and man being very similar [42,43].

The HCA receptors are all Gi coupled receptors and activation by their respective ligands in adipocytes causes a reduction in cAMP which then acts to inhibit lipolysis. The mechanism of action of GPR81 is shown in Figure 1.4 where lactate is produced from pyruvate via anaerobic glycolysis and released from the cell where it can bind to GPR81, activating the receptor. This inhibits adenylyl cyclase to lower levels of intracellular cAMP which downstream prevents the breakdown of triglycerides. Each ligand for the HCA receptors is released in response to different states and will inhibit lipolysis for different reasons. Arterial lactate is increased in states of hypoxia or intense exercise to prevent lipolysis in fat, and therefore lower FFA's. This feedback drives energy production towards pyruvate as this has a lower oxygen requirement per mole of ATP produced[44,45]. Both GPR109A/B have ketone body ligands which reach a sufficient concentration to activate their receptors during states of increased β-oxidation, be this fasting, a ketogenic diet or diabetic ketoacidosis. These molecules are formed in the liver as a by-product of β-oxidation of fatty acids. As the rate of lipolysis determines the amount of fatty acids available for β-oxidation, activation of GPR109A/B provides negative feedback for this system[27,29,46]. As GPR109B is only present in humans and higher primates, it is likely that these species require finer tuning for their

energy stores in adipocytes and have evolved to have another mechanism in place[32].

As previously stated, these receptors are also expressed on immune cells. Although the physiological role of GPR109A/B here is currently not understood, activation on these cells *in vitro* has been shown to increase levels of intracellular calcium[28,37,47]. On the other hand, a little more is understood about GPR81 and the immune system. Activation of GPR81 on mouse macrophages and human monocytes, suppresses Toll-Like Receptor pathways, preventing NLRP3 inflammasome activation and cell death[39,48].

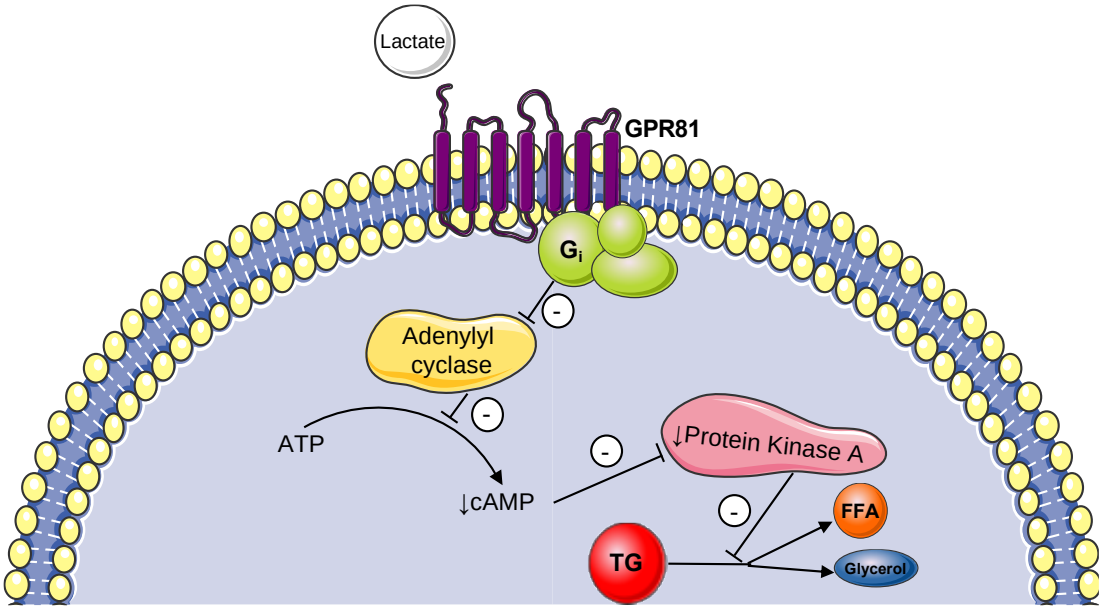

Figure 1.4 Schematic diagram of the anti-lipolytic effects of GPR81 activation in adipocytes

Lactate is formed intracellularly from glucose through glycolysis and is released. After binding to GPR81, the Gi signalling cascade inhibits adenylyl cyclase and halts ATP conversation to cAMP. A reduction in intracellular cAMP prevents the conformational change on protein kinase A needed to allow phosphorylation of hormone sensitive lipase and perilipin. These factors are therefore unable to hydrolyse triglycerides (TG) to free fatty acid (FFA) and glycerol. Figure based on Liu *et al.*[30] created using Servier Medical Art, Les Laboratoires Servier.

1.3.1 HCA receptors as a therapeutic target

Due to the anti-lipolytic effects of HCA receptor activation, it is unsurprising that the majority of the therapeutic drugs designed for these receptors are for the treatment of dyslipidemias. These aim to prevent the breakdown of lipids into FFA's via lipolysis inhibition, which drives glycolysis rather than β-oxidation, lowering blood glucose[49]. An excess of FFA release is also known to amplify insulin resistance[50] and therefore inhibition of lipolysis improves the insulin sensitivity in obese or diabetic patients. Furthermore, reducing the pool of FFA reduces the ability for the liver to produce low density lipoprotein (LDL) from very low density lipoprotein (VLDL)[51], thus improving the lipid profile. Before the identification of the endogenous agonists of GPR109A, nicotinic acid was discovered to activate the receptor which has been historically used as an anti-dyslipidemic drug[52]. Niacin also activates GPR109B in humans but at a lower affinity (EC_{50} values of 0.1 μM and 100 μM, for GPR109A and B, respectively)[53]. It has also been shown that niacin offers anti-atherosclerotic benefits, in particular when used in combination with statins[54]. Clinical trials have shown that this combination therapy not only lowers plasma LDL and raises HDL but also promotes cholesterol efflux in atherosclerotic plagues[54–56]. The major side effect of niacin as a drug is that it causes cutaneous flushing which severely impacts patient compliance of the drug. This is due to the expression of GPR109A on dermal Langerhans cells of the skin where activation causes the formation of prostanoids[57,58]. Synthetic ligands for GPR109A (both partial and full agonists) have been designed with some success[59,60]. The aim of these drugs are to reduce the flushing response of niacin, as this is not a Gi mediated effect[61], while preserving the beneficial anti-lipolytic effects. Although there are agonists designed to specifically activate GPR109B[62,63] they are not believed to have benefits over niacin due to the similarity in expression patterns between the two receptors. Research into these specific agonists is particularly difficult due to the lack of expression of the receptor in rodents without a transgenic mouse model to express GPR109B. Conversely, GPR81 has quite a different expression pattern than the other two HCA receptors, in particular, GPR81 is not expressed in

Langerhans cells and therefore activation of the receptor does not cause flushing[64]. This receptor has therefore recently become the target of many drug companies to produce specific GPR81 agonists to treat dyslipidemias and prevent cardiovascular risk without the adverse effects of GPR109A/B agonists[64–66].

Aside from treatment of dyslipidemias, GPR109A has been considered as an anti-inflammatory target, in particular in the treatment of psoriasis. Monomethylfumarate, an established anti-psoriatic, has been shown to activate GPR109A on immune cells but not GPR109B or GPR81[67], however this compound also causes side effects similar to niacin including flushing[68]. The anti-inflammatory effects of GRP109A activation also help to explain the anti-atherosclerotic effects of niacin which have been reported to be due to the receptors expression on macrophages in atherosclerotic plaques[56]. GPR81 is also expressed in immune cells where it has been shown to have positive anti-inflammatory effects in the liver and digestive system. Activation of GPR81 by the endogenous ligand lactate *in vivo* reduces inflammation and organ injury in a model of immune hepatitis in a *Gpr81*-dependant manner and was also shown to reduce the severity of acute pancreatitis and liver injury in mice[39]. In an experimental mouse model of colitis, GPR81 activation on immune cells with pharmacological agents decreased inflammatory cytokine expression and ameliorated colonic inflammation[48].

Experimental models of brain disease and injury have also been used to look at HCA receptor activation and their potential beneficial role here. GPR109A has been shown to be expressed on neuroinflammatory cells in the brain where activation reduces inflammation in mouse models of multiple sclerosis or stroke[69]. The role of GPR81 in the brain injury is controversial with studies reporting both positive and negative effects of GPR81 activation. It has been reported that GPR81 expression is upregulated in the brain in rodent models of stroke or cerebral ischemia and activation of the receptor by increased lactate may aggravate the injury[70–72]. Overexpression of GPR81 *in vitro*

increased cell vulnerability to ischemic injury and therefore antagonism of GPR81 was postulated as a therapeutic strategy for ischemic brain injury[72]. Inhibition of GPR81 with 3-hydroxy-butyrate prevented cell death and brain injury in both an *in vitro* model of oxygen-glucose deprivation as well as an *in vivo* mouse model of middle cerebral artery occlusion[72]. In stark contrast, activation of the receptor by 3,5-dihydrobenzoic acid was shown to prevent cell death by apoptosis and offer neuroprotection in the same models of both *in vivo* and *in vitro* brain ischemia[70].

Finally, the HCA receptors have also been implicated in certain types of cancer. The expression of GPR109A/B in the gastrointestinal (GI) tract has been investigated for its therapeutic target here. In colon cancer, the receptor is silenced and re-expression and activation of the receptor by its ligands causes tumour cell apoptosis[40]. GPR81 expression has been reported in multiple cancer cell lines including colon, lung, salivary gland, cervical and pancreatic where expression levels correlated with the rate of pancreatic cancer tumour growth and metastasis[73]. In breast cancer patients and cell lines, GPR81 expression has been found to be significantly higher in than that of normal cells or mammary tissue[74]. In this study, GPR81 knockdown using shRNA resulted in impaired breast cancer growth, supressed angiogenesis and increased apoptosis showing that knockdown of the receptor retards the development/metastasis of breast cancer.

1.3.2 Lactate and disease

Lactate is produced in the majority of tissues within the human body, with the highest levels of production in muscle[75]. An overview of lactate production and metabolism is shown in Figure 1.5. In humans, the main sources of lactate are glucose and alanine through their conversion into pyruvate[76]. Lactate is produced when oxygen stores are low, in anaerobic conditions. In aerobic conditions, pyruvate is produced from glucose via glycolysis and then enters the tricarboxylic acid (TCA) cycle, bypassing lactate production. However, under anaerobic conditions, lactate is the end product of glycolysis, requiring

no oxygen. Lactate and pyruvate are either produced or removed by the enzyme lactate dehydrogenase which is principally in the cytosol of the cell. This reaction includes the oxidation of NADH to NAD^+ in the thermodynamically favoured direction of pyruvate reduction to lactate or vice versa[77].

Lactate clearance, in healthy individuals, is carried out rapidly by the liver with additional clearance in the kidney[78]. The first step of clearance is the oxidation of lactate to pyruvate in the cytosol which is transported to the mitochondrial network by the mitochondrial pyruvate carrier (MPC) proteins[79]. Pyruvate can then generate endogenous glucose via oxaloacetate or can undergo oxidative metabolism via the generation of acetyl-CoA. Deterioration of either of these pathways can result in lactate accumulation.

In general, lactate elevation may be caused by increased production, decreased clearance, or a combination of the two[80]. As lactate is produced under anaerobic conditions, tissue hypoperfusion or hypoxia are the most common causes of elevated lactate production[81]. However, there are a multitude of causes for elevated plasma lactate in patients. These include shock, regional tissue ischemia, diabetes, drugs, toxins and pharmacological agents[80]. Liver dysfunction is also a key cause as this may contribute to both increased production and deceased clearance. There is a wealth of literature on lactate increases with excessive muscle activity and heavy exercise due to anaerobic metabolism[82]. Hyperlactatemia has also been associated with mortality in hospitals. A study from the Netherlands showed that plasma lactate levels >4 mmol/L at admission to the emergency department showed a scientifically higher risk of mortality than patients with lower levels of lactate[83]. While another study showed plasma lactate of even >2.6 mmol/L is a predictor of mortality within 30 days of hospital admission[84]. This shows the clinical significance of measuring plasma lactate and importance of lactate in disease.

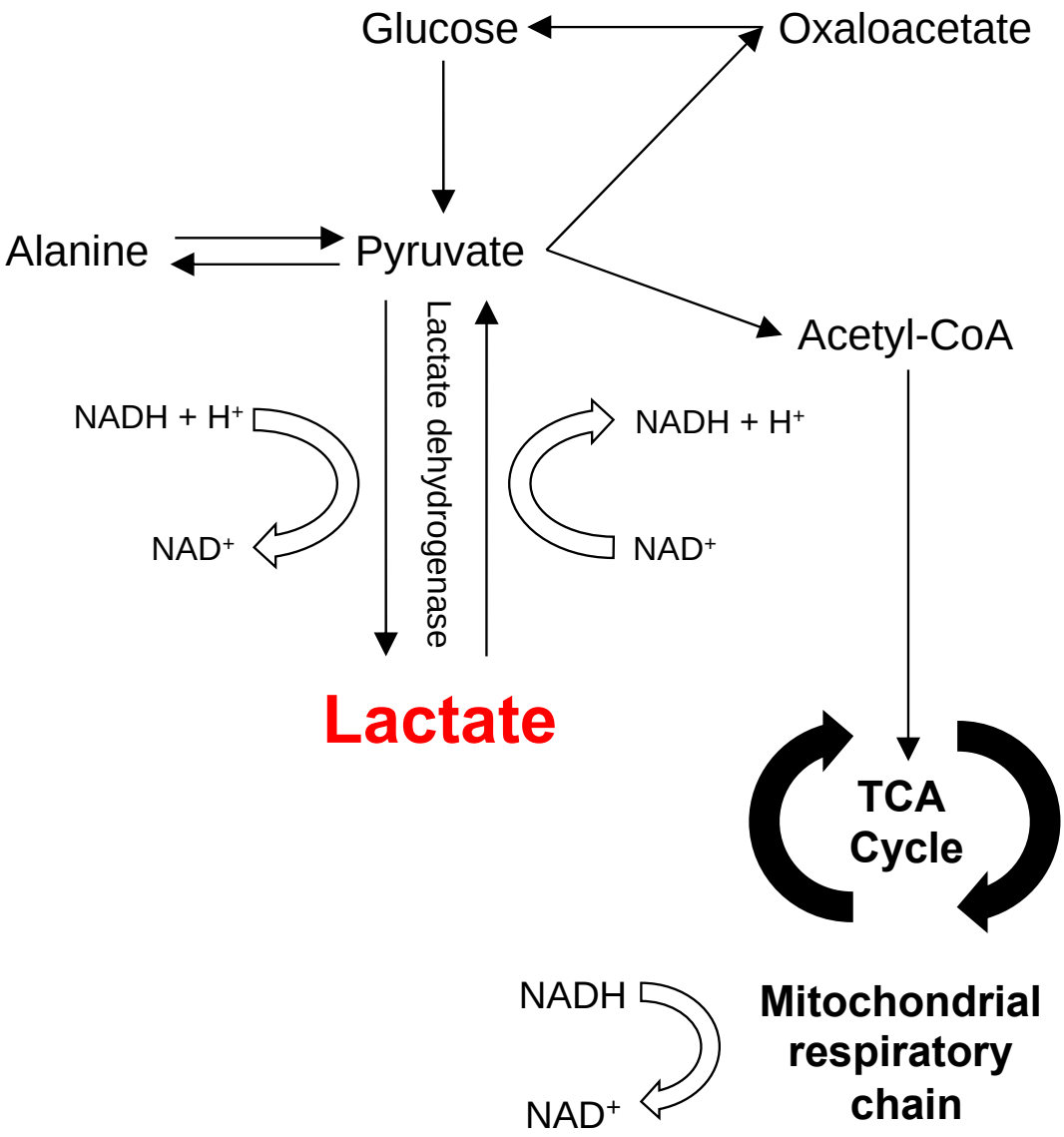

Figure 1.5 Schematic diagram of lactate metabolism

Lactate is formed from pyruvate by lactate dehydrogenase or vice versa. The majority of pyruvate is formed from either glucose or alanine in the cytosol. Lactate is metabolised by conversion to pyruvate which can either enter gluconeogenesis to produce glucose via oxaloacetate or enter the tricarboxylic acid (TCA) cycle to produce ATP via acetyl-coA.

1.3.3 GPR81 and vascular function

A role for GPR81 and its endogenous ligand lactate in the cardiovascular system has been suggested, specifically within the vasculature. Lactate is able to activate GPR81 with an EC_{50} of ~5 mM[31] while under normal physiological conditions, plasma lactate has a concentration of 0.5-2 mM, rising to 10-30 mM during intense exercise or prolonged hypoxia[30,31,85]. Although tissue levels of lactate are very rarely measured, in mice at baseline lactate in brown fat is ~2 mM[86] while after treadmill exercise muscle lactate is ~4 mM[87]. Tissue lactate is known to rise substantially under states of ischemia[80] which suggests that the receptor is either physiologically quiescent under basal conditions or that it is responsive to the local, rather than circulating, concentration of lactate in particular in states of ischemia[88]. Prior to the discovery that lactate was the endogenous ligand of GPR81, there were also reports that this compound was able to exhibit vasomotive effects. For example, it was historically reported that intravenous (IV) infusions of lactate in anaesthetised Spontaneously Hypertensive (SH) and Wistar rats causes a rapid and short lived increase in blood pressure compared to a saline control[89]. In this study, a non-physiological or pathophysiological concentration of lactate was used (0.5 M) with the aim of inducing panic in the mice which would have had multiple off target effects, including blood pH changes, which is an obvious caveat to this study. In contrast, lactate treatment *ex vivo* has been shown to cause direct vasodilatory effects. On preconstricted rat mesenteric resistance arteries, addition of lactate from 6 mM to 50 mM caused vasorelaxation which was shown to not be dependent on pH, the presence of the endothelium or nitric oxide[90]. In the same way, treatment of lactate on contracted isolated porcine retina caused significant increases in capillary blood vessel diameter suggesting dilation of these vessels[91]. Conversely, the retinal microvasculature from mice responded from basal tension to lactate by constricting and decreasing the luminal diameter[92]. In this study, hypoxia altered the effect of lactate to vasorelaxation and it was suggested that lactate may serve to constrict blood vessels when energy supplies are ample but in response to local metabolic need can switch to vasodilation once stores are

restricted. These effects were not confirmed to be GPR81 mediated, with the authors suggesting the findings were caused inhibition of Na^{+}/Ca^{2+} exchangers.

As previously discussed, a role for GPR81 in breast cancer has been studied. Although a negative effect in this disease state, the study showed that GPR81 is involved in angiogenesis and promotes the release of pro-angiogenic factors[74]. In the same way, both treadmill exercise (to increase plasma lactate concentration) as well as subcutaneous injections of lactate increased the expression of vascular endothelial growth factor A (VEGFA) and capillary density in the brain[42]. This finding was GPR81 specific with *Gpr81* null mice showing no difference to vehicle controls. In the support of a vasoactive role of GPR81, expression has been shown by a RFP reporter mouse line to be enriched in the pial fibroblast-like cells which line the vessels of the brain[42] as well as the smooth muscle cells of the mouse brain by single-cell RNA sequencing[93,93]. Using the GPR81-RFP reporter mouse alongside an endothelial cell marker, CD31, it was shown that expression did not co-localise[42]. There is currently a lack of data on the expression of GPR81 within the vasculature throughout the rest of body or at distinct localisation in the kidney.

The most recent study on the cardiovascular involvement of GPR81 was carried out by collaborators at AstraZeneca (Gothenburg, Sweden). They designed a specific agonist for GPR81, AZ13415538 (referred to in the study as AZ2 and for the rest of this thesis as AZ'5538), for the potential therapeutic use in metabolic disorders involving dyslipidaemias, in particular type II diabetes. This agonist activates GPR81 with an *in vivo* potency for GPR109A 40 and 7 times lower in humans and mice respectively. IV infusions of this agonist in dogs and rats found increases in blood pressure and decreased renal blood flow. *In vivo* rat studies with an infusion of the agonist over a 15 minute period resulted in blood pressure increases (~15 mmHg) and renal blood flow decreases (20-30% of basal)[65]. This was coupled with increased

urine flow followed by a delayed increase of ion excretion. The rise in blood pressure was rapid, suggesting an alteration in total peripheral resistance rather than blood volume and salt changes which involve long term homeostatic mechanisms[94]. Due to these adverse effects, it is unlikely that GPR81 agonists will progress to clinical trials but can be used as tool compounds to study the receptor and its function. During my MSc in Cardiovascular Biology, these findings were confirmed in rats. This suggests that there is a mechanism by which GPR81 is involved in the regulation of blood pressure *in vivo*. In addition to these findings, the authors also reported that in rats, the pressor response of AZ'5538 could be prevented with IV treatment of the mixed endothelin receptor antagonist bosentan. This indicates a link between the mechanism of GPR81 induced blood pressure increase and the endothelin system.

1.4 The endothelin system

There are three peptides in the endothelin family which activate two Gq protein coupled endothelin receptors which cause vasoactive effects. Endothelin-1 and endothelin-2 (ET-1 and ET-2) differ by only 2 amino acids in most mammals and activate both the endothelin A receptor (ETRA) and endothelin B receptor (ETRB) with equal affinity while endothelin-3 (ET-3) has a much lower affinity to ETRA in comparison to the other isoforms[95–97]. ET-1 is the most abundant isoform in humans and for that reason the majority of the literature focuses on this peptide as it is most relevant in the cardiovascular system.

ET-1 is synthesised continuously as pre-proendothelin (preproET-1) primarily by endothelial cells and has been located in all types of vessels. The peptide then undergoes a series of cleavage events to generate bigET-1 which is subsequently cleaved by endothelin converting enzymes (ECE) to produce mature ET-1[98,99]. This vasoactive peptide is produced and secreted in mammals in a dual pathway which is shown in Figure 1.6. In the first, constitutive, pathway bigET-1, ET-1 and ECE-1 are continuously released

from small secretory vesicles[100]. Much like lactate and GPR81, levels of ET-1 in plasma tend to be too low to activate ETRA and it is therefore believed to be a local paracrine mediator or blood pressure. However, endogenous continuous production of ET-1 by ECE from bigET-1 through the constitutive pathway has been shown to be necessary for maintenance of basal vascular tone through activation of ETRA[100]. The control of preproET-1 gene expression, and therefore the constitutive pathway, are largely controlled at a transcriptional level[101].

The other mechanism of ET-1 release is the regulated pathway. BigET-1, ET-1 and the ECE enzymes are stored in specialised Weibel-Palade storage granules which are unique to endothelial cells[102]. In the regulated pathway, an external stimulus (physiological or pathophysiological) causes the release of ET-1 from these bodies. Activation of the different receptors after release cause contrasting effects on vascular tone.

Upon release, ET-1 can activate ETRA (or a small number of ETRB) on smooth muscle cells of the vascular medial layer to cause direct vasoconstriction by increasing intracellular calcium concentration[103,104]. The complex of receptor and ligand is then internalised to the endosome to be recycled back to the cell surface. ET-1 can also activate ETRB on endothelial cells to cause release of vasodilatory compounds, including nitric oxide and prostacyclin to cause vasodilation in an autocrine manner which limits the vasoconstrictor response of ET-1 and maintain cardiovascular homeostasis[105]. Expression of the two ET receptors differs between tissues with higher levels of ETRB in the brain and whole kidney[106] while ETRA is enriched in the cardiovascular system and especially the vasculature of the kidney[101]. ET-1 is cleared rapidly from the circulation through the lungs, kidney and liver[107,108], and ETRB is believed to be the main receptor responsible for this[109].

ET-1 is also produced by cell types other than vascular endothelial cells, including other epithelial cells types[110], at lower levels. Vascular smooth

muscle cells (VSMC) are also able to produce ET-1 which can alter vascular responsiveness[111,112]. However the production in isolated aortae is significantly lower than in endothelial cells, making it less physiologically signficiant[113]. Immune cells including macrophages, dendritic cells and monocytes are able to produce ET-1, with the latter increasing ET-1 release in response to T-cell activation[110,114,115]. Finally, cardiomyocytes have been shown to express ET-1 where the peptide is involved in detrimental cell differentiation in hypoxia[116] and contractile function[117].

Until the suggestions by Wallenius *et al*., a direct connection between lactate (or GPR81) and ET-1 had not been reported. However, it is known that both lactate and endothelin are significantly increased during states of hypoxia both *in vitro* and *in vivo*[118–122]. There are also similarities reported in the actions of GPR81 activation and ET-1 actions on ETRA including increased BP pressure and reduced RBF[65,123–125]. Based on these findings, and the lack of GPR81 responses with endothelin receptor blockade, an unknown link between these two systems could be hypothesised.

Compounds to antagonise the endothelin receptors have been in use for many years both as tool compounds to study the endothelin system as well as a treatment for cardiovascular disorders. Anti-endothelin agents have been trialled for hypertension, CKD, heart failure and atherosclerosis to name a few[126]. The mixed antagonist Bosentan which targets both receptors was the first endothelin receptor antagonist to make it into the clinic for PAH[127]. While BQ-123 and BQ-788 have historically been used to study ETRA and ETRB, respectively[128,129].

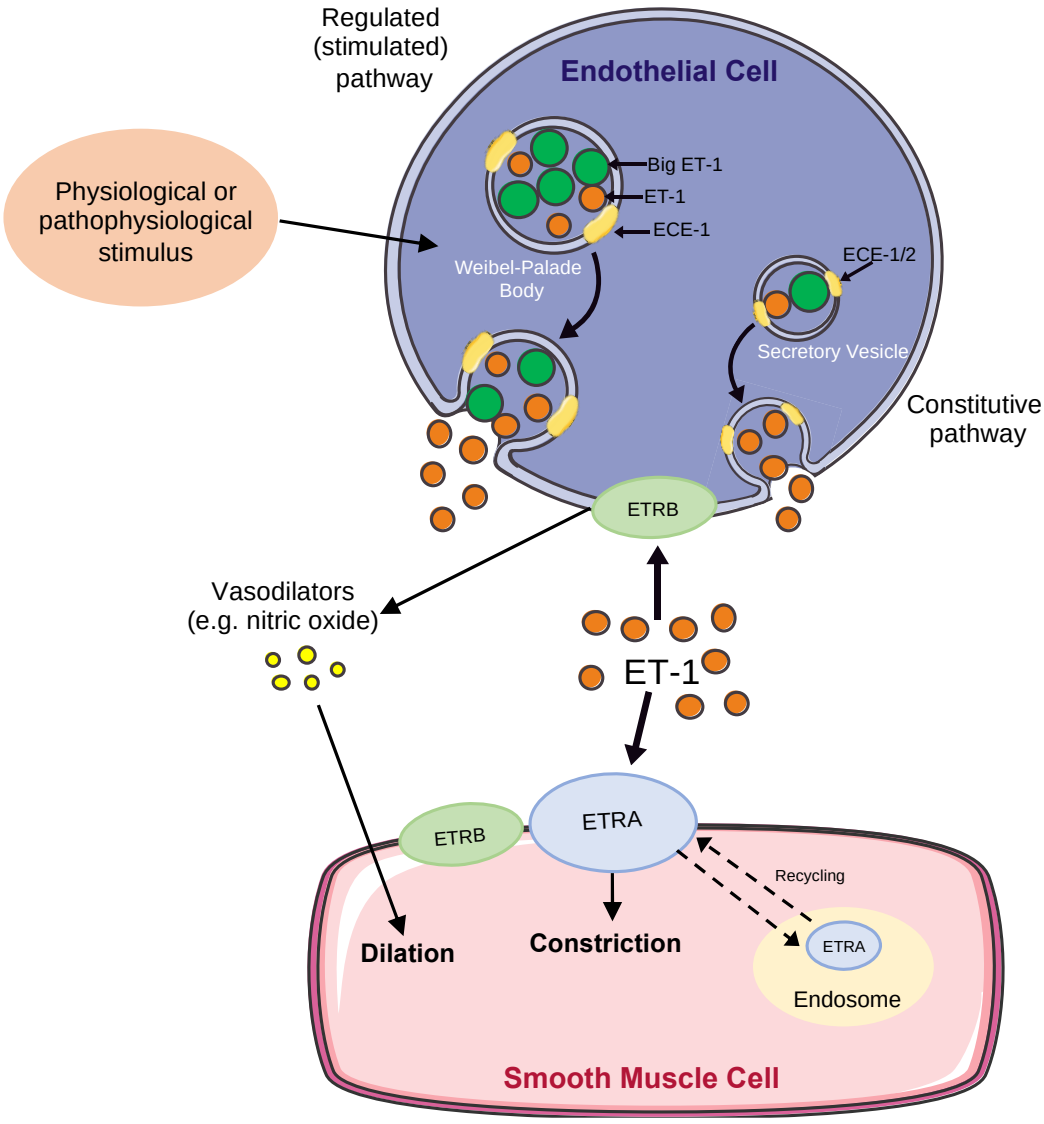

Figure 1.6 Endothelin-1 release and mechanisms of action

Endothelin-1 (ET-1) is first synthesised as big ET-1 in endothelial cells which is cleaved by endothelin converting enzyme (ECE) to form mature ET-1. The peptide is continuously released in the constitutive pathway where small vesicles release ET-1 from the cell to maintain normal vascular tone. ET-1 is also released by the regulated pathway in response to physiological or pathophysiological external stimuli. This releases ET-1 from Weibel-Palade bodies which are endothelial specific. Once released, the majority of ET-1 interaction is with endothelin A receptors (ETRA) on smooth muscle cells to cause vasoconstriction. A small population of endothelin B receptors (ETRB) are present on some smooth muscle cells and are able to mediate vasoconstriction. The ET-1/ETRA complex undergoes internalisation to the endosome and is recycled back to the cell surface. ET-1 is also able to interact with ETRB in an autocrine manner on endothelial cells to produce vasodilators such as nitric oxide to limit the constrictor response. Figure adapted from Maguire *et al.*[101] and created using Servier Medical Art, Les Laboratoires Servier[101].

1.5 Hypothesis and aims

The overarching hypothesis of my thesis is that:

GPR81 is a novel regulator of vasomotive tone and influences blood pressure in an endothelin-1-dependent manner.

To address this hypothesis, I aim to localise the expression of GPR81 in the kidney as well as within the vasculature of the mouse, to determine cardiorenal effects of GPR81 activation and utilise the *Gpr81* null mouse to assess the specificity of these actions. Secondly, I aim to identify and dissect the potential interaction between the GPR81 and endothelin systems. Finally, I will employ wire myography to evaluate the potential direct vasoactive role of GPR81.

Chapter 2 - Materials and Methods

2.1 Animal husbandry

Procedures were performed under the 1986 UK Home Office Animals (Scientific Procedures) Act, following ethical review by the University of Edinburgh. Experiments were performed on male C57BL/6JCrl (Charles River, Paris, France) or *Gpr81* wildtype or knockout mice[65] aged 10-12 weeks. Mice had with free access to standard chow and water and were housed at 22°C ± 1°C, 55% humidity and on a 12 hour light dark cycle (lights on at 07:00).

2.2 Expression of *Gpr81*

2.2.1 Tissue harvesting

Adult male C57BL/6JCrl mice were culled via asphyxiation with CO_2 prior to dissection. Aortae, whole decapsulated kidneys connected to the abdominal aorta with renal arteries and veins intact, and whole mesenteries were removed in ice cold physiological salt solution (PSS; 119.0 mM NaCl, 3.7 mM KCl, 2.5 mM $CaCl_2$, 1.2 mM $MgSO_4$, 25.0 mM $NaHCO_3$, 1.2 mM KH_2PO_4, 27.0 μM EDTA, and 5.5 mM D-glucose). Renal arteries were dissected from the kidneys and mesenteric arteries isolated. Renal and mesenteric arteries were pooled from 2 mice. Kidneys were placed immediately on dry ice and stored at -80^{o}C prior to RNA extraction. Vessels were stored in 1 mL RNAlater (Thermo Fisher, Paisley, UK) at 4^{o}C for 24 hours before removal from the solution and storing at -80^{o}C.

2.2.2 Extraction of RNA and conversion to cDNA

On dry ice, vessels were ground into a fine powder using a pestle (Thermo Fisher) before homogenisation and a modified protocol for the RNA extraction using the RNeasy Micro kit (Qiagen, Hilden, Germany) was carried out. 300 μL of RLT buffer (from the RNeasy kit) was added to the crushed vessels along with a 5 mm stainless steel homogenisation bead (Qiagen). Samples were homogenised in a TissueLyserII (Qiagen) at 30 Hz for 1 minute. Proteinase K (Thermo Fisher, diluted 1:60) was added to samples prior to incubation at 55^{o}C for 10 minutes. Samples were then centrifuged for 3 minutes at 10,000 rpm,

mixed with 350 µL 70% ethanol (Sigma Aldrich, St. Louis, MO, US) and transferred to a Micro-Elute spin column. The spin steps were then carried out according to manufacturer's protocol and RNA eluted in 14 µL RNase free water (Thermo Fisher).

RNA concentration and quality of all samples was assessed by a Nanodrop 1000 spectrophotometer (Thermo Fisher). cDNA was then synthesised following the High Capacity cDNA Reverse Transcription kit protocol (Applied Biosystems, CA, USA). 300 ng of vessel RNA was included in the reaction mix along with 10 µL of 2x RT buffer, 1 µL of 20x enzyme mix and made up to 20 µL with nuclease free water. Internal controls excluding the reverse transcriptase enzyme or RNA were run alongside. Samples were run in a Veriti thermocycler (Applied Biosystems) for 60 minutes at 37$_{o}$C followed by 5 minutes at 95$_{o}$C before storage of cDNA at -20$_{o}$C.

2.2.3 End point PCR for *Gpr81* expression

Primers for end point PCR for *Gpr81* were designed using NCBI Primer-Blast (Table 2.1). RNA samples from aortae, mesenteric arteries and renal arteries were diluted 1:5 in nuclease free water prior to PCR. Each reaction contained 10 µL VWR Red Taq DNA Polymerase 2x Master Mix (VWR, Lutterworth, UK), 0.4 µL of each 10 pmol/µL primer (IDT, IA, USA), 8.2 µL of nuclease free water and 1 µL cDNA. PCR was run in a Veriti thermocycler with the following conditions; initial activation 94°C for 5 minutes, 35 cycles of denaturation (30 seconds at 94°C), annealing (60 seconds at 56°C) and extension (60 seconds at 72°C) and final extension of 7 minutes at 72°C.

Gene name	Protein	Forward Primer	Reverse Primer	Product size
Hcar1	GPR81	ttggagatatcgcctgtcgc	ggctccaaacaacgttgacc	360bp

Table 2.1 End point PCR primers for *Gpr81*
Designed using NCBI Primer-Blast

12 µL of PCR product were run 12 µL of each sample run on a 2% agarose gel with ethidium bromide (1:10,000) at 80 v (300 mA) for 1 hour 30 mins before imaging.

2.2.4 qPCR for *Gpr81* expression

Quantitative polymerase chain reaction (qPCR) was performed in triplicate with the Roche Universal Probe Library (UPL) system using a Lightcycler 480 (Roche, West Sussex, UK). For each gene, a 7 point standard curve (1:10-1:640) was carried out containing a mix of all samples to be analysed to which each sample was normalised. Kidney and artery samples were diluted 1:20 prior to qPCR. Primers for GPR81, 18S and β-actin (Table 2.2) were designed with the UPL Assay Design Centre and used at a final concentration of 250 nM with UPL probes and PerfeCTa FastMix II (Quanta bio, Beverly, MA, USA). Gene expression was analysed as relative expression once normalised to the mean expression of the two housekeeping genes, 18S and β-actin.

Coding protein	Gene Name	Forward Primer	Reverse Primer	UPL probe number
18S	*Rn18s*	gccgctagaggtgaaattctt	cgtcttcgaacctccgact	93
β-Actin	*Actb*	ctaaggccaaccgtgaaaag	accagaggcatacagggaca	64
GPR81	*Hcar1*	ggtggcacgatgtcatgtt	gaccgagcagaacaagatgatt	4

Table 2.2 Primers and UPL probes used for Gpr81 qPCR
Primers designed using UPL Assay Design Centre.

2.2.5 Genotyping of *Gpr81*$^{-/-}$ mice

The global *Gpr81*$^{-/-}$ mouse line was created by AstraZeneca (Gothenburg, Sweden). Briefly, a conditional KO strategy was used for gene deletion, flanking *Gpr81* exon 1 with LoxP sites. A targeting vector containing a frt-flanked neo-selectable marker cassette was utilised, and the targeting construct was electroporated into a C57BL/6JOlaHsd-derived embryonic stem cell line. After homologous recombination, clones were injected into blastocysts to generate chimeric males that were then bred, and black-coated offspring were genotyped for correct integration into the *Gpr81* locus. The neo-

selectable marker cassette was deleted after subsequent breeding to mice expressing flp recombinase under the CAG promoter. *Gpr81* exon 1 was deleted after subsequent breeding to mice expressing Cre recombinase. Mice were then bred onto a C57BL/6NCrl background[65].

For the genotyping of offspring, genomic DNA was extracted from ear punch biopsies from weened pups using the 'HotSHOT' protocol[130]. Tissue was incubated with 75 µL of alkaline lysis reagent (25 mM NaOH, 0.2 mM EDTA in ddH_2O, pH 12) at 95^oC for 30 minutes before cooling to 4^oC on ice. Then, 75 µL of neutralisation buffer was then added (40 mM Tris-HCl in ddH_2O, pH 5). DNA could then be stored at -20^oC.

PCR was carried out using the Qiagen Multiplex PCR plus kit (Qiagen) with the following components: 2 µL genomic DNA, 12.5 µL 2x Master mix, 0.2 µM of each primer, 2.5 µL 5x Q solution and made up to 25 µL with RNase free water. Primer sequences for the genotyping are shown in Table 2.3. Samples were then run in a Veriti thermocycler for 5 minutes at 95^oC, 35 cycles of 95^oC for 30 seconds, 63^oC for 30 seconds and 72^oC for 90 seconds and a final step of 68^oC for 10 minutes.

Each sample had 2 µL of 6x DNA gel loading dye (Thermo Fisher) added before being run alongside a 100 bp DNA ladder (New England Biolabs, MA, USA) on a 2% agarose gel with 1:10,000 gel red (Scientific Laboratory Supplies, Newhouse, UK) at 100 V (300 mA) for 40 minutes. A product of 469 bp indicates a *Gpr81* null mouse, 254 bp indicates a wildtype while both show a heterozygote mouse. An example of a genotyping gel is shown in Figure 2.1.

Primer 1	Primer 2	Primer 3
aatgtaagcagttggcctgg	agaggcaggtggatctctga	cacaaaggagtcaaaagccc
WT band (p2-p3)	**KO band (p1-p2)**	
254bp	469bp	

Table 2.3 Genotyping primers for *Gpr81* mouse colony

Primers sequences provided by AstraZeneca (Gothenburg, Sweden).

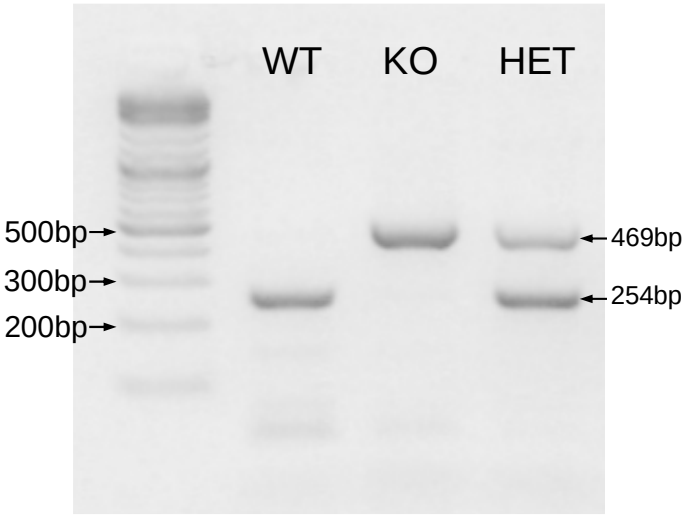

Figure 2.1 Representative genotyping gel the *Gpr81* mouse line

DNA samples extracted from ear clips from the Gpr81 mouse line underwent PCR before running on an agarose gel. A *Gpr81*$^{+/+}$ (WT), *Gpr81*$^{-/-}$ (KO) and *Gpr81*$^{+/-}$ (HET) shown here.

2.2.6 *In situ* hybridisation using RNAscope

RNAscope 2.5 HD red assay (ACD, Abingdon, UK) was carried out using manufacturer assay instructions[131] with some optimisation steps and are briefly explained below.

2.2.6.1 Sample preparation and pre-treatment

Gpr81$^{-/-}$ mice and WT littermates were culled via asphyxiation with CO_2 before the dissection of kidneys, renal arteries and aorta. One kidney was cut in a longitudinal manner while the other was cut transverse. All samples were stored in 10% neutral buffered formalin (Sigma) for 24 hours at room

temperature before being transferred to 70% ethanol (Sigma). Samples were dehydrated using an ethanol series followed by xylene. Samples were then embedded into paraffin blocks. Sections of 5 µm were mounted onto Superfrost Plus slides (Thermo Fisher) and airdried at room temperature.

Slides were baked at 60$_o$C in a dry oven for 2 hours before deparaffinising using 100% xylene then ethanol (both Sigma). Slides were baked at 60$_o$C for 30 minutes before sections were covered in hydrogen peroxide (ACD) and incubated at room temperature for 10 minutes. All slides were then washed in distilled water. For manual target retrieval, slides were submerged into boiling RNAscope 1X Target Retrieval Reagents solution for 15 minutes for kidney and both vessel types and then washed with 100% ethanol. Slides were again baked at 60$_o$C for 30 minutes. A barrier was then drawn around the tissue using Immedge hydrophobic barrier pen (Vector, Peterborough, UK) and left to dry overnight. Slides were then covered with RNAscope Protease Plus solution and incubated in a HybEZ oven (ACD) at 40$_o$C for 30 minutes and washed in distilled water.

2.2.6.2 RNAscope 2.5 HD red assay

To begin the assay, slides were covered with the appropriate mouse specific probe (Gpr81, positive control Ppib or negative control DapB) and incubated for 2 hours in the HybEZ oven at 40$_o$C. Slides were not allowed to dry out as they were hybridised with AMP1-6 and washed in RNAscope wash buffer in between. Signal was then detected by covering the slides with a 1:60 ratio of RNAscope Fast RED-B to Fast RED-A and incubated in the dark for 10 minutes at room temperature. Slides were then counterstained in 50% Gills 1 haematoxylin (Sigma) for 2 minutes before being submerged into 0.02% Ammonia water (Sigma). Slides were dried at 60$_o$C before mounting coverslips using EcoMount (Biocare, CA, USA).

2.2.6.3 Image acquisition

Slides were imaged using an Axio Scan SlideScanner (Ziess, Cambridge, UK). Images were then processed using QuPath[132] and Image J software[133] (Fiji). Success of the assay was judged by strong positive signal of PPIB (Peptidylprolyl Isomerase B) and no signal in dapB samples (an E.coli specific gene).

2.3 *In vivo* analysis of GPR81 activation

2.3.1 Terminal cannulation of vessels

The following protocol was carried out for all subsequent *in vivo* studies. Mice were anaesthetised with an interpretational (IP) injection of Inactin (sodium thiobutabarbital, Sigma, 120 mg/kg). Additional doses of anaesthesia were administered as required by monitoring toe pinch and blink reflexes. Lidocaine-HCl (2% w/w in 0.9% saline, Sigma) was injected to provide local anaesthetic at incision sites. Core body temperature was maintained at 37$_{o}$C using a servo-controlled heat plate (AD Instruments, Oxford, UK).

A ventral cervical skin incision was made and the muscles immediately beneath were dissected to expose the left jugular vein. Perivascular fat was gently removed with fine forceps, the anterior end ligated (size 5 suture silk, Fine Science Tools, CA, USA) and the vessel cannulated with 15 cm of P10 tubing (Smiths Medical, Kent, UK) attached to a 1mL syringe containing 0.9% saline. For studies requiring infusion of two substances at once, two 15cm sections of P10 tubing were inserted into the left jugular vein, for example in the renal clearance experiments. Cannulas were then tied in with a second ligature.

Next, the trachea was opened to maintain a clear airway. The muscles around the trachea were dissected to expose it and a small piece of P50 tubing (Smiths Medical) was inserted directly under the trachea to raise it slightly. An incision was made between tracheal cartilage rings and fluid build-up was cleared using small twists of tissue throughout experiments.

The carotid artery was cannulated for blood pressure and heart rate recording and for arterial blood collection. The artery was separated from the vagus nerve before anterior ligation. The posterior end was ligated with a vessel clamp to prevent blood loss. A small incision in the vessel was made where a length of P50 tubing with 1cm of P10 tubing at the end was inserted and tied in place. This tubing was attached to a 1 mL syringe containing 20 units/L porcine heparin saline (Sigma). The clamp was then removed to restore blood flow. The carotid cannula was connected to a ML224 Bridge Amp for arterial blood pressure monitoring through LabChart data acquisition software (both AD Instruments).

Finally, the bladder was catheterised for urine collection. A lower abdominal incision followed by one in the peritoneum was made so the bladder could be located and gently raised out. A hole was made in the bladder using a needle and a ~5 cm length of P50 tubing was inserted and tied in place.

Animals were equilibrated post-surgery for 30 minutes before a 15 minute infusion of 5% D-mannitol vehicle (pH 5) followed by AZ'5538 (1 µmol/kg bw/min; pH 5). Unless otherwise state, all IV infusion rates were 0.2 mL/10g/Hr using an AL2000 infusion pump (World Precision Instruments, FL, USA).

2.3.2 Pulse-wave Doppler ultrasound

Post-surgery, C57BL/6JCrl were mice placed in the supine position on a heat pad. Pulse-wave Doppler using a Vevo 770 with a 707B 30 MHz ultrasound probe (VisualSonics, Toronto, Canada) measured blood flow from the right renal artery. Peak velocity was measured at baseline and over 5 minute periods during IV administration of vehicle followed by AZ'5538 as above.

2.3.3 Doppler flow probe and needle flux probe placement

Doppler flow probe experiments were carried out in both C57BL/6JCrl mice and *Gpr81*$^{-/-}$ and wildtype littermates while needle flux probes were only used in the *Gpr81*$^{-/-}$ mouse line with wildtype controls.

For both procedures, mice underwent an additional midline laparotomy after the cannulation of vessels. This allowed the placement of either a Doppler transit time probe (Transonic, Ithaca, NY, USA) around the right renal artery (Surgilube gel (HR Pharmaceuticals, Pennsylvania, USA) was used for acoustic coupling) or Doppler flux probes (Transonic) inserted into the cortex and medulla of the right kidney. Probe position was confirmed post-mortem. All data was acquired through LabChart software (AD Instruments).

2.3.4 Renal clearance measurements

Renal clearance studies were carried out in both C57BL6/JCrl mice and the *Gpr81* mouse line. All mice underwent surgery as previously discussed with 2 IV lines in the right jugular vein. Mice were equilibrated post-surgery for 40 minutes where they received infusate (100 mM NaCl, 5 mM KCl, 15 mM $NaHCO_{3}^{-}$, and 0.25% FITC- inulin (Sigma), pH altered to 7.4 by bubbling with CO_2) at 0.2 mL/10g/Hr through one IV line) before the first urine collection period. The protocol was broken down into 3 collection periods where urine was collected into pre-weighed 500 µL Eppendorf tubes containing mineral oil to prevent sample evaporation and around 50 µL of blood was collected lithium-heparinised capillary tubes (Sarstedt, Nümbrecht, Germany) before and after the period which was spun for 5 minutes at 10,000 rpm to separate plasma. Firstly, over 40 minutes, mice continued to receive infusate along with 5% D-mannitol vehicle through the second IV line at 0.1 mL/10g/Hr, increasing the infusion rate to 0.3 mL/10g/Hr total. The next period of 15 minutes mice either continued to receive vehicle or AZ'5538 (1 µmol/kg/min at 0.1 mL/10g/Hr) along with infusate (in the studies in the *Gpr81*$^{-/-}$ mice and littermates, all mice received AZ'5538). For the final 40 minutes, mice continued with the same infusions. At the end of the experiment, terminal

plasma was collected in 500 µL lithium-heparinised tubes (Starstedt), mice were culled via cervical dislocation and kidneys weighed.

To calculate FITC-inulin concentrations, plasma and urine samples were diluted 1:100 and 1:10,000 in HEPES buffer (Sigma, 10 mM, pH7.4), respectively. A 9 point standard curve (10-0.04 µg/mL) and blank HEPES only sample were run alongside. 190 µL of each sample and standard was loaded in duplication into a Microfluor black 96 well plate (Thermo Fisher). Plates were read using an Infinite M1000 microplate reader (Tecan, Männedorf, Switzerland) with an excitation of 485 nm and emission of 538 nm

Glomerular filtration rate (GFR) was calculated from the FITC-inulin concentrations of plasma ([P_{inulin}]) and urine ([U_{inulin}]) samples determined from the standard curve. GFR was calculated as follows:

([U_{inulin}] x urinary flow rate)/ [P_{inulin}] = GFR

Where:
[U_{inulin}] = Urine FITC-inulin concentration
[P_{inulin}] = Plasma FITC-inulin concentration
GFR = Glomerular filtration rate

2.3.5 Measurement of urine and plasma electrolytes

Electrolyte analysis was carried out using a Spotchem EL SE-1520 (Arkray, Kyoto, Japan). Molar concentration of sodium, potassium and chloride were measured in each sample. Urine samples were diluted 1:1 in distilled water and terminal plasma left undiluted. Fractional excretion of each analyte was calculated as follows with sodium used as an example:

[U_{Na}] x urinary flow rate = eNa
[P_{Na}] x GFR = filtered load
(eNa/Filtered load) x 100 = FeNa (%)

Where:

$[U_{Na}]$ = Urine sodium concentration

$[P_{Na}]$ = Plasma sodium concentration

eNa = Sodium excretion

GFR = Glomerular filtration rate

FeNa = Fractional sodium excretion

2.3.6 Data analysis and statistics

Blood pressure data (taken at 1 kHz) were separated into systolic and diastolic blood pressure using cyclic measurements on LabChart. Doppler flow and flux data were also taken at 1 kHz and average cyclic data taken to remove pulsatilty. Data was down sampled prior to analysis and an average of 30 second periods were taken. All data are mean±SEM. Statistical comparisons (Graphpad Prism 6, La Jolla, CA) were made by using one or two-way analysis of variance (ANOVA) or *t*-test, as stated in figure legends along with group sizes. For two-way ANOVA, the main effects of the genotype or treatment, the interaction between these and time were assessed. The family P value was fixed at 0.05.

2.4 Assessment of endothelin and GPR81 interactions

As previously described (2.3.1), adult male C57BL/6JCrl mice were anaesthetised and underwent cannulation of the jugular vein and carotid artery. After a 30 minute equilibrium period, blood was sampled from the carotid line into lithium-heparinised tubes and separated to plasma. Mice were infused for 15 minutes with either 5% D-mannitol vehicle (pH 5) or AZ'5538 (15 µmol/kg; pH 5) at 0.2 mL/10g bw/hr. At the end of the experiment, another blood sample was taken. Mice were then euthanised by cervical dislocation for collection of kidneys and thoracic aorta onto dry ice. Plasma and tissues were stored at -80^{o}C before use.

2.4.1 Endothelin-1 protein expression

RIPA buffer (Sigma) was prepared by adding 1 cOmplete mini-protease inhibitor tablet (Roche) per 10 mL buffer. Whole kidneys were cut into quarters and 700 µL of buffer added to one quarter. Whole aorta samples had 300 µL buffer added. All samples underwent homogenisation with a 5 mm stainless steel bead at 30 Hz for 90 seconds using a TissueLyserII. Samples were then centrifuged at 10,000 g for 10 minutes at 4$_{o}$C, supernatants then kept on ice.

A BCA assay (Thermo Fisher) was carried out on tissue homogenates. Kidney and aorta samples were diluted 1/50 and 1/20 in RIPA buffer, respectively, prior to carrying out the assay in duplicate. The assay was conducted according to manufacturer's instructions and total protein content of the samples could then be calculated.

Plasma samples along with kidney and aorta homogenates then underwent the ET-1 Quantikine ELISA (R&D Systems, Abingdon, UK) according to manufacturer's instructions, in duplicate. Plasma samples were left undiluted while kidney homogenates were diluted 1/10 and aortae 1/3 in RIPA buffer.

Aorta and kidney homogenate ET-1 concentrations were normalised to total protein. A change in ET-1 concentration in plasma was calculated from before and after infusion values. This was due to small sample volumes for plasma.

2.4.2 Endothelin system gene expression

Frozen whole kidneys were cut into quarters prior to RNA isolation. 600 µL of RLT buffer were added before homogenisation for 1 minute at 30 Hz with a stainless steel bead in the TissueLyserII. Samples then underwent the RNeasy Mini kit protocol (Qiagen) according to standard protocol instructions. Extracted RNA was stored at -80$_{o}$C.

RNA was quantified and cDNA synthesised from 1 µg of RNA as described previously (2.2.2). cDNA samples were diluted 1/40 prior to qPCR using the

UPL system (2.2.4). Primers for the genes analysed can be found in Table 2.4. Relative gene expression was calculated by normalising to the mean of the two housekeeping genes 18S and TBP.

Coding protein	Gene Name	Forward Primer	Reverse Primer	UPL probe number
18S	*Rn18s*	gccgctagaggtgaaattctt	cgtcttcgaacctccgact	93
ET-1	*Edn1*	tccttgatggacaaggagtgt	cccagtccatacggtacga	29
ETRA	*Ednra*	tgtgagcaagaaattcaaaaattg	atgaggcttttggactggtg	34
ETRB	*Ednrb*	tcagaaaacagccttcatgc	gcggcaagcagaagtagaaa	83
GPR81	*Hcar1*	ggtggcacgatgtcatgtt	gaccgagcagaacaagatgatt	4
HPRT	*Hprt*	tcctcctcagaccgctttt	aacctggttcatcatcgctaa	95
TBP	*Tbp*	gggagaatcatggaccagaa	gatgggaattccaggagtca	97

Table 2.4 Primers and UPL probes used for qPCR

Primers designed using UPL Assay Design Centre.

2.4.3 *In vivo* blockade of endothelin receptors

C57Bl/6JCrl mice were anaesthetised and surgically prepared (as previously, 2.3.1) with two IV lines permitting separate infusion of AZ'5538 and the endothelin receptor antagonists. Bostentan (Stratech Scientific), BQ-123 (Tocris, Bristol, UK); and BQ-788, (Abcam, Cambridge, UK), or their corresponding vehicles (0.9% saline for Bosentan and BQ-123; 2.3% or 4.6% DMSO for BQ-788) were IV infused at 0.2 mL/10g bw/hr for 40 minutes, for the final 15 minutes, AZ'5538 was also infused at 15 µmol/kg. This altered the infusion rate to 0.4 mL/10g bw/hr for the final 15 minutes. Bosentan was used at 20 and 40 mg/kg[65] while BQ-123 and BQ-788 at 1 and 2 mg/kg[134]. These doses were based on previous literature in mice which suggest full receptor occupancy.

2.4.4 Data analysis and statistics

Differences in protein and mRNA expression of ET-1 and ET-1 related genes were analysed by unpaired t-tests. Blood pressure data (taken at 1 kHz) were separated into systolic and diastolic blood pressure using cyclic measurements on LabChart. Data was down-sampled prior to analysis and an average of 30 second periods were taken. All data are mean±SEM. Statistical comparisons (Graphpad Prism 6, La Jolla, CA) were made by using two-way

analysis of variance (ANOVA). Group sizes and statistical analysis used stated in figure legends. For two-way ANOVA, the main effect of the treatment was assessed, the interaction between these and time with Tukey's multiple comparison test to compare each dose to vehicle control. The family P value was fixed at 0.05.

2.5 Wire myography

2.5.1 General measurements of vascular tone by wire myography

Wire myography was used to assess vascular tone in aortae, renal arteries and second order mesenteric arteries isolated from adult male mice. All mice were culled by asphyxiation with CO_2 prior to isolation of the arteries which were stored in ice cold physiological salt solution (PSS; 119.0 mM NaCl, 3.7 mM KCl, 2.5 mM $CaCl_2$, 1.2 mM $MgSO_4$, 25.0 mM $NaHCO_3$, 1.2 mM KH_2PO_4, 27.0 μM EDTA, and 5.5 mM D-glucose), cleaned of fat, cut to ~2 mm lengths and then mounted onto a wire myograph (Danish MyoTech, Aarhus, Denmark). Wells of the myograph were filled with PSS (6 mL), which was perfused with 95% O_2 and 5% CO_2 at 37$_o$C. Basal tone was established for renal and mesenteric arteries and set at 7.34 mN for aortae. Due to the larger size of aortae, they were cut to exactly 2 mm in length while other arteries were measured after mounting. Vessels were then equilibrated for 30 minutes.

To establish vessel contractile capacity over the experimental time course and to normalise the absolute contractile force generated by vasoconstrictive drugs, vessels were depolarised by replacing the PSS with a high potassium physiological salt solution (KPSS; 125 mM KCl) at the beginning and end of the experiment. In the majority of studies, all vessels were subjected to increasing concentrations of phenylephrine (PE; Sigma 1 nM-1 μM aortae and 1 nm-3 μM for other vessels), sodium nitroprusside (SNP; Sigma 1 nM-3 μM), acetylcholine (ACH; Sigma 1 nM-3 μM) and endothelin-1 (ET-1, Sigma 1 pM-100 nM). Prior to assessment of vasodilatory drugs (SNP and ACH) vessels were preconstricted with PE to the half maximal response. ET-1 dose responses were always recorded last, after the final KPSS response due to

difficulties in washing ET-1 from the vessels. Drug additions to the PSS bath were kept below volumes of 100 µL.

2.5.2 Effect of AZ'5538 on vascular function

To assess AZ'5538 toxicity on vessels, adult male C57BL/6JCrl (Charles River) were culled and aortae and second order mesenteric arteries isolated and mounted. After basal tone was established and responses to KPSS were assessed, vessels were incubated for 15 minutes with varying concentrations of GPR81 agonist AZ'5538 (15.6,31.3, 62.5, 125 or 250 µM) or vehicle alone at the same volume (5% D-mannitol solution, pH 5, Sigma). Group sizes were between 2 and 5 and the ability of the vessel to constrict to KPSS before and after AZ'5538 were measured.

To determine changes in vascular function with AZ'5538 incubation, C57BL/6JCrl mice (n=8) were culled as previously described. Two sections of aortae, mesenteric arteries and renal arteries were dissected from each mouse and mounted onto the wire myography. Vessels were incubated with 30 µM AZ'5538 or 5% mannitol vehicle added to the 6 mL of PSS for 15 minutes before washing with PSS. Vessels were then subjected to increasing doses of PE, ACH, SNP and ET-1.

Preconstriction of vessels can alter vascular function to certain drugs, such as angiotensin II (ANG II), therefore this was assessed for AZ'5538. All three vessel types were mounted as previously described and split into two groups (n=8 for aorta and mesenteric, n=7 for renal arteries for each group). After assessing the vasoconstriction caused by KPSS, half of the wells were replaced with normal PSS while others were filled with a 25 mM KCl containing PSS to preconstrict vessels. Vessels were allowed to stabilise before a dose response carried out of AZ'5538 from 1 nM to 30 µM. Aortic vessels also went through this same protocol but with increasing concentrations of ANG II (10 pM-1 µM, Sigma) rather than AZ'5538.

2.5.3 ETRA blockade *ex vivo*

A concentration test for BQ-123 was carried out to assess a dose which successfully blocked ET-1 mediated vasoconstriction. Renal arteries from C57BL/6JCrl mice were mounted onto the wire myograph. KPSS responses were assessed before incubation for 30 minutes with water vehicle or BQ-123 at 1 µM, 3 µM, or 10 µM added to the PSS in the well (n=4 for each group). KPSS response was assessed again after incubation. Vessels were then incubated with the same treatment prior to ET-1 dose response to assess ETRA blockade.

In a separate experiment, with the aim of preventing AZ'5538-mediated vasoconstriction in renal arteries, vessels were incubated with either 1 µM BQ-123 or vehicle for 30 minutes followed by addition of 30 µM AZ'5538 or vehicle (n=8 for vehicle only and BQ-123 + AZ'5538, n=15 for vehicle + AZ'5538).

2.5.4 Assessment of vascular function in *Gpr81*$^{-/-}$ mice

Adult male *Gpr81*$^{-/-}$ and WT littermates were culled via asphyxiated with CO_2. Mesenteric and renal arteries were isolated and mounted onto the wire myograph (n=5-6). All vessels were assessed for responses to KPSS (at the beginning and end of experiment), PE, ACH, SNP, ET-1 and a 15 minute incubation with 30 µM AZ'5538.

In separate experiments, renal arteries from *Gpr81* null and WT mice were administered with increasing concentrations of AZ'5538 (1 nM-30 µM) (n=10-11 from 6 mice) before and after KPSS.

2.5.5 Statistical analysis for wire myography

Data was obtained using LabChart Software (AD Instruments) and taken at 1 Hz. All analysis was carried out using GraphPad Prism 8. Responses to KPSS, both absolute maximum mN value and percentage change from the beginning and end of the experiment were analysed by unpaired t-tests. Contractility data is presented as a percentage of the maximum KPSS response and dilatory as

a percentage of the vessel's preconstriction with PE both against –log of the molar drug concentration. All data are shown as mean±SEM. Non-linear regression provided dose response curves for PE, SNP, ACH, ET-1 and AZ'5538. Dose responses between groups were compared using two-way ANOVA as well as comparing EC/IC_{50} and $\%E/I_{max}$ from the non-linear regressions formed using an extra sun-of-square F test. BQ-123 toxicity data was compared using a one-way ANOVA with a Dunnett's post hoc test. All statistical analysis details and group sizes are in the figure legends.

Chapter 3 - Expression of GPR81 and *in vivo* receptor activation

3.1 Introduction

Although it has been known for over a decade that GPR81 is expressed in the kidney as well as other cardiovascular tissues[30], the function in these tissues is still not understood. With the exception of adipocytes, there is a lack of data on cell-type specific localisation of the receptor. There have been previous studies implying expression of the receptor in the vasculature[42], in particular in vascular smooth muscle[93]. There have also been reports of a potential vasoactive role of the receptor, with a more recent study finding that activation of GPR81 *in vivo* caused an increase in mean arterial blood pressure (MABP) of ~15 mmHg in both rats and dogs[65]. I aimed to define the potential role of GPR81 activation in blood pressure regulation.

To help understand the physiological role of GPR81, my collaborators at AstraZeneca (Gothenburg, Sweden) have provided the specific GPR81 agonist AZ13415538 (referred to as AZ'5538). *In vitro* EC_{50} values for GPR81 are 74 nM, 310 nM and 180 nM for adipocytes from human, rat and mouse, respectively. Along with this compound, AstraZeneca have also provided the *Gpr81*-null mouse line. Homozygote *Gpr81*$^{-/-}$ mice have a global deletion of the single exon *Gpr81* gene and are on a C57BL/6NCrl background. There have been no reported adverse phenotypes of this genetic deletion[65]. This mouse line allows confirmation of on-target GPR81 effects of AZ'5538 in the *in vivo* studies.

The objective of this chapter was to localise the receptor in the kidney and vasculature and to use AZ'5538 as a tool to investigate the effects of GPR81 activation on blood pressure and renal haemodynamics in mice.

I hypothesise is that *Gpr81* is expressed within the vasculature, including that of the kidney, and that activation of GPR81 by AZ'5538 will cause specific cardiorenal effects. I aimed to address this hypothesis by, firstly, determining the expression of *Gpr81* mRNA in whole kidney and artery homogenate followed by localising *Gpr81* expression in specific areas of the kidney, aorta

and renal arteries. Next I will investigate the effect of acute AZ'5538 infusion on blood pressure, heart rate, renal blood flow and kidney function in wildtype C57BL/6JCrl mice. And finally assess the specificity of any changes seen with AZ'5538 infusion by utilising the *Gpr81*$^{-/-}$ mouse as a negative control.

3.2 Results

3.2.1 Renal and vascular expression of *Gpr81*

End point PCR was used to identify *Gpr81* mRNA expression in the aorta, renal and mesenteric arteries of wildtype C57BL6/JCrl mice (Figure 3.1, see Table 2.1 for primer details).

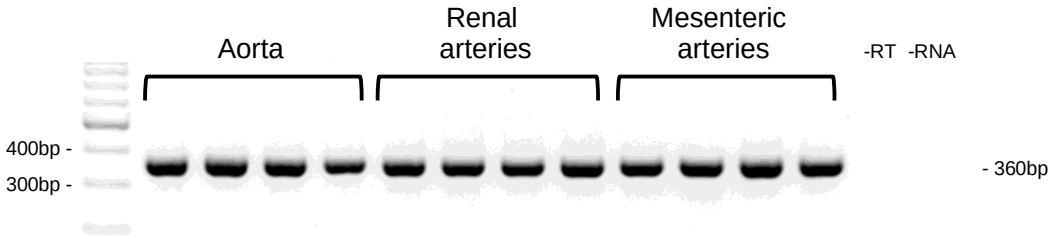

Figure 3.1 *Gpr81* expression in the mouse vasculature by end point PCR

RNA was extracted and reverse transcribed from C57BL/6JCrl mouse vessels. Negative controls were samples where reverse transcription enzyme or RNA were left out at the cDNA conversion step. All samples underwent end point PCR before gel electrophoresis. n=4 for all vessel types, pooled from 2 mice for renal arteries and mesenteric arteries.

qPCR was also utilised as a second technique to confirm *Gpr81* expression in the vasculature. Expression for *Gpr81* was found in aorta, renal and mesenteric arteries (Figure 3.2).

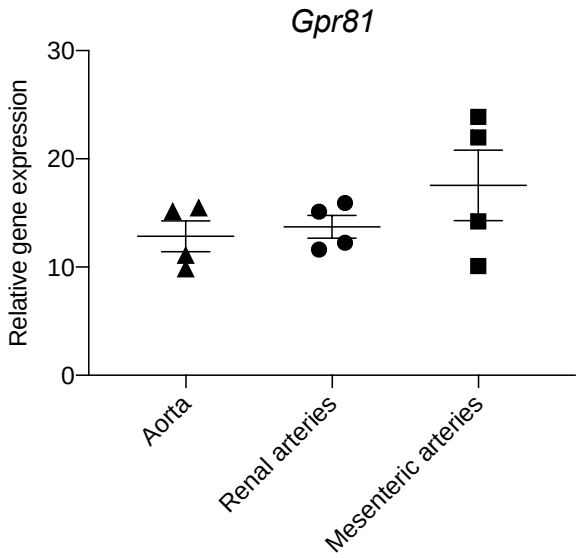

Figure 3.2 Gpr81 expression in the mouse vasculature by qPCR

RNA was extracted and reverse transcribed from C57BL/6JCrl mouse arteries. n=4 for all, pooled from 2 mice for renal arteries and mesenteric arteries. Gene expression was normalised to the average of housekeepers, 18S and β-actin.

RNAscope in situ hybridization was used to localise GPR81 within kidney, aorta and renal artery sections. This was carried out in *Gpr81*$^{-/-}$ and WT littermate mice. In whole kidney sections, no positive staining was found in *Gpr81*$^{-/-}$ mice (Figure 3.3 and Figure 3.4). *Gpr81* was expressed in both the cortex and medulla of the WT animal kidneys (Figure 3.3 and Figure 3.4). The staining in the cortex was localised mainly in the glomeruli (Figure 3.3), particularly at the vascular poles (indicated by the stars), consistent with localisation in afferent or efferent arterioles.

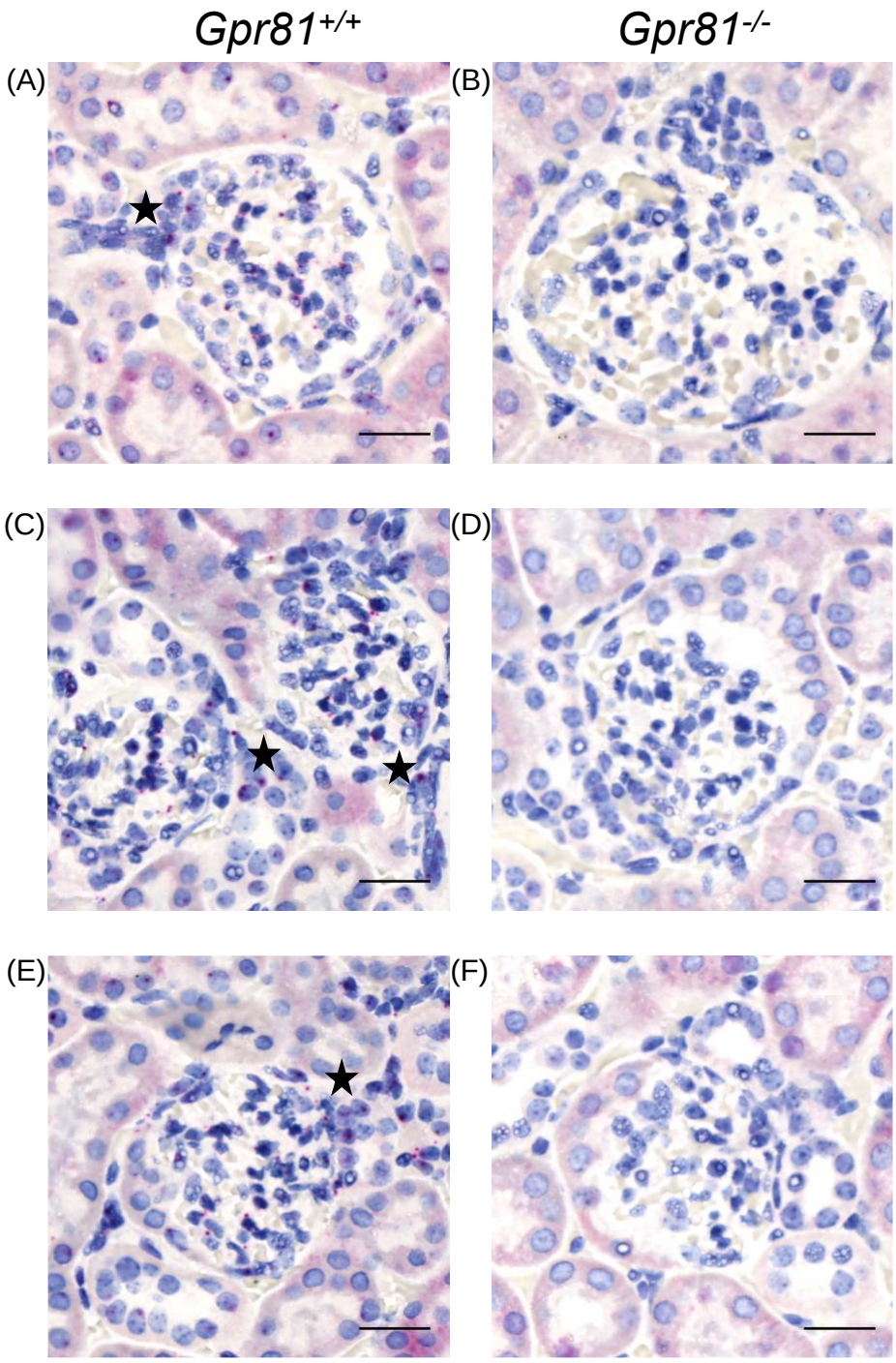

Figure 3.3 *Gpr81* expression in the kidney glomerulus by RNAscope in situ hybridisation

Mouse kidney cut longitudinally prior to in situ hybridisation. Positive *Gpr81* mRNA expression shown by red punctuated dots, nuclei stained blue and tubules pale pink. Expression found in wildtype mouse glomeruli of the kidney cortex (A, C and E) where the star indicates staining at arterioles of the glomerulus. No staining seen in *Gpr81*$^{-/-}$ mouse kidney cortex (B, D and F). Scale bars represent 25 µm.

Expression for *Gpr81* was found in the medulla of kidney sections and did not colocalise with the nuclear stain (Figure 3.4).

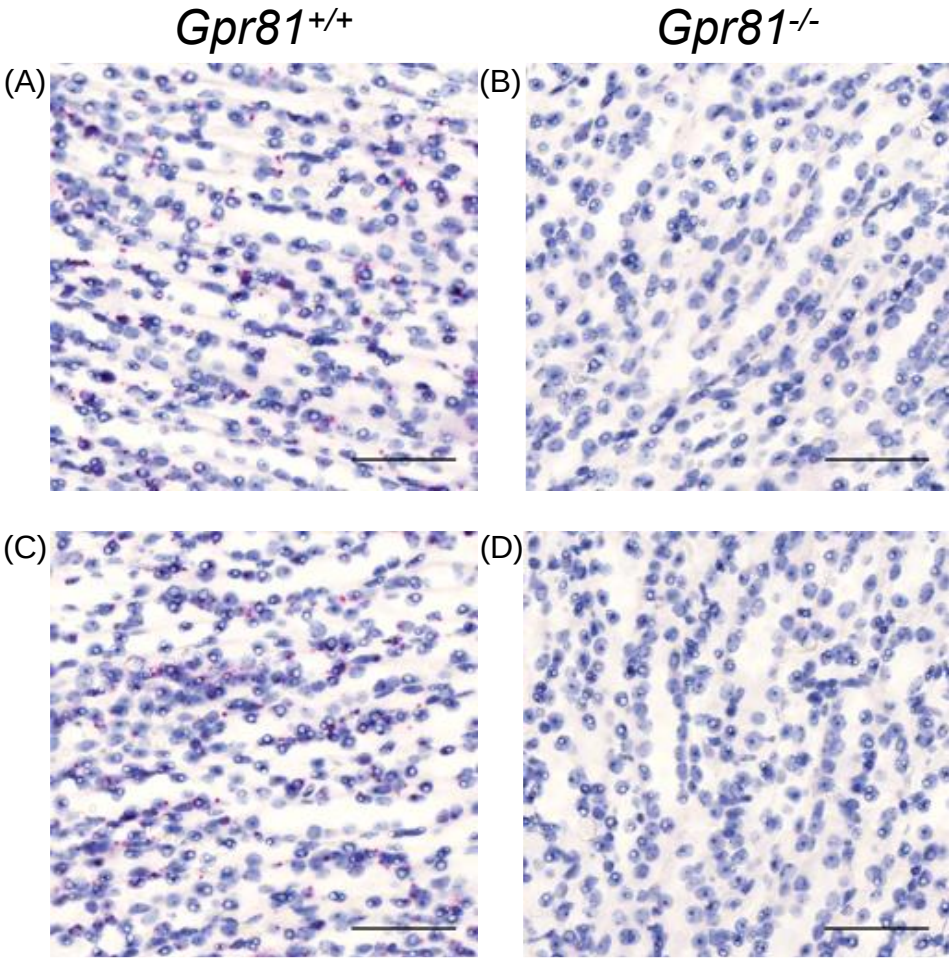

Figure 3.4 *Gpr81* expression in the kidney medulla by RNAscope in situ hybridisation

Mouse kidney cut longitudinally prior to in situ hybridisation. Positive *Gpr81* mRNA expression shown by red punctuated dots and nuclei stained blue. *Gpr81* expression found in the medulla of the kidney in wildtype mice (A and C) while no staining is seen in *Gpr81-/-* mouse kidney medulla (B and D). Scale bars represent 50 µm.

Although at lower levels, some staining to indicate *Gpr8*1 expression was also present in the blood vessels in the kidney cortex in wildtype mice (Figure 3.5).

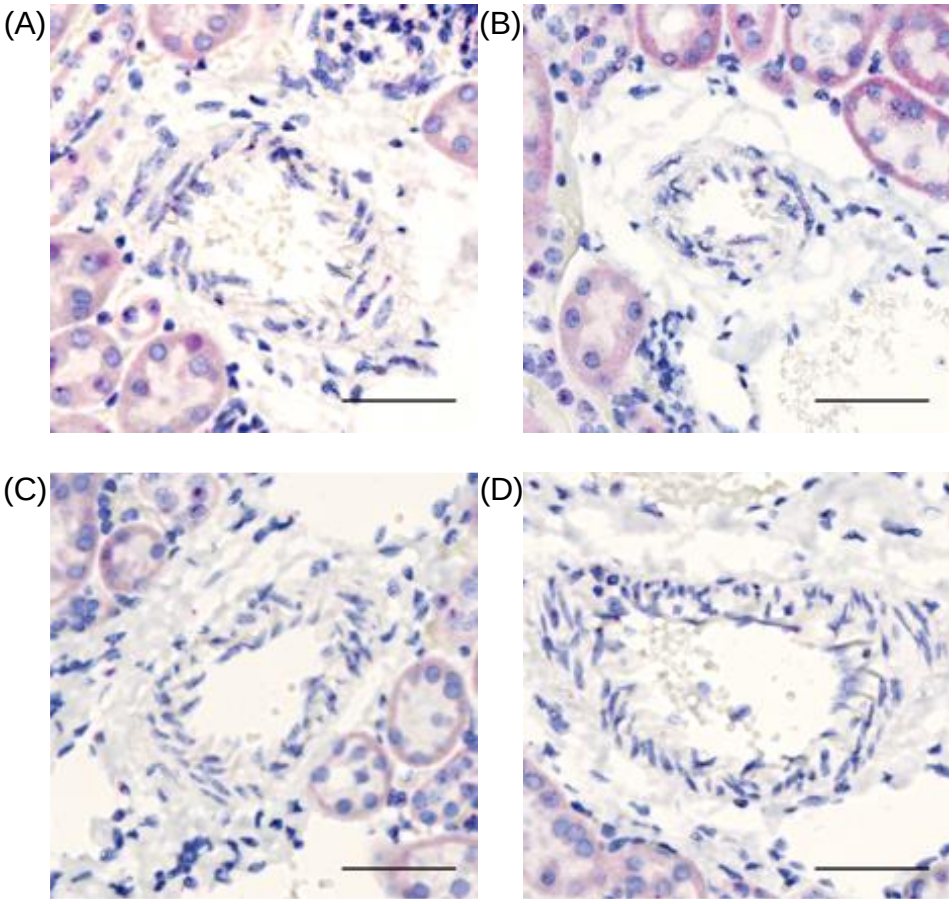

Figure 3.5 *Gpr81* expression in vessels in the kidney cortex of wildtype mice by RNAscope *in situ* hybridisation

Mouse kidney cut transverse prior to *in situ* hybridisation. Positive *Gpr81* mRNA expression shown by red punctuated dots, nuclei stained blue and tubules are pale pink. All panels show vessels in the kidney cortex of *Gpr81*$^{+/+}$ mice. Scale bars represent 50 µm.

Both in the aorta and renal arteries (Figure 3.6 and Figure 3.7), positive staining is seen in the medial layer of the arteries, consistent with localisation to vascular smooth muscle cells, indicated by black arrows. No staining was visible in arteries from *Gpr81*$^{-/-}$ mice (Figure 3.6and Figure 3.7 (B) and (D) for both).

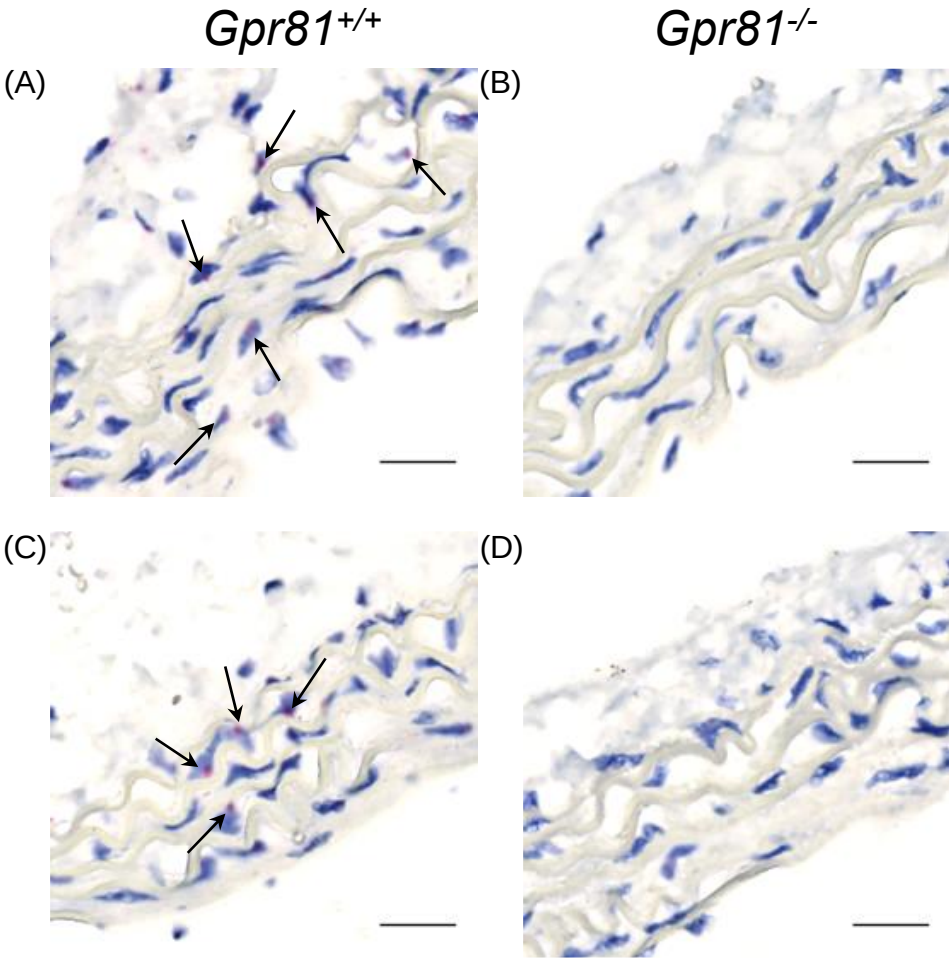

Figure 3.6 *Gpr81* expression in the aorta of mice by RNAscope *in situ* hybridisation

Positive *Gpr81* mRNA expression shown by red punctuated dots and nuclei stained blue. Arrows indicate *Gpr81* staining in *Gpr81*$^{+/+}$ mouse aortae (A and C) while no staining is seen in *Gpr81*$^{-/-}$ vessels (B and D). Scale bars represent 20 µm for all.

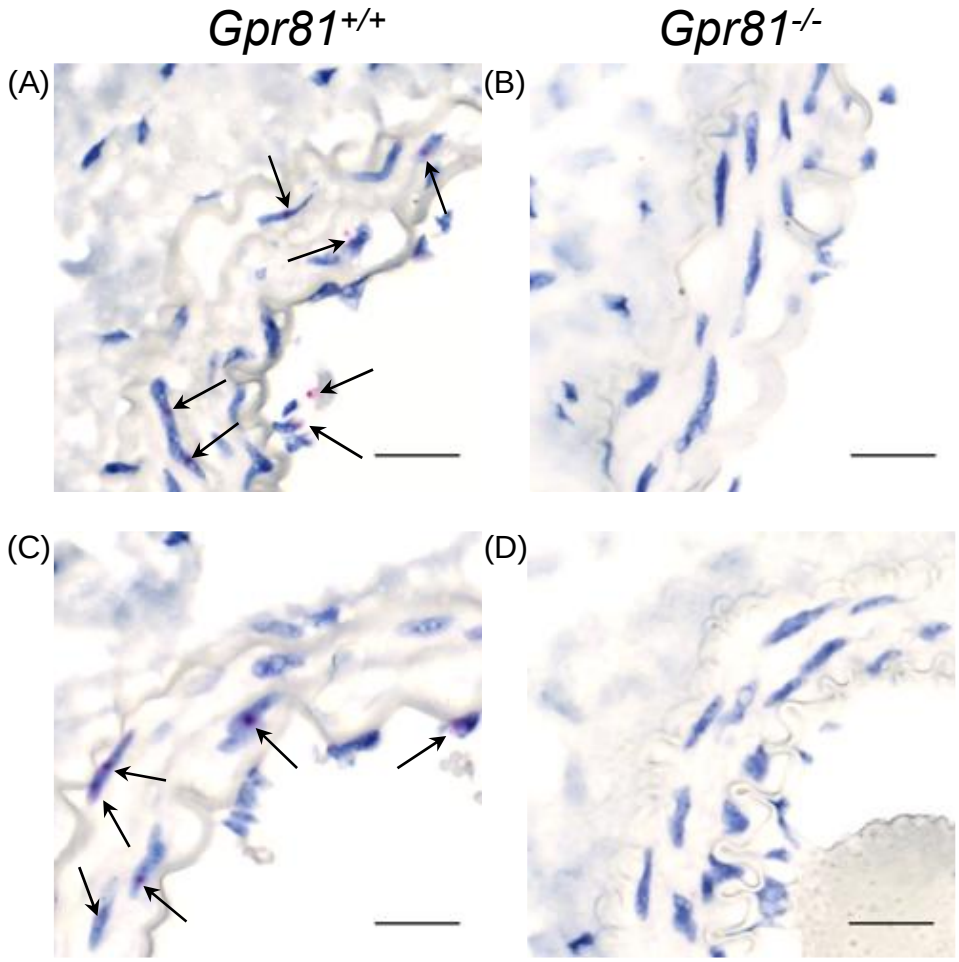

Figure 3.7 *Gpr81* expression in the renal arteries of mice by RNAscope *in situ* hybridisation

Positive *Gpr81* mRNA expression shown by red punctuated dots and nuclei stained blue. Arrows indicate *Gpr81* staining in *Gpr81*$^{+/+}$ mouse renal arteries (A and C) while no staining is seen in *Gpr81*$^{-/-}$ vessels (B and D). Scale bars represent 20 µm.

3.2.2 In vivo activation of GPR81 with AZ'5538 in wildtype mice

Heart rate (HR), systolic (SBP) and diastolic (DBP) blood pressure were measured in terminally anesthetized male C57BL/6JCrl mice. Baseline values were 284±15 bpm, 85.6±3.8 mmHg, and 68.9±4.6 mmHg for HR, SBP, and DBP, respectively. AZ'5538 significantly increased both SBP and DBP compared to 5% mannitol vehicle (Figure 3.8(A) and (B)). The peak blood pressure increase was 13.4±1.6 mmHg and 11.3±1.1 mmHg for SBP and DBP respectively (Figure 3.8(D)). Heart rate decreased with infusion of AZ'5538;

5% mannitol vehicle infusion caused a slight tachycardia (Figure 3.8(C) and (E)).

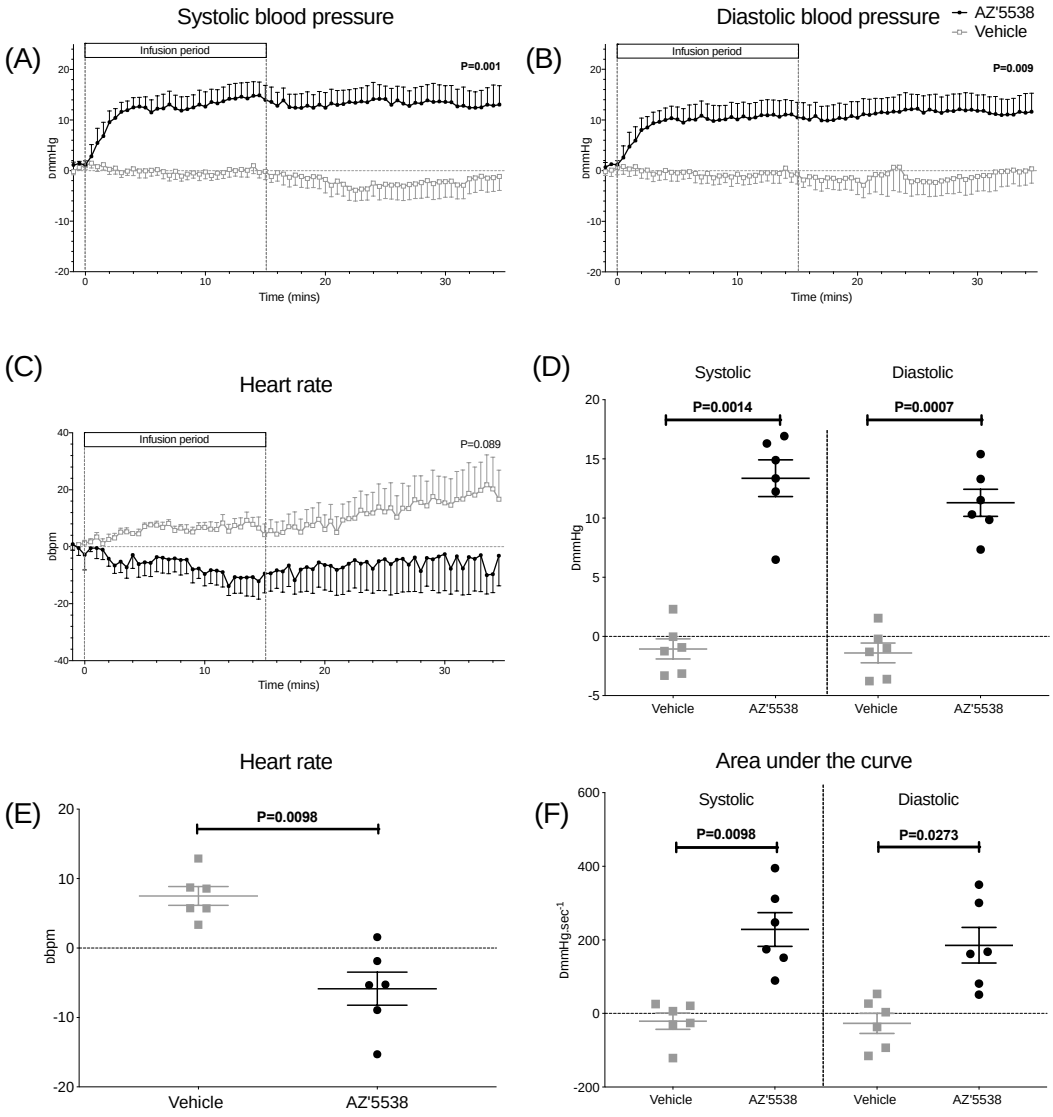

Figure 3.8 AZ'5538 infusion increases blood pressure and decreases heart rate

Vehicle and GPR81 agonist AZ'5538 were infused intravenously into C57BL/6J mice over a 15 minute period at 1µmol/kg/min. Activation of GPR81 increased (A) systolic and (B) diastolic blood pressure and decreased (C) heart rate compared to 5% mannitol vehicle control, all assessed by two-way ANOVA where the P value given is that of the drug treatment. At the end of the infusion, differences in (D) systolic and diastolic blood pressure and (E) heart rate were analysed by paired t tests. (F) Area under the curve was assessed for the blood pressure responses. All data are mean±SEM from baseline, n=6

All mice received a second infusion of AZ'5538, 35 minutes after the first administration. The pressor response to the second administration was

attenuated, particularly in DBP (Figure 3.9), suggesting receptor de-sensitization.

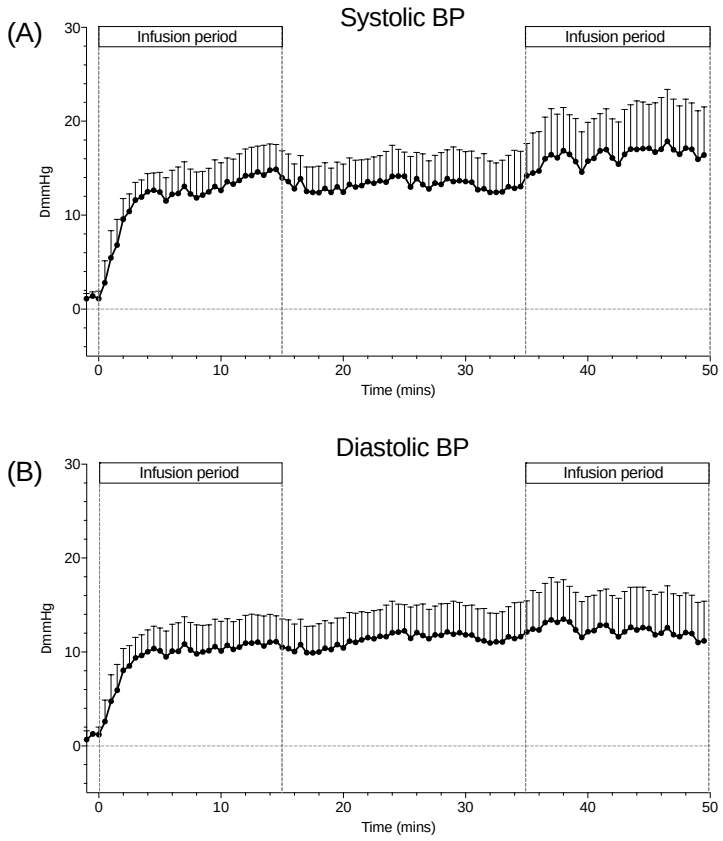

Figure 3.9 A second infusion of AZ'5538 has a blunted pressure response

C57BL/6JCrl mice were infused with AZ'5538 for 15 minutes with a 20 minute window of no infusion followed by a second 15 minute infusion. Traces show (A) systolic and (B) diastolic blood pressure. All data are mean±SEM from baseline, n=6.

Renal blood flow (RBF) was measured in two different groups of mice by two different methods. First, by direct Doppler ultrasound with a probe around the right renal artery. Baseline RBF was 0.60±0.11 mL/min which was significantly decreased with AZ'5538 infusion by ~50% (Figure 3.10(A), plateau of -0.33±0.12 mL/min; ANOVA drug treatment P=0.027; time and interaction P<0.0001). Renal vascular resistance (RVR) was calculated by normalising to mean arterial blood pressure and this was significantly increased (Figure 3.10(B), ANOVA drug treatment P=0.019; time and interaction P<0.0001).

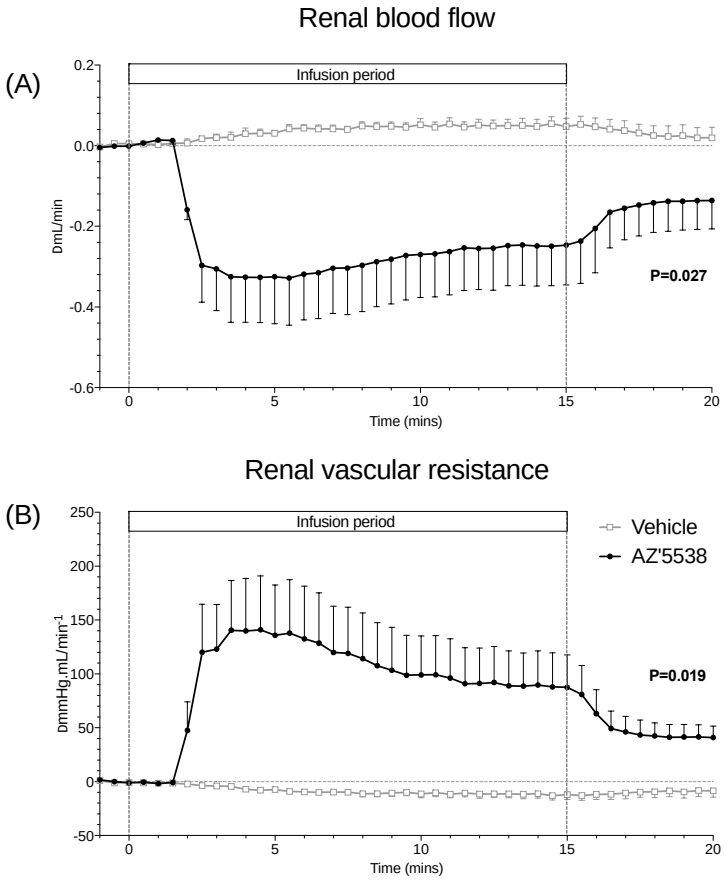

Figure 3.10 Renal blood flow is decreased with AZ'5538 infusion measured by Doppler flow probe

C57BL/6JCrl mice were infused with 5% mannitol vehicle followed by AZ'5538. (A) change in renal blood flow measured by Doppler ultrasound flow probe around the right renal artery. (B) Renal vascular resistance calculated by normalising to blood pressure. All data are mean±SEM from baseline, n=4 and analysed by two-way ANOVA where the P value given is that of the drug treatment.

Renal blood pressure was also measured by pulse-wave Doppler ultrasound. Baseline velocity was 275.2±10.4 mm/sec which was decreased by ~30% (Figure 3.11, peak decrease of -181.8±12.8 mm/sec; ANOVA drug treatment P=0.0002, time and interaction P<0.0001).

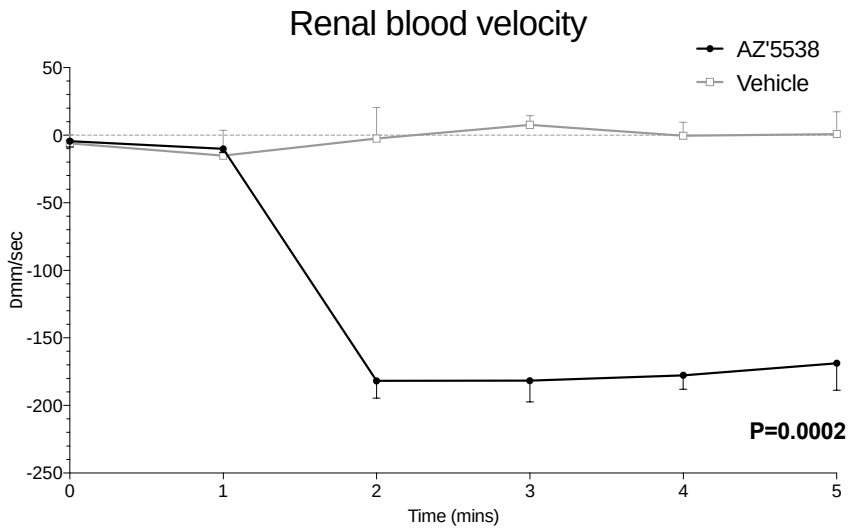

Figure 3.11 Renal blood flow is decreased with AZ'5538 infusion measured by pulse-wave Doppler ultrasound

C57BL/6JCrl mice were infused with 5% mannitol vehicle followed by AZ'5538. Pulse-wave Doppler ultrasound used to measure change in right renal artery blood velocity Data are mean±SEM from baseline, n=4 and analysed by two-way ANOVA where the P value given is that of the drug treatment.

Mice were infused with a solution containing FITC-inulin, permitting the calculation of GFR by inulin clearance. After a baseline urine collection, mice were infused either with AZ'5538 or vehicle and data are presented as the net change (delta or Δ) from baseline values. Urine flow rate was significantly affected by AZ'5538: the Δ value was significantly different from zero in the drug treated group but not vehicle (Figure 3.12(B)). Baseline GFR was lower in the vehicle treated group (Figure 3.12(C), vehicle=119.0±7.7 µL/min AZ'5538=148.4±18.1 µL/min). Vehicle infusion had no effect on GFR; in contrast AZ'5538 reduced GFR and the Δ was significantly different from zero. (Figure 3.12(D)).

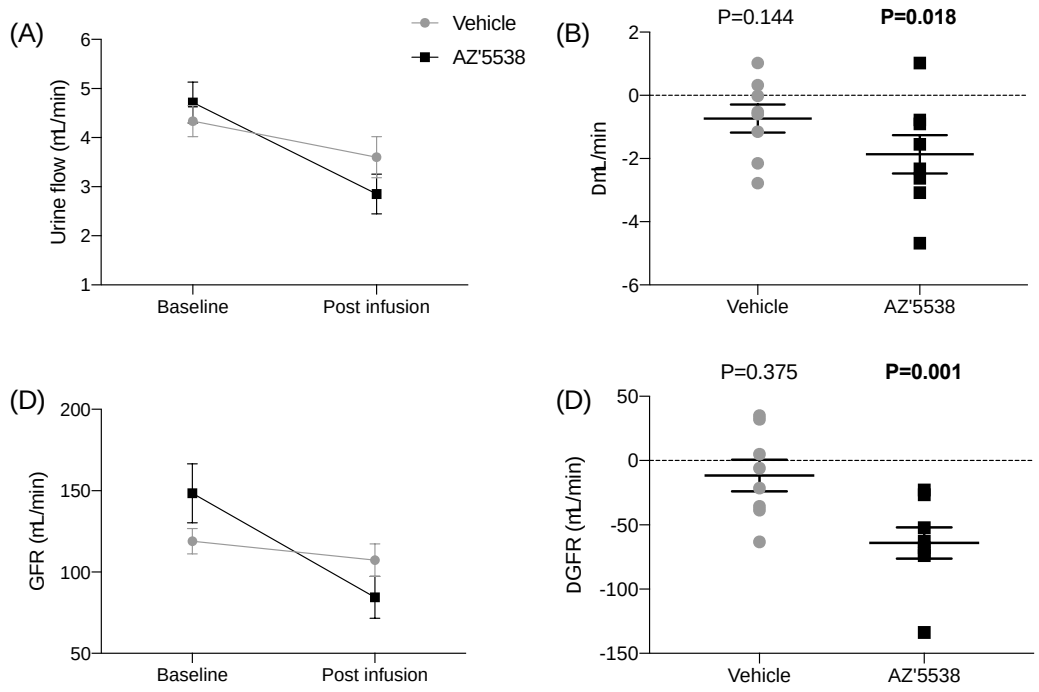

Figure 3.12 Kidney function is decreased with AZ'5538 infusion

Mice were infused continuously with 0.25% FITC-inulin with either 5% mannitol vehicle or AZ'5538 at. Urine was collected to measure (A) flow rate and (B) changes in urine flow (C) GFR and (D) the change in GFR from baseline for vehicle or AZ'5538. (B) and (D) analysed by one sample t and Wilcoxon test to assess if changes were different from 0. All data are mean±SEM from baseline, n=8.

AZ'5538 did not change fractional sodium chloride and plasma concentrations of Na and Cl were not different between groups (Figure 3.13(A-D)). Plasma potassium was significantly higher in mice receiving AZ'5538 but it is not certain whether this was an effect of the drug since plasma K was measured only in a large, final blood sample and was not able to be measured accurately in the urine samples (Figure 3.13(E)).

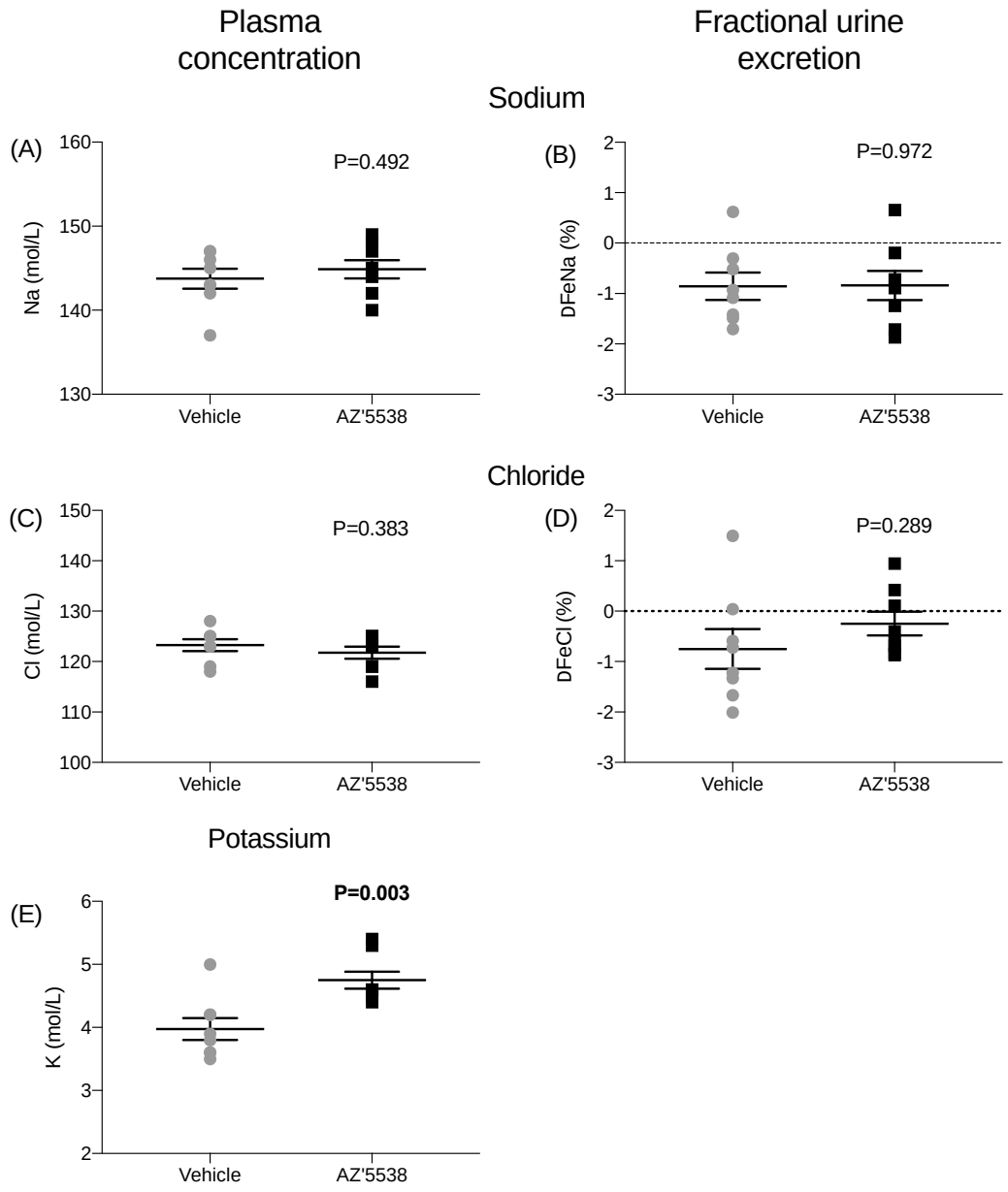

Figure 3.13 Changes in plasma and urine electrolyte concentration with AZ'5538 infusion

C57BL/6JCrl mice were infused with either 5% mannitol vehicle or 1 µmol/kg/min AZ'5538. Terminal plasma was analysed for (A) sodium, (C) chloride and (E) potassium concentration. Urine was collected pre and post infusion and the change in fractional (B) sodium and (D) chloride excretion measured by normalising to GFR. All data are mean±SEM from baseline, n=8 and analysed by unpaired t-test.

3.2.3 Cardiorenal effects of AZ'5538 and GPR81 specificity

At baseline, under terminal anaesthesia, there were no differences between male *Gpr81*$^{-/-}$ mice and WT littermates in SBP, DBP, HR, RBF (measured by Doppler flow probe) or GFR (Table 3.1).

	Gpr81$^{+/+}$	P=	*Gpr81*$^{-/-}$
SBP (mmHg)	73.3±18.8	0.749	71.0±17.3
DBP (mmHg)	59.7±14.3	0.990	59.6±17.3
HR (bpm)	281±57	0.612	293±48
RBF (mL/min)	0.63±0.40	0.461	0.48±0.18
GFR (µL/min)	270.2±28.4	0.587	289.0±17.9

Table 3.1 *Gpr81*$^{-/-}$ and wildtype littermates show no differences in baseline cardiorenal parameters

Systolic blood pressure (SBP), diastolic blood pressure (DBP), heart rate (HR), renal blood flow (RBF; right kidney) and glomerular filtration rate (GFR; both kidneys) in *Gpr81*$^{+/+}$ and *Gpr81*$^{-/-}$ littermates under terminal anaesthesia. Data are mean±SEM analysed by unpaired t-test. For SBP, DBP and HR n=10. RBF and GFR were measured in separate groups of mice (n=5 for RBF; n=6 for GFR).

In the wildtype mice, infusion of AZ'5538 increased SBP (Figure 3.14 (A), P<0.0001 genotype, time and interaction) and decreased HR (Figure 3.14 (B) ANOVA genotype P=0.025, time P=0.003 and interaction P<0.0001). AZ'5538 was without effect in *Gpr81*$^{-/-}$ mice. Similarly, RBF, measured by Doppler ultrasound probe, decreased significantly with AZ'5538 infusion in WT mice but remained unchanged in *Gpr81*$^{-/-}$ mice (Figure 3.14 (C), ANOVA genotype P=0.008 interaction and time P<0.0001). Renal vascular resistance, calculated from RBF and BP, did not show significant differences between genotypes (Figure 3.14 (D), ANOVA genotype P=0.151, time P=0.022 and interaction P=0.0002). Perfusion in the cortex and medulla of the right kidney was measured using Doppler needle probes. AZ'5538 induced a significant reduction in perfusion of the cortex, but only in WT mice (Figure 3.14 (E), genotype P=0.0003, time and interaction P<0.0001). Medullary flux was also

reduced in the medulla of WT mice but not in the *Gpr81*$^{-/-}$ (Figure 3.14 (F), genotype P=0.070, time and interaction P<0.0001). Overall, the blood pressure and blood flow effects were qualitatively similar between *Gpr81*$^{+/+}$ and C57BL/6JCrl mice although a higher increase in systolic blood pressure was seen in the C57BL/6JCrl mice.

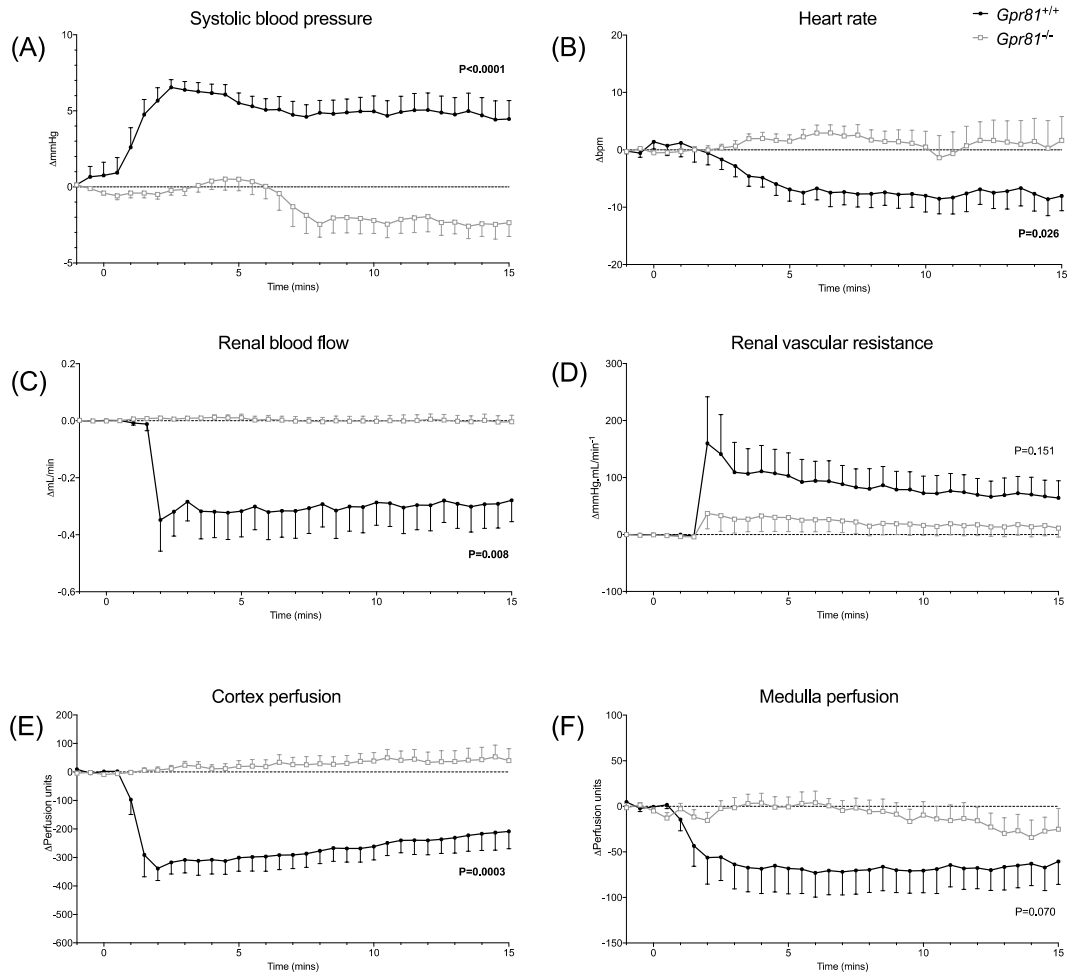

Figure 3.14 Infusion of AZ'5538 into *Gpr81*$^{-/-}$ mice causes no cardiorenal effects

Gpr81$^{-/-}$ mice and WT littermates were anaesthetised and infused with AZ'5538 at 15 µmol/kg. Changes in (A) blood pressure and (B) heart rate were measured via the carotid artery (A and B, n=10). Renal blood flow assessed by Doppler flow probe around the right renal artery and normalised to MABP to calculate renal vascular resistance (C and D, n=5). In other animals, cortex and medulla perfusion was measured by Doppler needle probes (E and F, n=6). All data are mean±SEM from baseline and analysed by two-way ANOVA where the P value given is that of genotype differences.

In a separate experiment, the effect of GPR81 activation on glomerular filtration rate (GFR) was assessed using inulin clearance. Baseline GFR was not different between genotypes (Table 3.1). AZ'5538 caused a significant decrease in GFR from baseline (Figure 3.15(D), ΔGFR = -125.3±48.4 µL/min; P=0.001; n=6) in WT mice. The GPR81 agonist did not significantly change GFR in *Gpr81*$^{-/-}$ animals (Figure 3.15(D), ΔGFR = -39.0±83.2 µL/min; P=0.303; n=6).

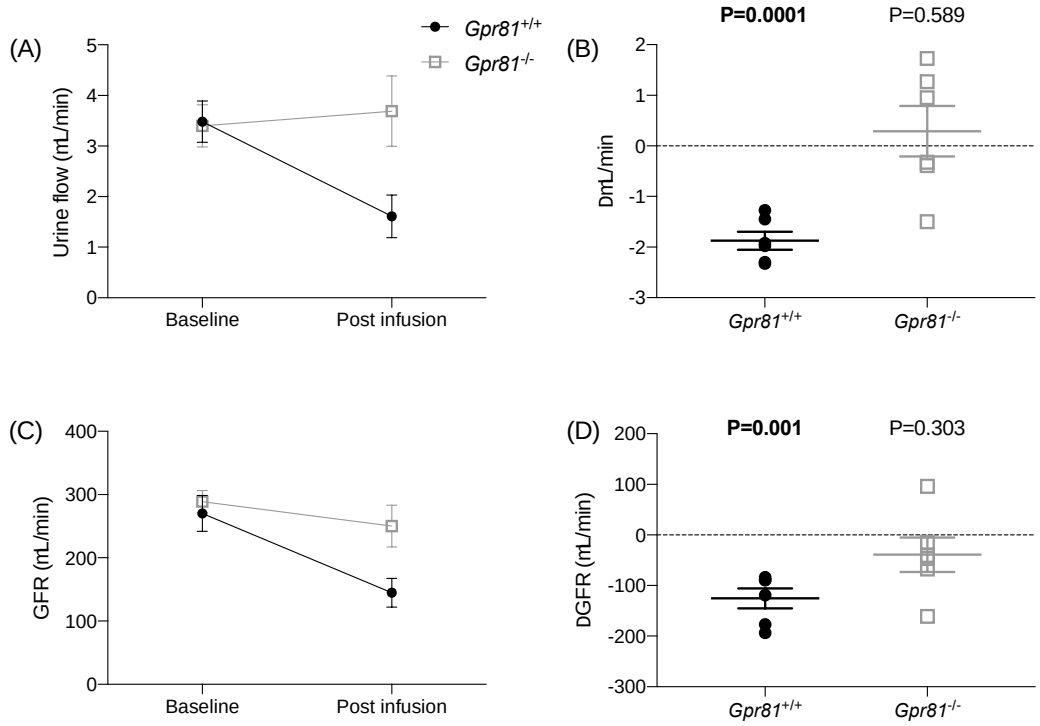

Figure 3.15 Infusion of AZ'5538 into *Gpr81*$^{-/-}$ mice does not alter kidney function

Gpr81$^{-/-}$ mice and WT littermates were infused continuously with 0.25% FITC-inulin and AZ'5538 at 1 µmol/kg/min. Urine was collected to measure; (A) urine flow, (B) changes in urine flow, (C) GFR, and (D) the change in GFR from baseline for vehicle or AZ'5538. (B) and (D) analysed by one sample t and Wilcoxon test to assess if changes were different from 0. All data are mean±SEM from baseline, n=6.

There were no differences seen between *Gpr81*$^{-/-}$ and WT littermates in terminal plasma concentrations of sodium or chloride (Figure 3.16 (A) and (C)). There were also no differences between genotypes for the baseline excretion rate or change in fractional excretion of the same electrolytes (Table 3.2 and Figure 3.16 (B) and (D). There was however a difference in the terminal plasma

concentration of potassium (Figure 3.16 (E)) with higher levels seen in WT animals (WT = 4.58±0.16 mol/L, KO = 3.83±0.19 mol/L, P=0.012). This is the same trend that was seen in C57BL/6JCrl mice between vehicle and AZ'5538 suggesting this is GPR81 specific.

	Gpr81$^{+/+}$	P=	*Gpr81*$^{-/-}$
Sodium (nmol/min)	731±205	0.651	897±290
Chloride (nmol/min)	1122±209	0.657	1286±292

Table 3.2 No difference between the baseline urinary excretion rate of sodium and chloride in *Gpr81*$^{-/-}$ and wildtype littermates

Baseline urinary excretion rate of sodium and chloride corrected to urinary flow rate of *Gpr81*$^{-/-}$ mice and wildtype litter mates. All data are mean±SEM from baseline, n=6 and analysed by unpaired t-test.

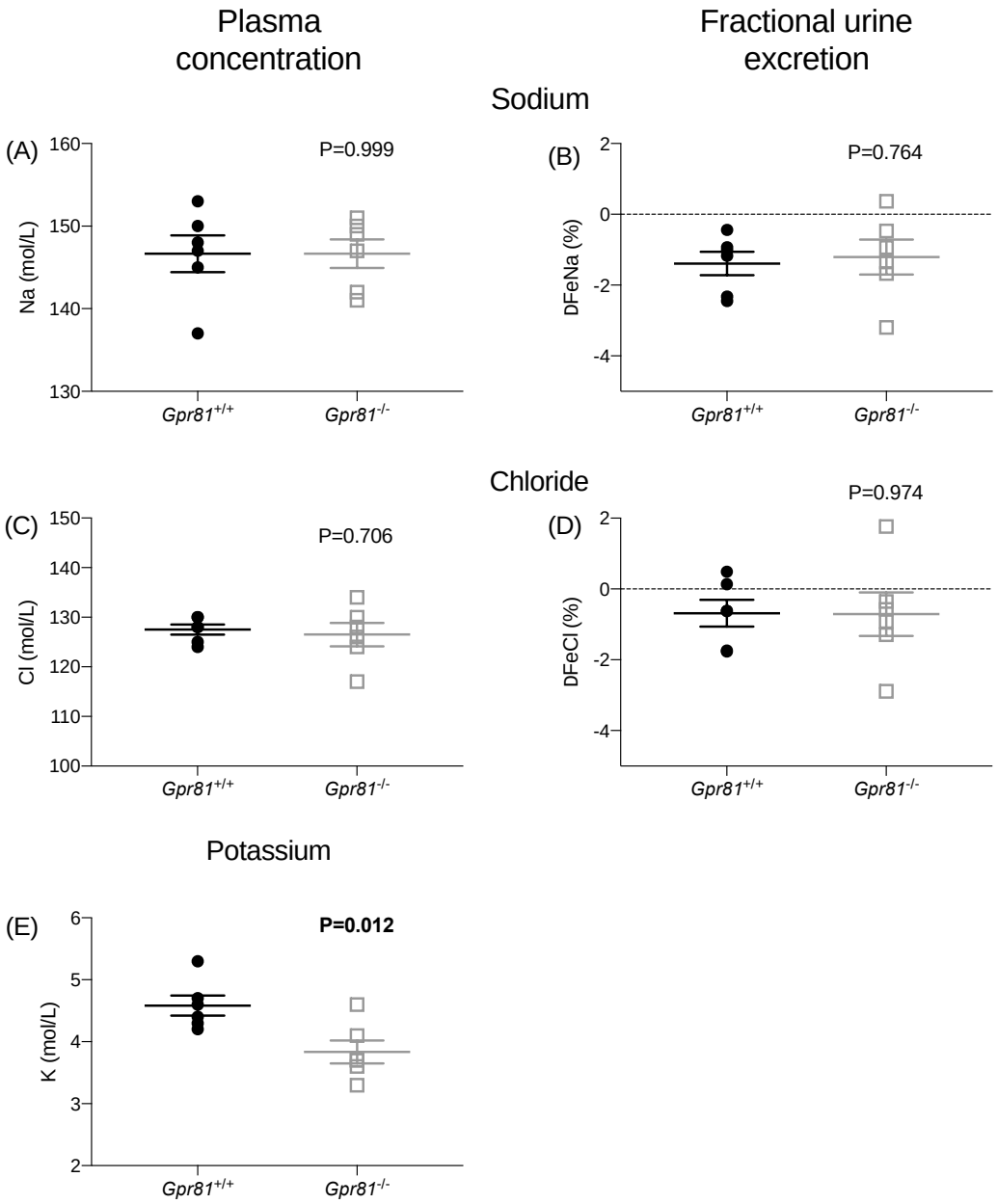

Figure 3.16 Changes in plasma and urine electrolyte concentration with AZ'5538 infusion in *Gpr81-/-* mice

Gpr81-/- mice and WT littermates were infused with 1 µmol/kg/min AZ'5538. Terminal plasma was analysed for (A) sodium, (B) chloride and (C) potassium concentration. Urine was collected pre and post infusion and the change in fractional (D) sodium and (E) chloride excretion measured by normalising to GFR. All data are mean±SEM from baseline, n=6 and analysed by unpaired t-test.

3.3 Discussion

In this chapter, the renal and vascular expression were assessed along with the *in vivo* activation of GPR81. Expression of *Gpr81* mRNA was found in whole arteries of wildtype mice and further identified in vascular smooth muscle cells of the aorta and renal arteries, along with the glomeruli and vessels of the kidney cortex and throughout the medulla. Infusion of the GPR81 specific agonist AZ'5538 into wildtype mice caused a rapid increase in BP, decreased HR, RBF and GFR. Utilising the *Gpr81*$^{-/-}$ mouse, the specificity of the acute *in vivo* cardiorenal effect of AZ'5538 infusion was confirmed along with a *Gpr81* specific reduction in cortical and medullary perfusion.

3.3.1 Renal and vascular expression of *Gpr81*

Initial studies that found lactate to be the endogenous ligand for GPR81 also presented the range of tissues that the receptor is expressed in. The majority of GPR81 expression is found in adipose tissue, with higher levels in brown than white adipose[30]. *Gpr81* mRNA expression across a range of non-adipose tissue was also reported, with expression in the highly vascularized tissues of heart, skeletal muscle and kidney being ~10% of that in adipocytes[30]. Another study did not detect GPR81 expression in skeletal muscle[42], although expression may be below the detection threshold of the GPR81-RFP reporter used in these mice.

With the knowledge that the GPR81-RFP mouse had low levels of expression[42] and having received anecdotal advice that the GPR81 antibodies had cross-reactivity with other GPCRs of the same family (Kristina Wallenius, personal communication), end point PCR and qPCR were used as a starting point followed by *in situ* hybridisation using the RNAscope system to determine the vascular and renal expression of *Gpr81* mRNA. Housekeepers for qPCR were determined by assessing a panel in each vessel type. 18S and β-actin had the most stable expression in all artery types. Robust *Gpr81* mRNA was detected each of the three arteries examined using both methods of detection. Although not shown here, in my MSc mini project based on GPR81, a positive

control of white adipose and negative control of adipose from a *Gpr81*$^{-/-}$ mouse was used to confirm specificity of the primers and PCR[135]. *In situ* hybridization further localized *Gpr81* to the smooth muscle layer of arteries, consistent with fluorescent-reporter expression in the vessel wall of pial arteries in the mouse brain[42] and with single cell RNA sequencing experiments detecting the receptor in cerebral and lung vascular smooth muscle cells[93]. Within the kidney, *Gpr81* was additionally expressed in glomerular arterioles and within perivascular cells, particularly in the renal medulla. A limitation is that co-localisation has not yet been carried, but others have reported renal afferent arteriole expression in the mouse and dog[65]. In the cerebral microcirculation, GPR81 colocalizes with PDGFRβ expressing cells and in leptomeningeal cells[42], i.e. in cell populations interacting closely with the capillary microcirculation supporting our findings within the vasculature.

3.3.2 AZ'5538 induced GPR81-specific cardiorenal effects

There are many states in which GPR81 would be activated by increased circulating lactate levels including tissue ischemia, cardiac arrest, liver failure, pharmacological agents and of course, hypoxia[80]. The study of GPR81 using endogenous ligand lactate is difficult due to many off target effects, however, the recent development of potent GPR81 agonists to treat dyslipidemia[65,66,136] provide tools with which to probe the cardiovascular physiology of GPR81[65,66,136]. In a recent study, structurally distinct compounds developed by AstraZeneca increased SBP by ~15mmHg in rats and dogs[65], the pressor effect in mice was much less pronounced (~5 mmHg) but data from *Gpr81*$^{-/-}$ mice suggested this was GPR81-mediated. Our studies in mice unequivocally demonstrate that AZ'5538 increases blood pressure dependent on the expression of GRP81. No differences were seen at baseline between *Gpr81*$^{-/-}$ and wildtype littermates however this is problematic to interpret as these mice were under terminal anaesthetic, although previous reports also report no phenotypic differences between genotypes[65]. A surprising finding was that AZ'5538 caused hyperkalaemia in a GPR81-dependent manner. Due to this rapid effect, it is suspected this is redistribution of potassium across cells rather

than a balance problem. It is also unexpected to see that there were no alterations in renal sodium handling, as this would be expected. A decrease in GFR along with RBF would suggest there should also be alterations in sodium excretion however these were not seen here. However, it could be that this response is delayed and therefore not seen due to the short time frame although there is a change in urine flow rate seen in this time frame. I have further shown that GPR81 activation reduces flow through the renal artery, perfusion of the cortex (and, to a lesser extent, the renal medulla) and decreases GFR. Since BP is rising, the data are likely to reflect vasoconstriction at the level of the renal artery and afferent arteriole, causing a change in total peripheral resistance. This is supported by the rapid onset of the blood pressure increase and the decrease in heart rate. It is difficult to unambiguously interpret the regional hemodynamic effects of GPR81 activation but in our experience, regional blood flow effectively autoregulates, at least in the cortex[137]. Given the expression of the receptor in perivascular cells, these data may reflect regulation of capillary flow by GPR81 activation, but this is speculative. Of note, there were not any difference in basal blood pressure or blood flow in *Gpr81*$^{-/-}$ mice identified, supporting the concept that the receptor is functionally quiescent at physiological concentrations of lactate [137].

There are still key pieces of information missing to completely understand the GPR81 mediated *in vivo* effects. Firstly, delivery of AZ'5538 directly to the kidney, through the renal artery would be beneficial. This is a technique currently being worked up but is yet to be fully optimised. This would show us if renal delivery is sufficient to cause vasoconstriction of the renal artery and a decrease in renal blood flow or whether this is a systemic effect as seen with IV delivery via the jugular vein. It is also necessary to rule out a CNS effect of GPR81 activation, particularly as it is known that there is expression in the brain[43]. To confirm the increased blood pressure is not due to increased sympathetic drive, ganglionic blockade using hexamethonium could be infused prior to AZ'5538 and the blood pressure response analysed.

In the studies in this chapter, male adult *Gpr81*$^{-/-}$ and wild type littermates were used. Therefore, a limitation is that both female and heterozygote mice were not examined. In the studies carried out by AstraZeneca, they also only used male mice and rats while the dog studies included both males and females[65]. Although it was not feasible in the time frame of this PhD to analyse both sexes and all three genotypes, it would be very interesting to repeat these experiments with both. I expect there would be a lower response in heterozygote mice to AZ'5538 but whether this would be significantly different is of interest.

3.3.3 Molecular mechanisms of GPR81 activation

The cellular mechanism underpinning GPR81-mediated vasoconstriction is not known. The expression profile of GPR81 which has been discussed in this chapter suggests involvement of lactate/GPR81 in vascular function, similar to that reported for other GPCRs activated by metabolic intermediates. Thus, niacin, which activates GPR109a, reduces the production of reactive oxygen species by arterial endothelial cells[138] and also promotes vasodilation by stimulating prostaglandin production[139]. For lactate/GPR81, however, functional data are limited. Increasing lactate concentration in the brain, either through exercise or by exogenous administration, promotes angiogenesis[42]. This effect is GPR81-dependent since lactate-induced angiogenesis does not occur in knockout mice. Lactate also vasoconstricts rat retinal microvessels[92] but it is not known whether this is GPR81-mediated or relates to other actions of lactate on cell membrane transporters[92]. In a similar way it has been shown that lactate stimulated GPR81 on Müller cells of the mouse retina contributes to new blood vessel formation and GPR81-null mice show reduced vascularisation in the retina[140]. Infusion of very high concentrations of lactate increases blood pressure in rats[89] but this most likely reflects the sympathoexcitation induced by panic, rather than activation of GPR81 in blood vessels [92].

In adipocytes, GPR81 couples to Gi, downregulating cAMP production and protein kinase A signaling[141] and this signalling pathway influences lipolysis inhibition. There is evidence to suggest that activation of Gi pathways have vascular influence, in particular due to the lowering of intracellular cAMP levels. For example, succinate activation of GPR91, which is coupled to G_i, acutely increases blood pressure in rats[142] and has direct effects on arterial contractility[143]. In a similar way, activation of Gi pathways by GPCR kinase 5 (GK5) lowers cAMP in vascular smooth muscle, causing a sustained increase in blood pressure[144]. Activation of A1 receptors by adenosine also constricts the renal afferent arteriole by a Gi-mediated cascade within smooth muscle cells[145], this is of particular interest due to our suggestion of GPR81 expression in the renal arterioles and particularly, in smooth muscle cells of these vessels. Activation of these receptors is also known to cause hyperkalaemia[146], an effect seen with AZ'5538.

Reciprocally, mechanisms which increase cAMP have been shown to promote relaxation of vessels. This has been demonstrated in rat mesenteric[147] and pig interlobar[148] arteries using a range of pharmacological agents to increase intracellular cAMP. In rat mesenteric arteries, it was shown that increased cAMP decreased intracellular calcium concentration in smooth muscle cells which caused the relaxation of vessels[147].

This chapter indicates that GPR81 activation regulates macro- and microvascular perfusion within the kidney. The physiological requirement for such a system is not clear since this would operate to vasoconstrict regions of high anaerobic cellular metabolism. Perhaps it serves to constrain and regulate flow into relatively ischemic areas of the kidney, mitigating against hyperaemic damage. Importantly, renal tissue lactate levels are high in conditions of ischemic injury and other studies have shown the potential benefit of GPR81 antagonism in ischemic brain injury[72] and cancer[73,74,149]. Thus, blockade of the GPR81 system could be therapeutically tractable to prevent vascular damage during ischemic renal injury. Further detail into the

mechanism of action of GPR81-mediated vasoconstriction will aid in the therapeutic potential of the receptor[73,74,149].

3.3.4 Summary of chapter findings

- *Gpr81* mRNA expression was found in whole artery and kidney homogenates
- Specifically, *Gpr81* was localised to the arterioles of the kidney glomeruli, the medulla and the smooth muscle of the aorta and renal arteries
- No expression of *Gpr81* mRNA was found in the *Gpr81*$^{-/-}$ mouse
- AZ'5538 infusion caused a rapid increase in BP, decrease in HR, RBF, capillary perfusion and GFR
- All *in vivo* effects were GPR81 specific as they were not seen in the *Gpr81*$^{-/-}$ mouse

Chapter 4 - Investigating the interaction between GPR81 and the endothelin system

4.1 Introduction

Having demonstrated that the blood pressure and haemodynamic effects of AZ'5538 were GPR81-mediated, the next aim was to understand the mechanisms behind these actions. In 2017, Wallenius *et al.* published data showing that the pressor effect of AZ'5538 (referred to there as AZ2) could be partially prevented by bosentan, a mixed endothelin A and B receptor antagonist[65]. My studies localised GPR81 expression in the vascular smooth muscle, and the rapid increase in BP and reduction in renal blood flow support the concept of peripheral vasoconstriction and an association between GPR81 and ET-1, the most potent endogenous vasoconstrictor[101].

I hypothesised that activation of GPR81 *in vivo* using AZ'5338 would cause activation of the endothelin system and that inhibition of this pathway would prevent the pressor effect of GPR81 activation. In this chapter, I collected tissue and plasma from mice treated with AZ'5538 or vehicle to measure ET-1 protein or mRNA expression of associated genes. I also blocked endothelin receptors, using both mixed and specific antagonists, to assess the impact on the AZ'5538 induced rise in BP.

4.2 Results

4.2.1 Expression of endothelin system components with GPR81 activation

ET-1 concentration was measured in the plasma before and after infusion of AZ'5538 or vehicle and is presented as the change in ET-1 concentration. There was a significant increase in plasma ET-1 (Figure 4.1, Vehicle 0.13±0.10 pg/mL and AZ'5538 0.44±0.10 pg/mL, P=0.045).

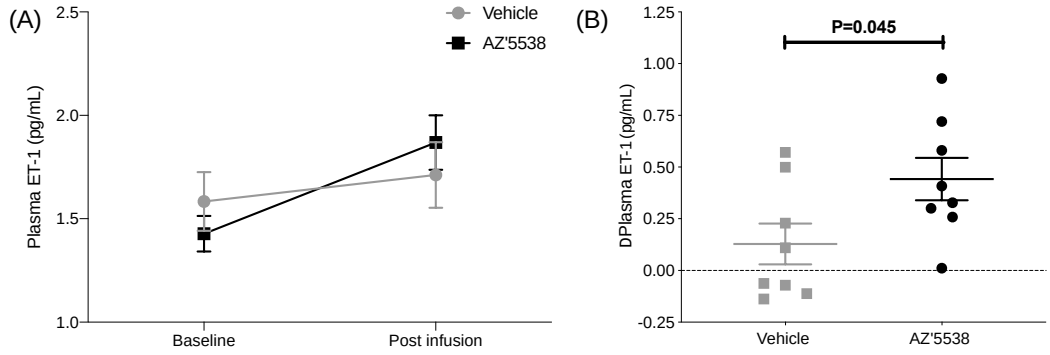

Figure 4.1 Infusion of AZ'5538 increases circulating ET-1

C57BL/6JCrl mice were anaesthetised and infused with either vehicle or 1 µmol/kg/min AZ'5538 for 15 minutes. ET-1 protein was measured by ELISA in plasma samples (A) before and after infusion and (B) change in protein level calculated. Data are mean±SEM analysed by unpaired t-test, n=8.

There were no differences between terminal ET-1 concentrations in kidney and aorta homogenates from mice treated with vehicle or AZ'5538 (Figure 1.2 (A) and (B), respectively).

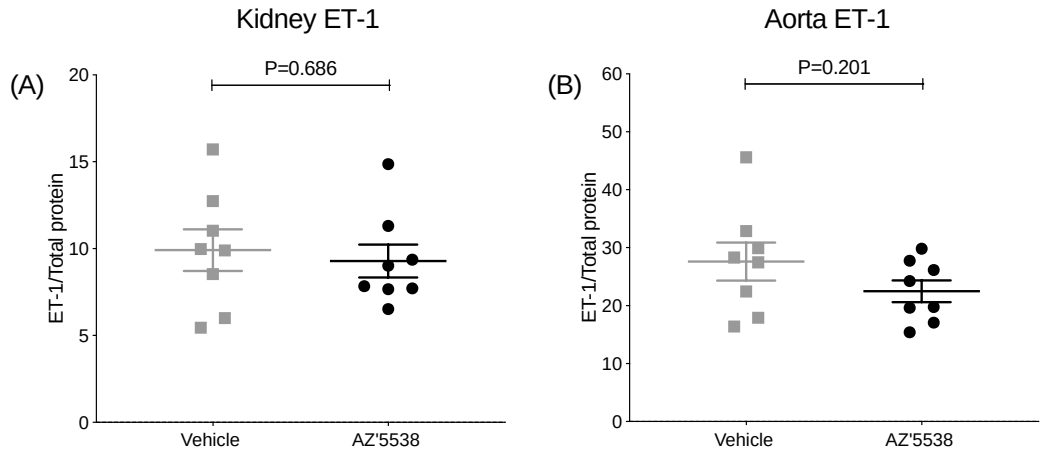

Figure 4.2 Infusion of AZ'5538 does not change ET-1 levels in the tissue

C57BL/6JCrl mice were anaesthetised and infused with either vehicle or 1 µmol/kg/min AZ'5538 for 15 minutes. ET-1 protein was measured by ELISA in (A) whole kidney homogenate and (B) aorta homogenate and normalised to total protein. Data are mean±SEM analysed by unpaired t-test, n=8.

In terms of gene expression, AZ'5538 infusion did not alter expression of GPR81 or ETRA (*Ednra*) in the whole kidney (Figure 1.3 (A) and (C)). However, renal expression of ET-1 (*Edn1*) and ETRB (*Ednrb*) were both lower in mice that had received an infusion of AZ'5538 (Figure 1.3 (B) and (D)).

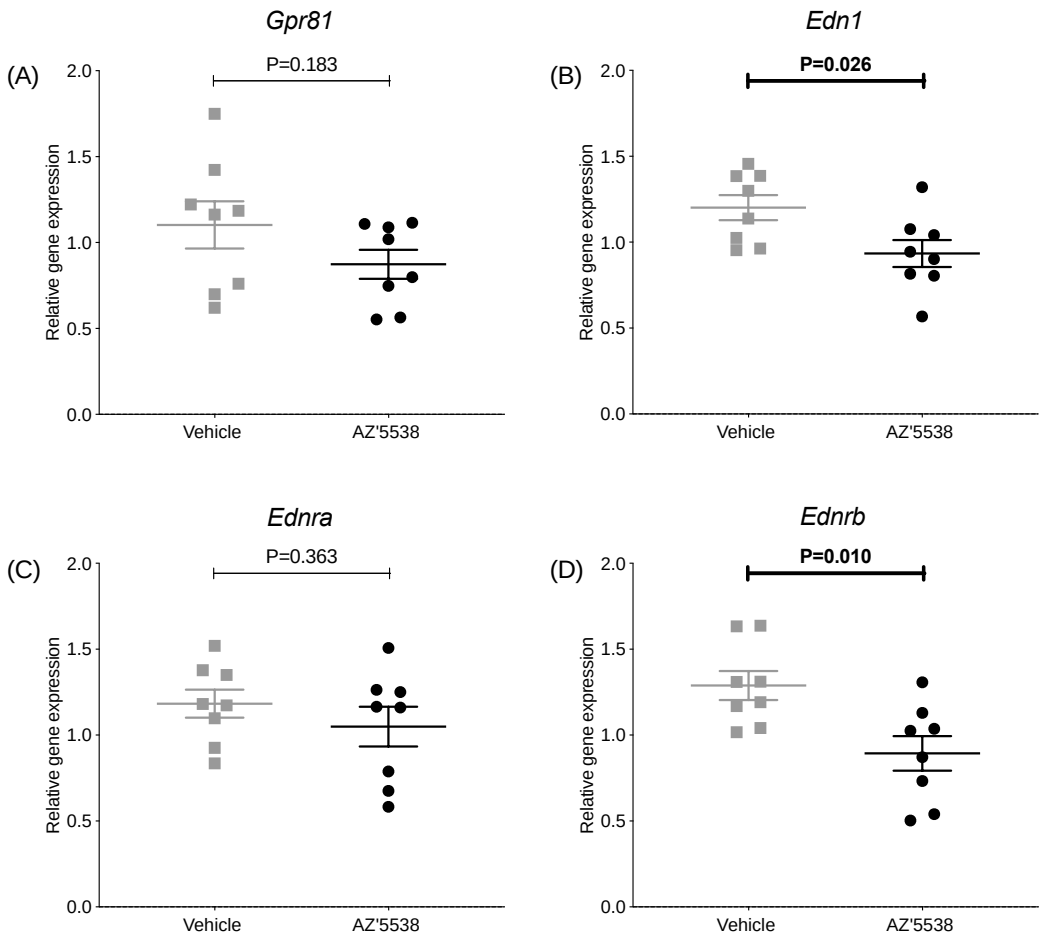

Figure 4.3 Infusion of AZ'5538 alters mRNA expression of the endothelin system

C57BL/6JCrl mice were anaesthetised and infused with either vehicle or 1µmol/kg/min AZ'5538 for 15 minutes. Gene expression was measured by qPCR in whole kidneys for (A) *Gpr81* (GPR81), (B) *Edn1* (ET-1), (C) *Ednra* (ETRA) and (D) *Ednrb* (ETRB) and normalised to housekeeper expression (*Rn18s* and *Tbp*). Data are mean±SEM analysed by unpaired t-test, n=8.

4.2.2 Blockade of endothelin receptors and GPR81 activation *in vivo*

To assess functional cross talk between GPR81 and the endothelin system, C57BL/6JCrl mice were pre-treated with the mixed endothelin receptor antagonist, bosentan prior to infusion of AZ'5538. Bosentan alone at 20 mg/kg or 40 mg/kg had no effect on systolic or diastolic blood pressure compared to vehicle (Figure 4.4).

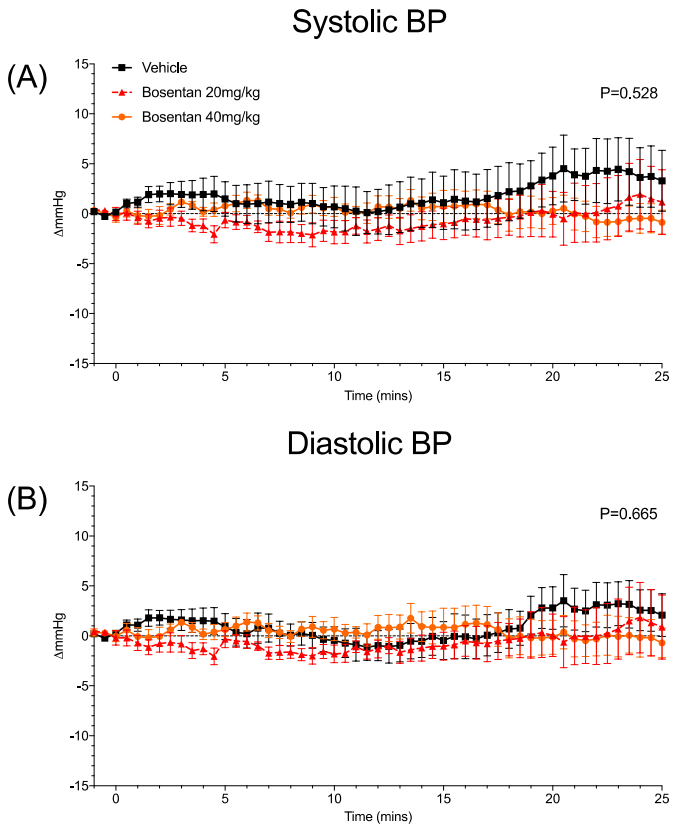

Figure 4.4 Mixed endothelin receptor antagonist Bosentan has no effect on baseline BP

Vehicle and two doses of Bosentan were infused intravenously into C57BL/6JCrl mice over a 25 minute period. (A) Systolic and (B) diastolic blood pressure was recorded during infusion of Bosentan. Data are mean±SEM from baseline and were analysed by two-way ANOVA with the P value given that of the drug treatment, n=5.

Bosentan pre-treatment at either 20 mg/kg or 40 mg/kg partially diminished the pressor effect of AZ'5538 (Figure 4.5, Bosentan treatment P=0.024, time P<0.0001 and interaction P=0.064). Multiple comparisons statistics showed significant differences between vehicle treated mice and Bosentan at the lower dose of 20 mg/kg but not the higher dose for both SBP and DBP (Table 4.1).

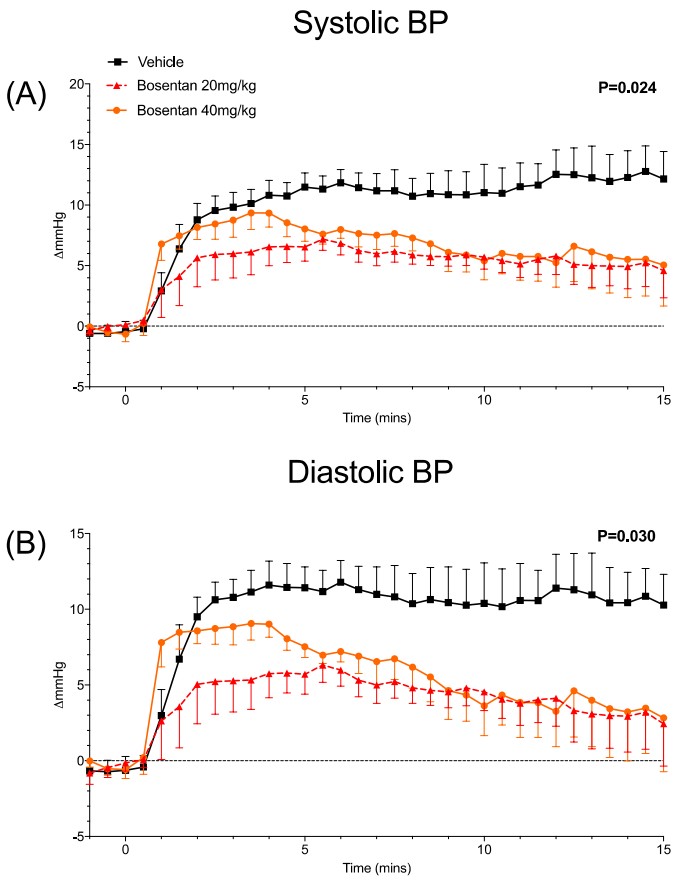

Figure 4.5 Effect of mixed endothelin receptor antagonist Bosentan on GPR81 mediated blood pressure changes

Vehicle and two doses of Bosentan were infused intravenously into C57BL/6JCrl mice over a 25 minute period prior to being infused alongside AZ'5538 for 15 minutes at 1 µmol/kg/min. Bosentan at 20 mg/kg and 40 mg/kg were compared to vehicle. (A) Systolic and (B) diastolic blood pressure were recorded. All data are mean±SEM from baseline, n=5, analysed by two-way ANOVA with Tukey's multiple comparisons test where the P value given is that of antagonist treatment.

		Vehicle vs 20mg/kg	Vehicle vs 40mg/kg
Bosentan	SBP	0.017	0.071
	DBP	0.021	0.081

Table 4.1 Multiple comparison statistics for Bosentan pre-treatment

Data were analysed by two-way ANOVA with Tukey's multiple comparisons test. P values given for the main effect of the bosentan pre-treatment compared to vehicle for both systolic (SBP) and diastolic (DBP) blood pressure. Significant values given in red. n=5.

To resolve this effect further, the experiment was repeated using pre-treatment with either BQ-123, to block the endothelin A receptor (ETRA) or BQ-788, to block the endothelin B receptor (ETRB). BQ-123 or BQ-788 alone, at both doses, did not change baseline BP (Figure 4.6).

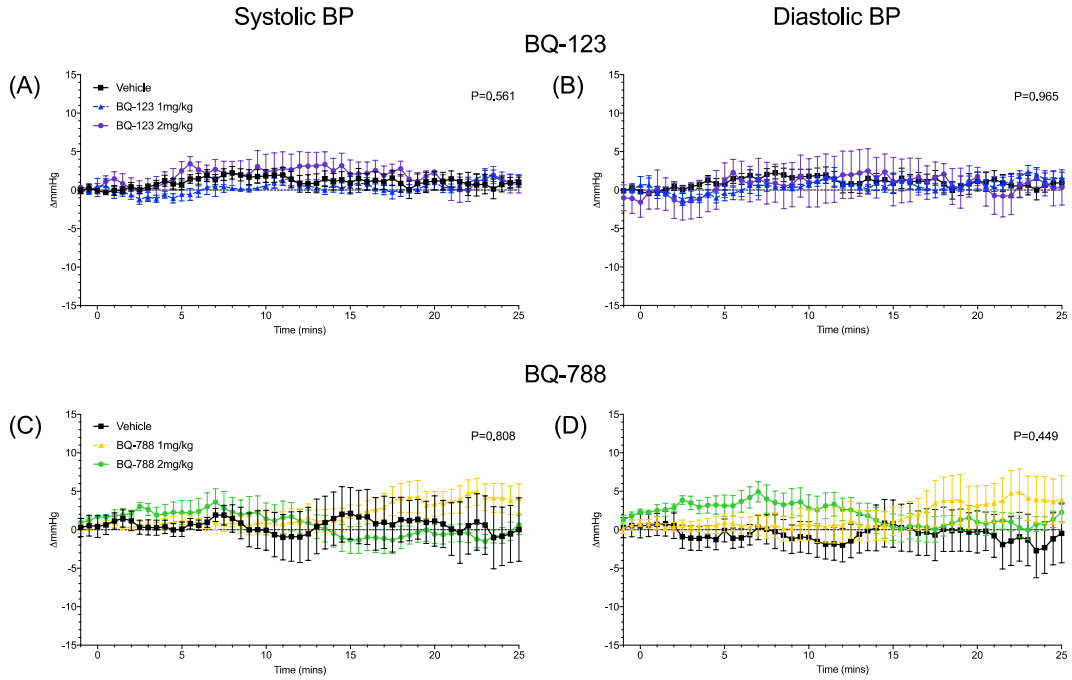

Figure 4.6 Endothelin receptor antagonists BQ-123 and BQ-788 have no effect on baseline BP

Vehicle and two doses of antagonists were infused intravenously into C57Bl/6JCrl mice over a 25 minute period. (A and C) Systolic and (B and D) diastolic blood pressure was recorded during infusion of (A and B) ETRA antagonist BQ-123 and (C and D) ETRB antagonist BQ-788. Data are mean±SEM from baseline and were analysed by two-way ANOVA with the P value given that of the drug treatment, n=4-7.

At 1 mg/kg, BQ-123 did not diminish the pressor response to AZ'5538 but the higher dose of 2 mg/kg of BQ-123 significantly blunted the blood pressure increase (Figure 4.7 (A) and (B), BQ-123 treatment P=0.044, time P<0.0001 and interaction P=0.988). Blockade of ETRB using BQ-7-88a had no effect on the pressor response to AZ'5538, (Figure 4.7 (C) and (D)).

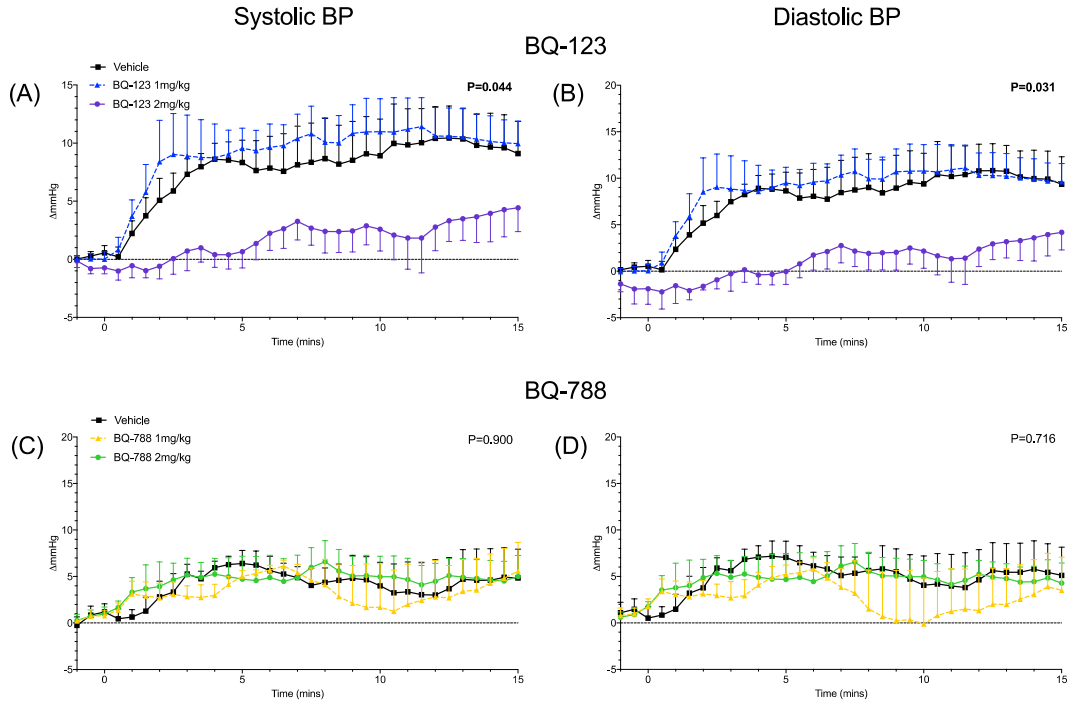

Figure 4.7 Effect of specific endothelin receptor antagonists BQ-123 and BQ-788 on GPR81 mediated blood pressure changes

Vehicle and two doses of (A and B) ETRA antagonist BQ-123 and (C and D) ETRB antagonist BQ-788 were infused intravenously into C57Bl/6JCrl mice over a 25 minute period prior to being infused alongside AZ'5538 for 15 minutes at 1 µmol/kg/min. Antagonists were compared to vehicle. (A and C) Systolic and (B and D) diastolic blood pressure were recorded. All data are mean±SEM from baseline, n=4-7, analysed by two-way ANOVA with Tukey's multiple comparisons test where the P value given is that of antagonist treatment.

Multiple comparison statistics show a difference between vehicle and BQ-123 2 mg/kg in DBP and a trend towards a difference in SBP while no differences were seen between vehicle and BQ-123 at a lower dose or BQ-788 (Table 4.2).

		Vehicle vs 1mg/kg	Vehicle vs 2mg/kg
BQ-123	SBP	0.832	0.064
	DBP	0.922	0.038
BQ-788	SBP	0.944	0.970
	DBP	0.666	0.994

Table 4.2 Two-way ANOVA multiple comparison statistics for specific endothelin receptor antagonist pre-treatment

Data for ETRA specific antagonist BQ-123 and ETRB antagonist BQ-788 were analysed by two-way ANOVA with Tukey's multiple comparisons test. P values given for main effect of BQ-123 or BQ-788 pre-treatment compared to vehicle. Significant values given in red. n=4-7.

4.3 Discussion

4.3.1 GPR81 and ET-1 expression

In this chapter, it was found that activation of GPR81 with AZ'5538 for 15 minutes in mice caused an increase in plasma ET-1 with no change in the tissue protein expression. This suggests release of stored ET-1 into the circulation rather than *de novo* synthesis and processing of pre-pro endothelin due to the short 15 minute time course of the experiments.

Mature ET-1 (as well as the precursor big ET-1) is held in storage granules within endothelial cells, known as Weibel-Palade bodies[150]. These structures release their contents in response to either chemical or mechanical stimulus which cause release of the contents, including ET-1, or degranulation and breakdown of the Weibel-Palade bodies where they fuse with the membrane[102,151]. This is part of the regulated stimulated pathway for ET-1 release[102]. For example a cold pressor test in healthy human forearms increases plasma ET-1 within 2 minutes[152], a time course which is much too fast for production of new ET-1. Mechanical stretch *in vitro* on endothelial cells also showed degranulation of the storage granules and ET-1 release[153]. In terms of signal transduction pathways it has been shown that increasing intracellular calcium concentration or activating protein kinase C in human endothelial cells releases ET-1[154,155] which presents the possibility that unknown pathways may mediate this response, for example GPR81 activation. My data did not confirm this pathway of release but the measurement of a marker of Weibel-Palade bodies, for example P-selectin[102], would, in future studies, help to determine if this is indeed the source of ET-1. If the release of ET-1 is due to degranulation of these structures, then an increase in other components of the granules will also be seen, therefore an increase in both ET-1 and von Willebrand factor would show breakdown of Weibel-Palade bodies[156,157].

In the kidney samples, a decrease in both ET-1 and ETRB gene expression was seen. This could potentially suggest negative feedback into the endothelin

system with an increase in circulating levels. ETRB decreasing could also be to prevent vasodilation caused by this receptor, encouraging activation of ETRA. Nevertheless, the time course of this experiment is 15 minutes, making it unlikely that agonist treatment induced changes in gene expression. It is therefore possible that this is not a true effect of GPR81 activation. It is currently unknown whether GPR81 activation long term alters the transcription of the genes associated with the endothelin system.

There are similarities in the effects seen with ET-1 and AZ'5538 infusion *in vivo* including increased blood pressure and reduced renal blood flow. The role of ET-1 in direct vasoconstriction is well known however studies have shown that exogenous ET-1 in many animal models including dogs, rabbits and rats causes a reduction in renal blood flow and glomerular filtration rate[123–125], similar to the findings here. ET-1 vasoconstricts both afferent and efferent arterioles[158,159], the suggested location of expression of *Gpr81* mRNA in the kidney cortex.

Since GPR81 is a G_i coupled receptor, the receptor exerts it's effects by lowering intracellular levels of cAMP, altering downstream pathways. Importantly, it has been shown that cAMP can influence vasomotor tone indirectly, via the endothelin pathway. An inverse relationship between cellular cAMP and ET-1 production is established[160,161] and agents that inhibit cAMP in vascular smooth muscle augment ET-1 production[162]. These studies in human primary VSMCs showed decreases in both ET-1 peptide and pre-proendothelin mRNA expression in cells treated with agents which increase cAMP concentration (Ro-20-1724, cicaprost and forskolin) over a 24 or 48 hour period[160,161].

Although plausible, the literature doesn't provide any direct evidence connecting lactate (or GPR81) and ET-1, beyond the pharmacological studies of Wallenius *et al.*[65] and those outlined here. However, there are studies which help to explain this indirectly. A study by Barrett-O'Keefe *et al.* performed in 8

adult male humans reported both the concentration of plasma lactate and ET-1 during exercise[163]. While no connection between these variables was made in the paper, I have plotted the data and identified a positive correlation (Figure 4.8). This suggests a system where GPR81 may be the primary sensing system, responding to locally increased extracellular lactate to stimulate ET-1 release and constrain vasodilation during exercise to optimise muscle perfusion while protecting MABP.

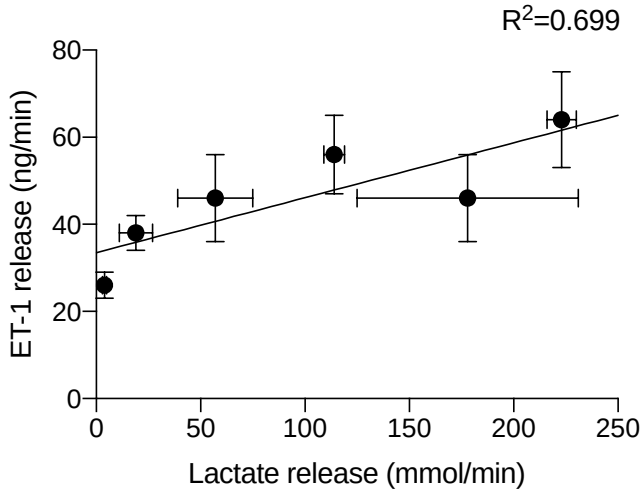

Figure 4.8 Correlation between plasma ET-1 and lactate release during exercise

Graph plotted from data from Barrett-O'Keefe *et al.*[163]. Human subjects underwent increasing levels of exercise (knee extensor paradigm). ET-1 or lactate release was calculated from femoral venous and arterial plasma samples by ELISA and blood gas analysis, respectively. Net release was calculated using the following equation: (venous concentration − arterial concentration) × {leg blood flow × [101 − (haematocrit/100)]}. Data are mean±SEM, n=8, linear regression shown which has a significant correlation, P=0.038.

Similarly, hypoxia, which also increases extracellular and circulating lactate levels, has been associated with ET-1 increases. This has been shown both *in vitro* in bovine endothelial cells[119] as well as *ex vivo*. In rat mesenteric arteries, hypoxia resulted in increased ET-1 release[120]. The same was seen in porcine coronary arteries[121] and it was also suggested that ET-1 counteracts the hypoxia induced vasodilation with local vasoconstriction. They suggest that the hypoxic vasodilation in the coronary system is essential in states of low

oxygen but ET-1 may counteract this to maintain normal blood pressure throughout other organ systems to overall sustain MABP.

4.3.2 Endothelin receptors involvement in GPR81 activation

ET-1 as a ligand is able to exhibit opposing vascular effects depending on the receptor type and localisation of the receptor which it activates (Figure 1.6). Here it was shown that the pressor effect of AZ'5538 was partially prevented using a pre-treatment of a mixed endothelin receptor antagonist Bosentan. A more substantial effect was seen with the lower dose of Bosentan in comparison to the higher. This can be explained by the increased level of ETRB blockade with the higher dose, opposing the ETRA blockade. The AZ'5538 blood pressure increase was fully prevented by pre-treatment with an ETRA antagonist, BQ-123 with no effects of BQ-788 (ETRB antagonist). BQ-788 and the vehicle (2.3/4.6% DMSO) resulted in a smaller increase in BP with AZ'5538 in comparison to AZ'5538 alone or with saline as a vehicle pre-treatment. This may be due to the DMSO component, especially when used at the higher concentration of 4.6%. It was shown that DMSO vehicle alone did not cause a direct effect on BP however it did blunt the response to AZ'5538 compared to saline somewhat. It has been previously shown that DMSO can have effects on blood pressure, a study in dogs showed a transient increase in both systolic and diastolic blood pressure with IV infusion[164] and this is a caveat for the interpretation of my data.[164]. It is, however, clear from the BQ-123 study that the GPR81 effect is ETRA-dependent. This is supported by a study also using BQ-123 but in canine kidneys. It was shown that reductions in renal blood flow and glomerular filtration caused by ET-1 were abolished with ETRA antagonism while a ETRB antagonist had no effect on these parameters[19]. The ETRB antagonist, Sarafotoxin 6c, did increase urine flow and sodium excretion in these animals however this is not an effect seen with GPR81 activation, in fact, I have shown a decrease in urine flow and no change in sodium excretion.

Expression of the two endothelin receptor types are very different and ETRA tends to be localised to where I or others have also found *Gpr81* expression. While ETRA is expressed on smooth muscle cells where they cause a cascade leading to vasoconstriction, ETRB is predominately located on endothelial cells causing vasodilation[101]. The tissue type distribution of ETRA is also different to ETRB and supports the findings presented in this chapter. ETRA is much more highly expressed in cardiovascular tissue, including the vasculature, while ETRB is at higher levels in the brain[165]. Even though at lower levels than ETRB in the brain, ETRA is enriched in pial arteries[166] which is of particular interest as *Gpr81* mRNA expression has been localised here[42]. In the medulla of the kidney, ETRA is located on pericyte cells along the vasa recta which provides the medullary microcirculation and vasoconstriction here has been shown to be ETRA dependant[167]. From the *in situ* hybridisation studies, high levels of expression were also seen here for *Gpr81*.

I propose a mechanism by which increased local concentrations of extracellular lactate activates GPR81 on smooth muscle cells, lowering cAMP and causing activation of ETRA and causing vasoconstriction.

4.3.3 Summary of chapter findings

- Activation of GPR81 with AZ'5538 increases circulating ET-1 but not tissue protein levels.
- The GPR81 pressor response is ETRA mediated and not ETRB.
- A longer study is needed to determine changes in gene expression.

Chapter 5 - GPR81 mediated changes in vascular tone and function by wire myography

5.1 Introduction

In previous chapters I have presented *in vivo* data indicating GPR81-specific effects on blood pressure and renal blood flow. Given the rapidity of onset and the localisation of the receptor in the vascular smooth muscle, I hypothesised that systemic vasoconstriction occurred due to a direct contractile effect of GPR81 activation on smooth muscle of both resistance and conduit arteries through the vasculature. I address this hypothesis in the current chapter, using wire myography to measure vascular contractility in isolated aortae, mesenteric and renal arteries.

Wire myography is a technique that allows the assessment of known vasoactive drugs and compounds with unknown vasoactive roles, such as GPR81 agonist AZ'5538. It also enables the comparison between treatments, genotype and artery types to help understand mechanisms underlying changes in vascular tone.

In this chapter, I aim to use wire myography to, firstly, evaluate the potential vasoactive effects of AZ'5538 on aortae, mesenteric and renal arteries from wildtype mouse arteries by incubating vessels with the drug and carrying out dose response protocols with known vasoactive drugs. Secondly, I will determine if these effects are blocked by ETRA antagonism, as the *in vivo* changes are by prior incubation with BQ-123. Next I will characterise differences between wildtype and *Gpr81*-null mouse vasoreactivity to compounds of known vasoconstrictive or dilatory function (for example phenylephrine, acetylcholine and sodium nitroprusside). And finally, I plan to assess if any vascular changes seen with AZ'5538 treatment *ex vivo* are specific to GPR81 using arteries from the *Gpr81*-null mouse and wildtype littermates.

5.2 Results

5.2.1 GPR81 activation has direct vascular effects ex vivo

The ability of vessels to vasoconstrict in the presence of high potassium before and after incubation with the GPR81 agonist, AZ'5538, was assessed in C57BL/6JCrl mouse aortae and mesenteric arteries (Figure 5.1). A value of 0% shows no change vasoconstrictive ability from the beginning to the end of the experiment. In both aortae and mesenteric arteries at concentrations above 31.3 µM of AZ'5538 the viability of the vessels went below zero, suggesting damage to the vessels from the incubation. Therefore, 30 µM was taken forward as the highest concentration of AZ'5538 which did not affect the reactivity of vessels.

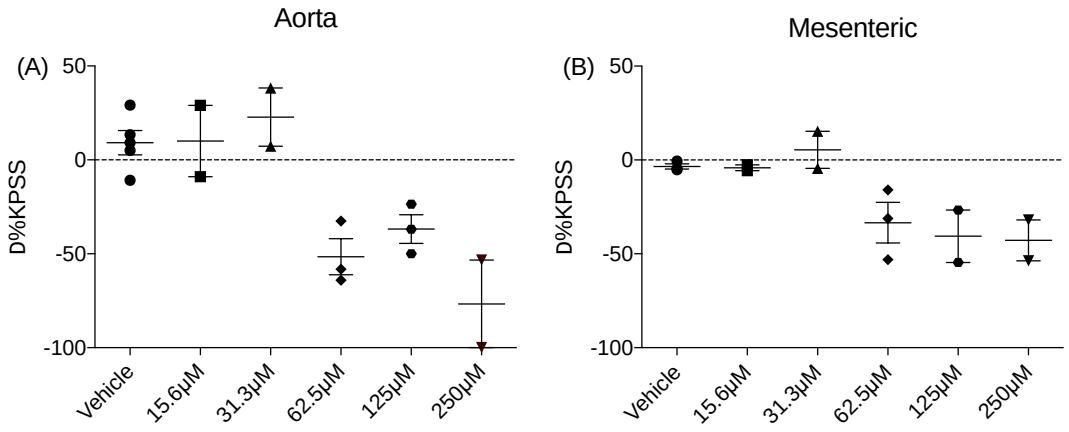

Figure 5.1 Concentration test of AZ'5538 on isolated aortae and mesenteric arteries

Percentage change in (A) aortae and (B) mesenteric arteries response to KPSS (125mM KCl) before and after addition of 5% mannitol vehicle or AZ'5538 to the wire myograph for 15minutes (n=2-5). Data was not analysed for statistical significance due to low n numbers.

Aortae, mesenteric and renal arteries were all selected for wire myography. Incubation of aortae and mesenteric arteries from basal tension with AZ'5538 or vehicle showed no differences (Figure 5.2(A) ANOVA drug treatment P=0.668, time P=0.056 and interaction P=0.917 and (B) drug treatment P=0.268, time P=0.262 and interaction P=0.126, respectively). Renal arteries showed a time-dependent increase in vasoconstriction with AZ'5538 treatment

which plateaued at ~10 minutes (Figure 5.2(C) ANOVA drug treatment P=0.005, time P=0.001 and interaction P<0.0001).

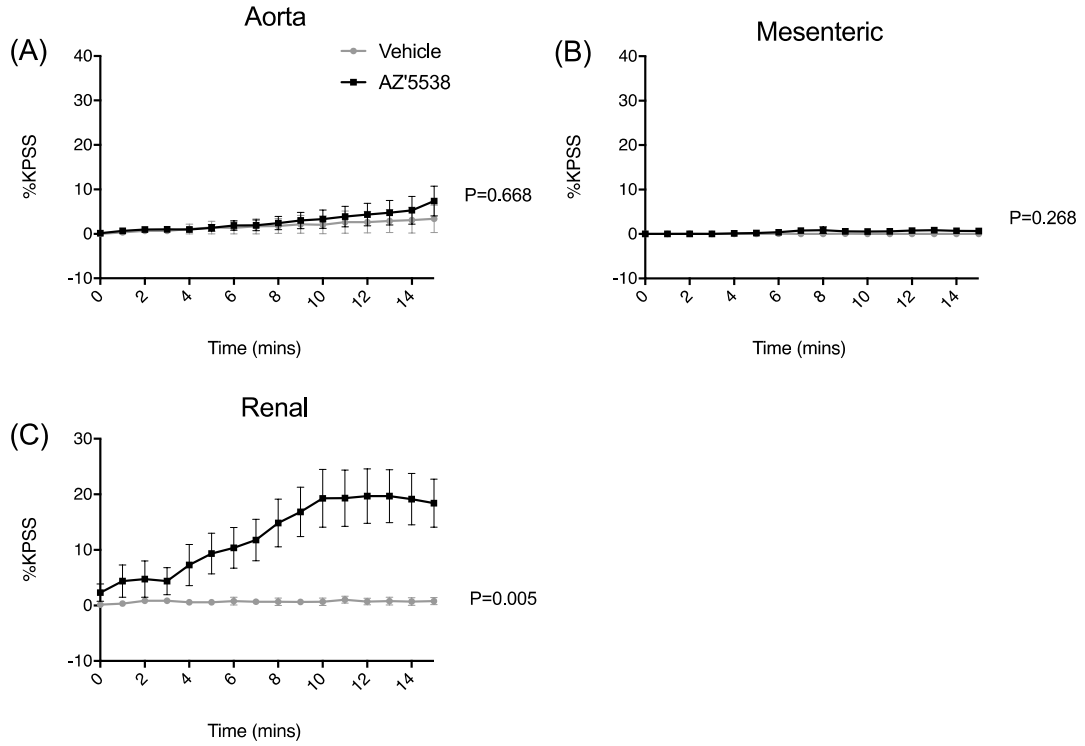

Figure 5.2 AZ'5538 causes vasoconstriction in the renal artery but not aorta or mesenteric arteries

Sections of (A) aortae, (B) mesenteric arteries and (C) renal arteries were incubated for 15 minutes with 30 μM AZ'5538 (black squares) or 5% mannitol vehicle of the same volume (grey circles) (n=8 for all). Data is presented as a percentage of the response to KPSS and was analysed by two-way ANOVA.

All vessels which were subjected to AZ'5538 or vehicle incubation then went through a series of dose response experiments with known vasoconstrictors and dilators. The overall vessel responses to PE were decreased in mesenteric and renal arteries (Figure 5.3(C) and (E)) as well as their maximal response to this drug (Table 5.1) while there were no changes in the aorta (Figure 5.3(A) and Table 5.1). The endothelium-dependent vasodilator ACH was attenuated with AZ'5538 treatment with ANOVA drug treatment statistics being significant for all vessel types (Figure 5.4(A), (C) and (E)). The IC_{50} was also decreased for all vessel types (Table 5.1 Changes in vascular reactivity in vessels treated with AZ'5538). The aorta showed no change in maximal

response, mesenteric arteries showed a decreased maximal response while renal arteries showed an increase (Table 5.1). There were no differences in responses to SNP (an endothelium-independent nitric oxide donor) for any of the vessel types (Figure 5.4(B), (D) and (F) and Table 5.1). With the range of ET-1 concentrations used it was not possible to fit a full non-linear regression and therefore EC_{50} and E_{max} values could not be calculated or analysed. There were no differences between two-way ANOVA results from ET-1 on any vessel type (Figure 5.3(B), (D) and (F)).

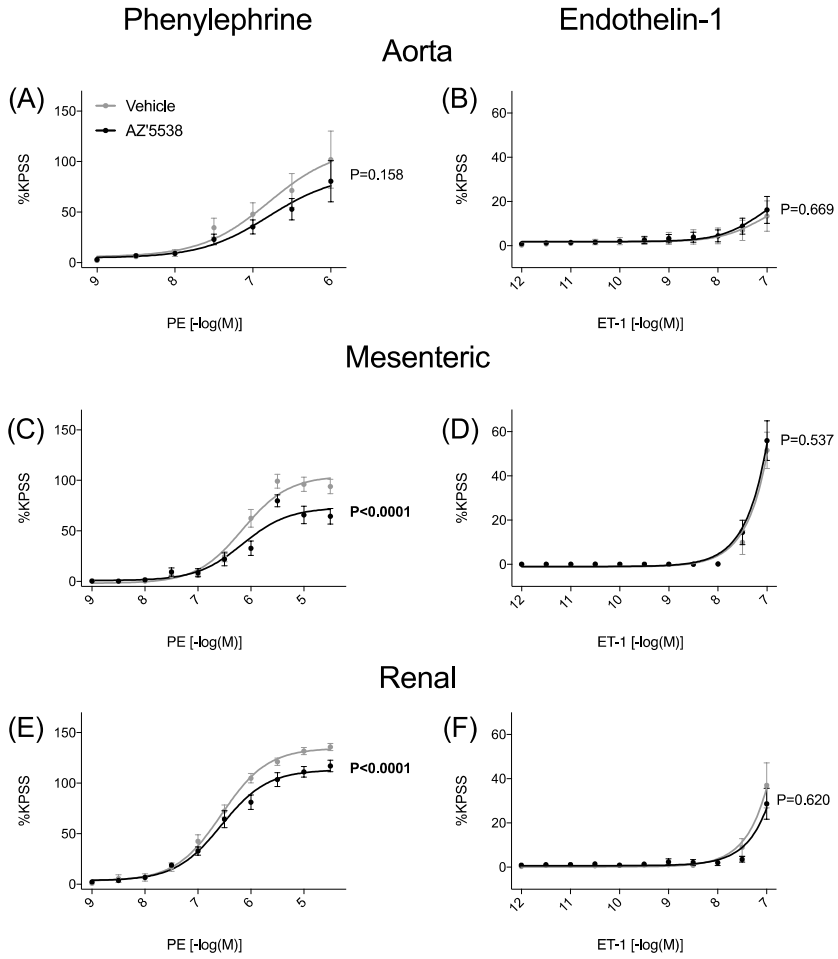

Figure 5.3 AZ'5538 alters vascular response to vasoconstrictors *ex vivo*

Aorta (A and B), second order mesenteric arteries (C and D) and renal arteries (E and F) were incubated with vehicle (grey circles) or 30 μM AZ'5538 (black squares) before being subjected to increasing concentrations of vasoconstrictors PE (A, C, E), and ET-1 (B, D, F) (n=8 for all). Data shown as a percentage force of the maximum response to KPSS. All curves shown as non-linear regression and analysed by two-way ANOVA where the P value given is the effect of AZ'5538 versus vehicle.

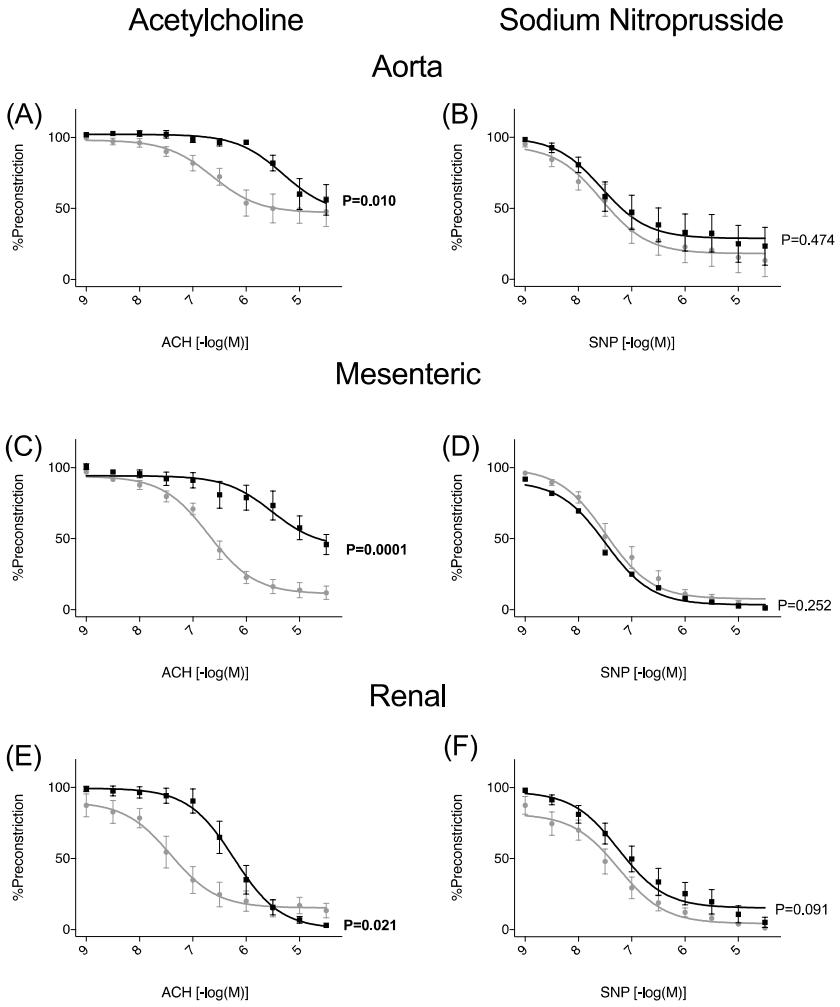

Figure 5.4 AZ'5538 alters vascular response to vasodilators *ex vivo*

Aorta (A and B), second order mesenteric arteries (C and D) and renal arteries (E and F) were incubated with vehicle (grey circles) or 30 μM AZ'5538 (black squares) before being subjected to increasing concentrations of ACH (A, C, E) and SNP (B, D, F) (n=8 for all). Data shown as a percentage to their individual vasoconstriction to half maximal with PE prior to dose response. All curves shown as non-linear regression and analysed by two-way ANOVA where the P value given is the effect of AZ'5538 versus vehicle.

			-LogEC$_{50}$/IC$_{50}$	SD	P value	%E$_{max}$/I$_{max}$	SD	P value
Aorta	PE	Vehicle	6.87	0.30	0.696	110.30	19.89	0.627
		AZ'5538	6.67	0.28		93.63	17.84	
	ACH	Vehicle	6.63	0.21	<0.0001	47.04	4.17	0.935
		AZ'5538	5.31	0.21		46.26	8.18	
	SNP	Vehicle	7.57	0.21	0.996	18.15	4.36	0.112
		AZ'5538	7.57	0.25		28.84	4.88	
Mesenteric	PE	Vehicle	6.17	0.08	0.854	104.30	4.06	<0.0001
		AZ'5538	6.14	0.14		73.47	4.59	
	ACH	Vehicle	6.70	0.08	0.001	11.15	2.54	0.013
		AZ'5538	5.52	0.27		44.06	8.16	
	SNP	Vehicle	7.38	0.09	0.100	6.21	2.30	0.648
		AZ'5538	7.61	0.10		4.70	2.30	
Renal	PE	Vehicle	6.57	0.05	0.657	134.30	2.67	<0.0001
		AZ'5538	6.53	0.07		113.90	3.24	
	ACH	Vehicle	7.41	0.17	<0.0001	15.28	3.72	0.014
		AZ'5538	6.23	0.10		0.54	4.55	
	SNP	Vehicle	7.40	2.85	0.141	5.91	4.54	0.123
		AZ'5538	7.09	3.62		13.26	4.58	

Table 5.1 Changes in vascular reactivity in vessels treated with AZ'5538

EC/IC$_{50}$ is expressed as -log[Molar conc] and E/I$_{max}$ as a percentage of the KPSS response for each drug (n=8 for all). Statistically significant (P<0.05) values are given in red. Statistics calculated from non-linear regressions formed using an extra sun-of-square F test.

To confirm that the dose of AZ'5538 followed by four drug dose response experiments did not affect vessel viability, the percentage change in KPSS response was analysed and no differences were seen between AZ'5538 and vehicle in any vessel (Figure 5.5).

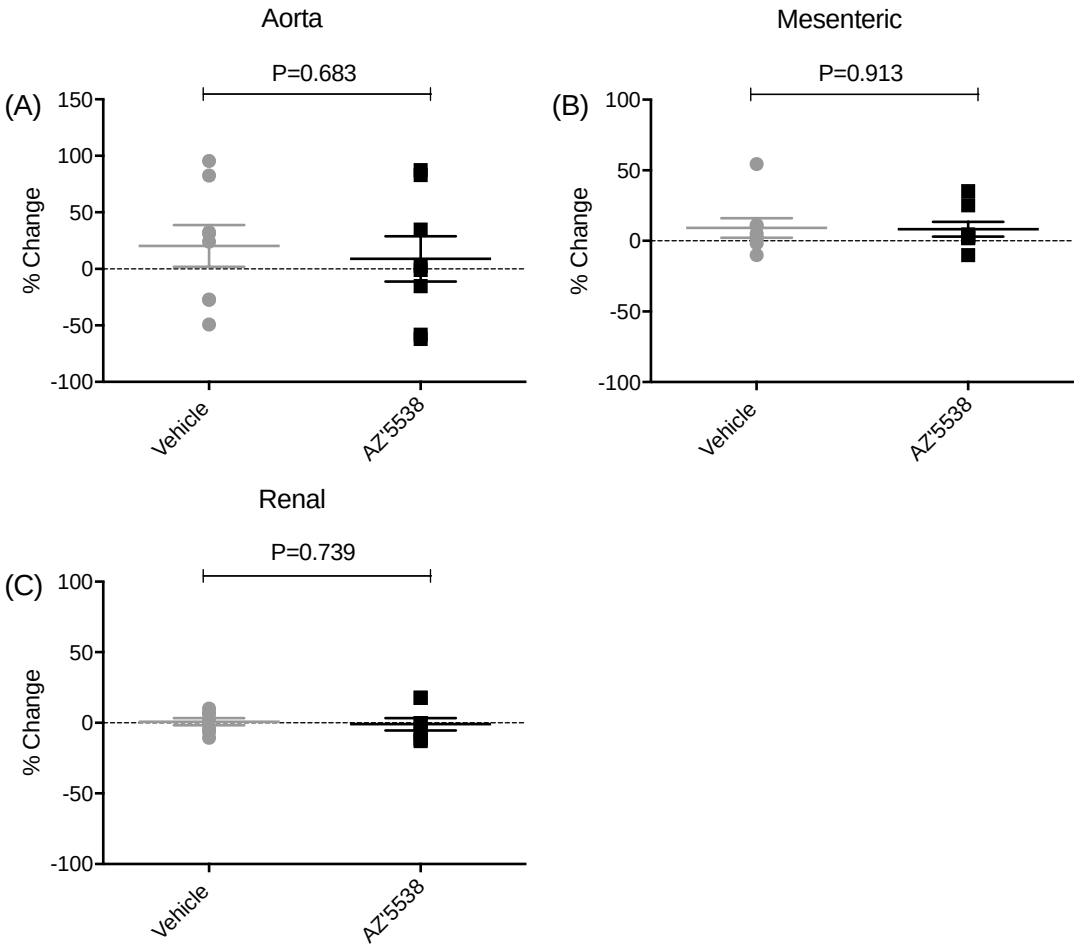

Figure 5.5 AZ'5538 does not alter the ability of vessels to vasoconstrict by KCl depolarisation

(A) Aortae, (B) mesenteric arteries and (C) renal arteries were depolarised with 125 mM KCl at the beginning and end of the experiment to determine viability of the vessels where vehicle treated (grey circles) and AZ'5538 treated (black squares) were compared (n=8 for all). Data was analysed by t-test.

Preconstriction of vessels can alter their response to vasoactive compounds. An example of this ANG II where preconstriction of some vessels is required to elicit a vasoconstrictive response[168], as shown in Figure 5.6. For this reason, all three vessel types underwent dose-response protocols with increasing

doses of AZ'5538 from basal tension in normal PSS or with an increased potassium concentration (Figure 5.7). As with a single incubation of the drug, aortae showed no difference in vasoactivity from basal (Figure 5.7(A) ANOVA preconstriction P=0.453, [AZ'5538] P=0.232, interaction P=0.170). At basal conditions there was no effect of AZ'5538 on mesenteric vessels however with preconstriction there was a dose-dependent decrease in tension (Figure 5.7(B) preconstriction P=0.272, [AZ'5538] P=0.033, interaction P<0.0001). For renal arteries there is a dose-dependent increase in vasoconstriction at basal tone (Figure 5.7(C)). Conversely, preconstriction of renal arteries changed AZ'5538 from being vasoconstrictive to vasodilatory (ANOVA preconstriction P=0.007, [AZ'5538] P=0.387 and interaction P<0.0001). Although these are opposing effects on the vessel, they start to alter tone at the same point (around 3µM).

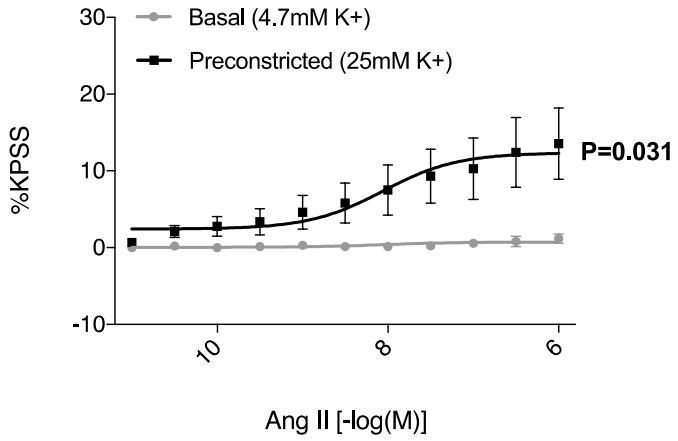

Figure 5.6 Vasoconstriction of aortae with and without prior preconstriction with KCl

Aortae (n=8 per group) were incubated with normal PSS (4.7 mM K_+, grey circles) or a higher potassium salt solution (25 mM K_+, black squares). Vessels were then subjected to increasing doses of ANG II. Data shown as non-linear regression curves as a percentage to maximum KPSS response and was analysed by two-way ANOVA with the statistical significance given on the figure as the difference between the two potassium treatment groups.

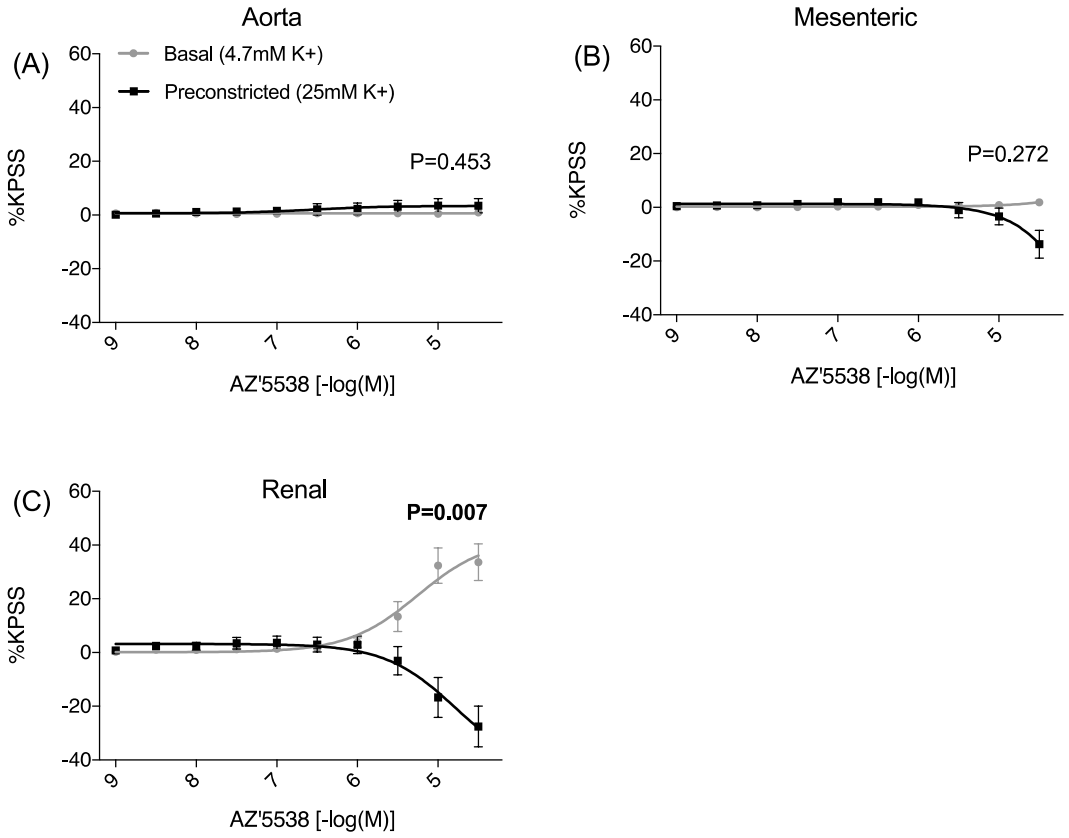

Figure 5.7 Preconstriction of vessels with KCl alters AZ'5538 mediated vasoconstriction

(A) Aortae, (B) mesenteric arteries and (C) renal arteries were incubated in normal PSS (4.7 mM K_+, grey circles) or increased KCl PSS (25 mM K_+, black squares) (n=8 for aorta and mesenteric, n=7 for renal arteries) prior to increasing doses of AZ'5538. Data is shown as non-linear regression curves and was analysed by two-way ANOVA with the statistics given between KCl concentration groups.

5.2.2 Blockade of ETRA does not prevent GPR81 mediated vasoconstriction

With the aim to inhibit the vasoconstriction caused by AZ'5538 on renal arteries, a range of concentrations of BQ-123 were analysed *ex vivo* in the wire myography set up. None of the doses of BQ-123 had any effect on basal vascular tone of renal arteries with no change in tone larger than 2% of KPSS response (Figure 5.8(A)). There was a significant difference in the different drug doses by two-way ANOVA (BQ-123 doses P=0.050, time P=0.125, interaction P=0.737) however this is probably due to the small differences seen between doses. No significant differences were seen in the viability of the

vessels before and after BQ-123 treatment (Figure 5.8(B)) however there was a slight decrease as the doses increased (mean vehicle 0.03%, BQ-123 1 µM -3.96%, 3 µM -5.12%, and 10 µM -9.15%). All doses were able to inhibit the vasoconstrictive response of ET-1 on renal arteries (two-way ANOVA comparison at 300 µM ET-1 between vehicle and 1 µM BQ-123 P=0.0002, 3 µm BQ-123 P=0.0003, and 10 µM BQ-123 P<0.0001). The lowest dose of BQ-123 (1 µM) was taken forward due to this having the smallest effect on KPSS response.

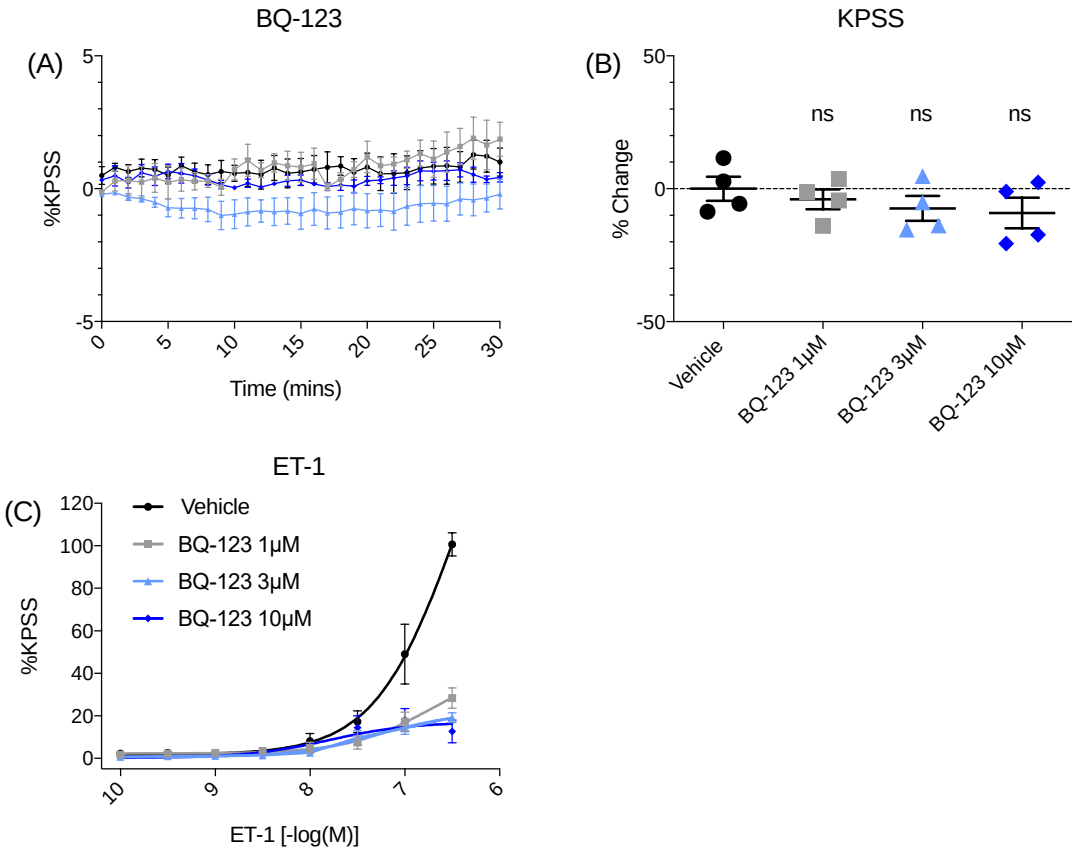

Figure 5.8 Ex vivo blockade of ETRA using BQ-123

Renal arteries of C57BL/6JCrl mice treated with vehicle or BQ-123 at varying concentrations for 30 minutes (n=4 for all groups). (A) response of vessels to BQ-123 incubation given as a percentage of response to KPSS. (B) percentage change of vessel vasoconstriction with KPSS before and after BQ-123 treatment compared using one-way ANOVA with each BQ-123 concentration compared to vehicle. (C) renal arteries treated with increasing concentrations of ET-1 after BQ-123 incubation. Compared using two-way ANOVA with multiple comparisons where each dose of ET-1 saw vehicle compared to all doses of BQ-123. Data presented as a percentage of response to KPSS.

Renal arteries were incubated with BQ-123 or vehicle before the addition of AZ'5538 or vehicle to determine if this could inhibit the vasoconstrictive response. All vessels treated with AZ'5538 showed a time-dependant increase in vasoconstriction which plateaued at around 10 minutes (Figure 5.9, P<0.0001 for both groups), as seen in Figure 5.2(C).The group treated with BQ-123 prior to AZ'5538 showed an attenuated response to the drug (P=0.017) but did still cause vasoconstriction in comparison to vehicle alone.

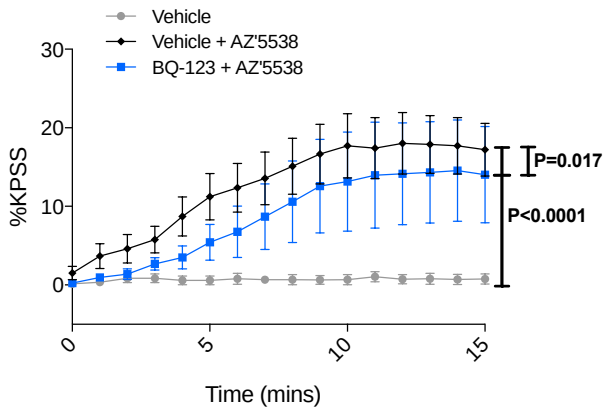

Figure 5.9 Blocking ETRA *ex vivo* does not prevent AZ'5538 induced vasoconstriction

Renal arteries incubated with vehicle (grey and black lines) or 1 µM BQ-123 (blue lines) for 30 minutes followed by 30 µM AZ'5538 (black and blue lines, n=15 and 8 respectively) or vehicle (grey lines, n=8) for 15 minutes. Data presented as a percentage of the response to 125 mM KCl and analysed by two-way ANOVA mixed effect analysis with Tukeys multiple comparisons test.

5.2.3 Differences in vascular tone between Gpr81 null and WT mice

Differences between mesenteric and renal arteries from mice lacking GPR81 expression and their WT littermates were assessed to determine the vascular role of GPR81. As anticipated, the force of mesenteric contraction to high potassium was greater than renal arteries (Figure 5.10). No differences were seen between genotypes for either artery type (Figure 5.10(A) WT 5.45±2.31 mN KO 4.72±3.35 mN (B) WT 2.81±1.78 mN KO 2.85±1.56 mN, for mesenteric and renal respectively).

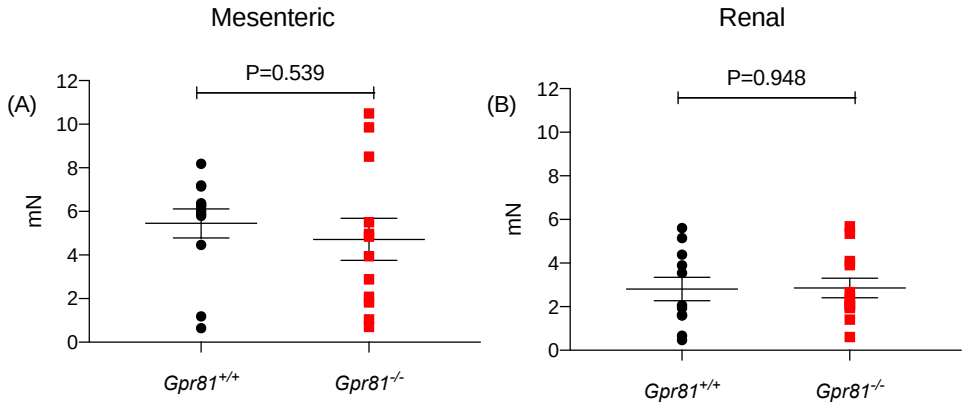

Figure 5.10 *Gpr81*$_{-/-}$ and *Gpr81*$_{+/+}$ mice have no differences in depolarisation response

(A) Mesenteric (n=12) and (B) renal arteries (n=11-12) from *Gpr81* null (red squares) and WT (black circles) show no differences in response to 125 mM KCl containing KPSS. Data analysed by unpaired t-test.

Known vasoactive drugs were analysed to assess any potential differences between genotypes. No differences were seen between *Gpr81*$_{+/+}$ and *Gpr81*$_{-/-}$ mesenteric and renal arteries to vasoconstrictors PE or ET-1 (Figure 5.11(A), (B), (G), (H) and Table 5.2). As previously, a full dose-response curve for ET-1 was not reached therefore non-linear regression data was not possible to calculate. There were also no differences between genotypes in renal arteries treated with SNP (Figure 5.11(F) and Table 5.2) however mesenteric arteries from *Gpr81*$_{-/-}$ showed a leftward shift in the curve, increasing the IC_{50} and suggesting increased potency (Table 5.2, WT IC_{50} 6.76±0.26 -log[M], KO 7.91±0.15 -log[M], P=0.005). For both vessel types, differences were seen in the responses to the endothelium-dependent vasodilator ACH. Renal arteries exhibited a genotype difference in two-way ANOVA statistics (Figure 5.11(D) P=0.046) as well as an increased I_{max} value in the *Gpr81*$_{-/-}$ mice, implying an inability of these vessels to completely vasodilate with this drug (Table 5.2, WT I_{max} 16.61±4.72%, KO 29.98±3.65, P=0.028). Conversely, mesenteric arteries from *Gpr81*$_{-/-}$ mice showed an increased IC_{50} for ACH compared to WT meaning they dilated to a lower concentration of the vasodilator while showing no difference in I_{max} (Table 5.2, WT IC_{50} 7.17±0.16 -log[M], KO 7.73±0.17 -

log[M], P=0.046). Mesenteric arteries from wildtype mice incubated with 30 µM AZ'5538 from basal tone showed no affect (Figure 5.11(I)), consistent with Figure 4.2 (B). These arteries from *Gpr81*$^{-/-}$ showed no difference and no vasoconstriction was seen. Renal arteries also showed no difference between genotypes when treated with AZ'5538 (Figure 5.11(J)). Both renal arteries from wildtype and *Gpr81*$^{-/-}$ mice gradually vasoconstricted over time, plateauing at around 11 minutes and with a maximum contraction of 22.25±16.40% of KPSS response for WT and 22.23±12.78% for *Gpr81* null mice.

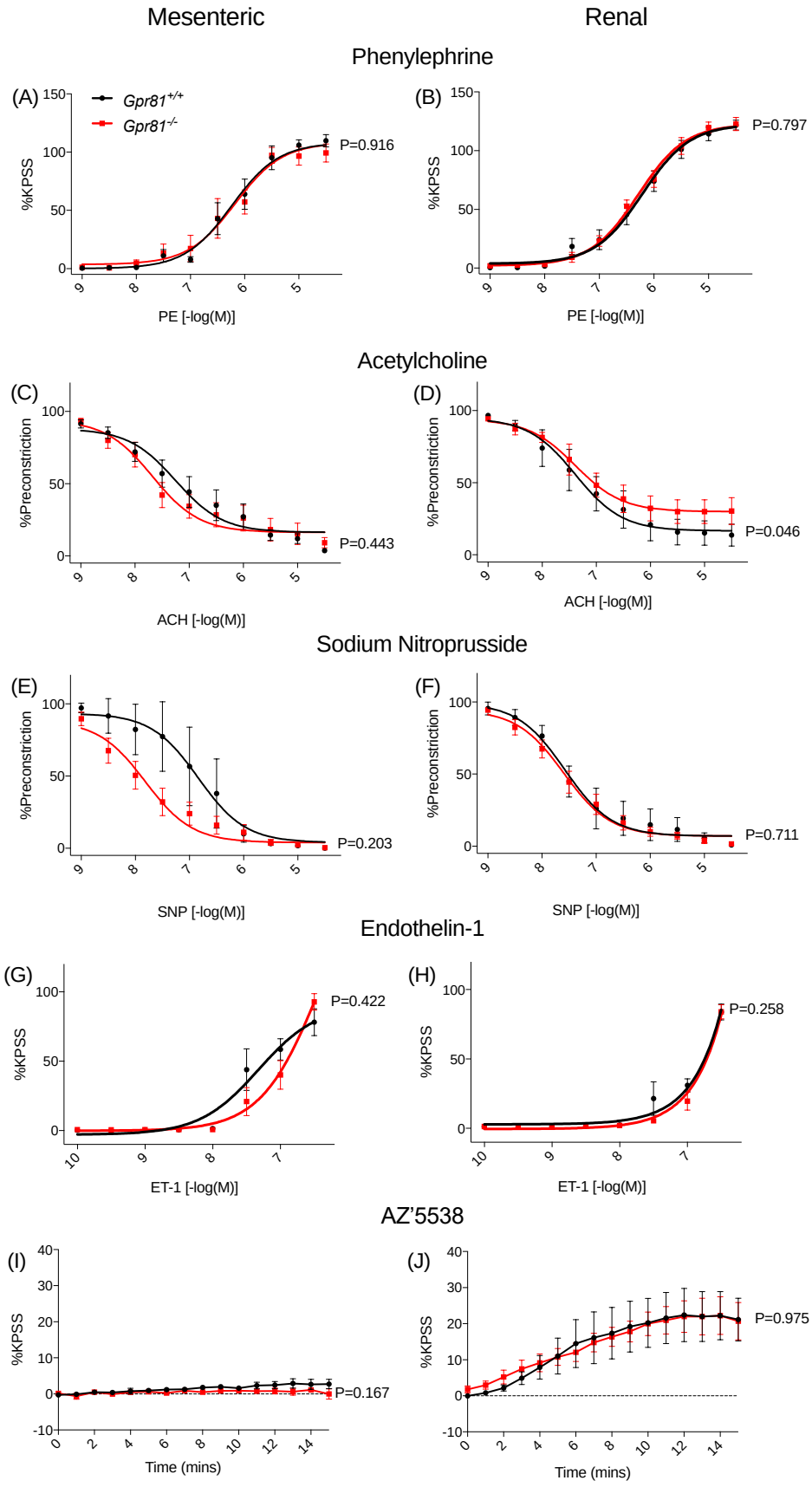
Mesenteric
Renal
Phenylephrine
(A)
(B)
Gpr81+/+
Gpr81-/-
%KPSS
PE [-log(M)]
P=0.916
P=0.797
Acetylcholine
(C)
(D)
%Preconstriction
ACH [-log(M)]
P=0.443
P=0.046
Sodium Nitroprusside
(E)
(F)
SNP [-log(M)]
P=0.203
P=0.711
Endothelin-1
(G)
(H)
ET-1 [-log(M)]
P=0.422
P=0.258
AZ'5538
(I)
(J)
Time (mins)
P=0.167
P=0.975

Figure 5.11 Differences in response between *Gpr81*$^{-/-}$ and *Gpr81*$^{+/+}$ mouse vessels to known pharmacological vasoconstrictors and dilators

Mesenteric arteries (A,C,E,G,I) and renal arteries (B,D,F,H,J) from *Gpr81* WT (black circles and KO (red squares) mice subjected to increasing concentrations of PE (A,B), ACH (C,D), SNP (E,F), ET-1 (G,H). For these drugs, curves shown are non-linear regressions. Vessels were also incubated with 30 μM AZ'5538 for 15 minutes (I, J). n=5-6. PE, ET-1 and AZ'5538 are displayed as a percentage force of the maximum response to KPSS while vasodilators ACH and SNP as a percentage to their individual vasoconstriction to half maximal with PE. All data was analysed by two-way ANOVA where the P value given is the effect of the genotype.

			-LogEC$_{50}$/IC$_{50}$	SD	P value	E$_{max}$/I$_{max}$	SD	P value
Mesenteric	PE	WT	6.18	0.11	0.717	112.70	5.43	0.260
		KO	6.24	0.14		103.30	6.23	
	ACH	WT	7.17	0.16	0.046	13.62	3.72	0.376
		KO	7.73	0.17		18.25	3.30	
	SNP	WT	6.76	0.26	0.005	-0.77	8.70	0.372
		KO	7.91	0.15		6.91	2.88	
Renal	PE	WT	6.23	0.09	0.701	121.10	4.46	0.666
		KO	6.27	0.06		123.60	3.34	
	ACH	WT	7.39	0.21	0.997	16.61	4.72	0.028
		KO	7.39	0.20		29.98	3.65	
	SNP	WT	7.60	0.16	0.906	8.10	3.91	0.642
		KO	7.58	0.09		6.07	2.20	

Table 5.2 Differences in vascular reactivity between *Gpr81*$^{-/-}$ and *Gpr81*$^{+/+}$ mice

EC/IC$_{50}$ is expressed as -log[Molar conc] and E/I$_{max}$ as a percentage of the KPSS response for each drug. n=5-6. Statistically significant (P<0.05) values are given in red. Statistics calculated from non-linear regressions formed using an extra sun-of-square F test.

To determine if differences between vessels treated with AZ'5538 or vehicle (Figure 5.3, Figure 5.4 and Table 5.1) were GPR81-specific effects, mesenteric and renal arteries were from both *Gpr81*$^{-/-}$ and wildtype littermates were all incubated with the agonist prior to dose response curves. Although differences were seen in C57BL/6JCrl mouse vessels to PE with and without AZ'5538 treatment (Figure 5.3 (B) and (C)), there were no differences here between genotypes (Figure 5.12 (A) and (B) and Table 5.3). Previously, there were differences in mesenteric and renal arteries incubated with AZ'5538 in their response to ACH. The IC_{50}, I_{max} and ANOVA drug treatment statistic were all significantly different for both vessel types (Figure 5.4(E) and (F) and Table 5.1) however when this was examined in animals lacking the *Gpr81* gene, the only difference seen was the I_{max} for mesenteric vessels (Figure 5.12 (C) and (D) and Table 5.3). There was a genotype difference in the *Gpr81*$^{-/-}$ and *Gpr81*$^{+/+}$ mouse mesenteric artery response to SNP (Figure 5.12 (E)) as well as a reduced IC_{50} value (Table 5.3, WT IC_{50} 7.36±0.10 -log[M], KO 7.75±0.07 -log[M], P=0.006) whereas no difference was seen in wildtype animals between AZ'5538 and vehicle (Figure 5.4(H) and (I)). No differences were seen with ET-1 treatment in either group (Figure 5.12(G) and (H)).

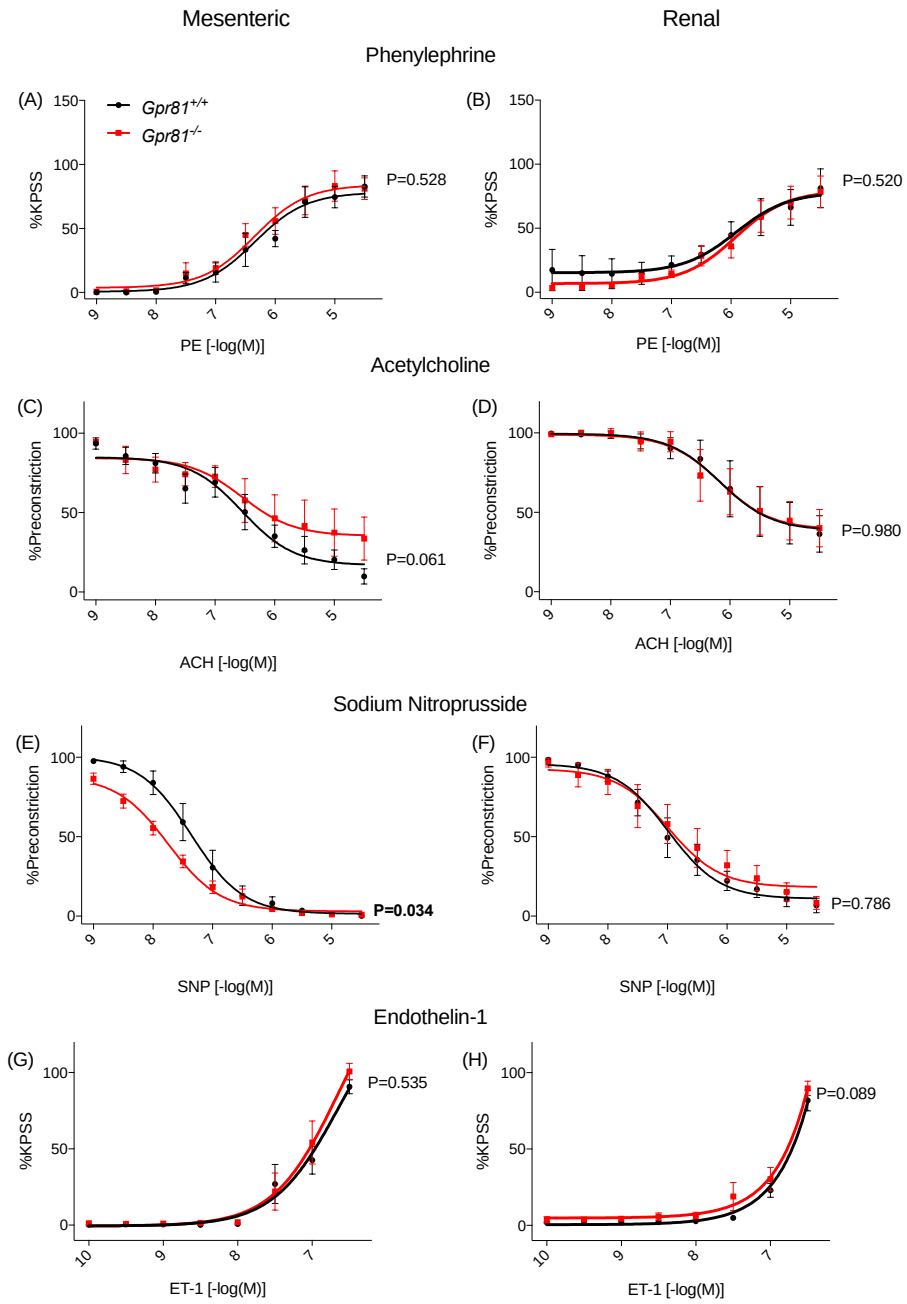

Figure 5.12 Differences in response between *Gpr81*$^{-/-}$ and *Gpr81*$^{+/+}$ mouse vessels to known pharmacological vasoconstrictors and dilators after AZ'5538 incubation

Mesenteric arteries (A, C, E, G) and renal arteries (B, D, F, H) from *Gpr81* WT (black circles and KO (red squares) mice were all treated with GPR81 agonist AZ'5538 (30 µM for 15 minutes). All vessels were then subjected to increasing concentrations of PE (A, B), ACH (C, D), SNP (E, F), ET-1 (G, H). For these drugs, curves shown are non-linear regressions. n=6 for all. PE and ET-1 are displayed as a percentage force of the maximum response to KPSS while vasodilators ACH and SNP as a percentage to their individual vasoconstriction to half maximal with PE. All data was analysed by two-way ANOVA where the P value given is the effect of the genotype.

			-LogEC$_{50}$/IC$_{50}$	SD	P value	E$_{max}$/I$_{max}$	SD	P value
Mesenteric	PE	WT	6.18	0.16	0.213	81.75	5.55	0.962
		KO	6.49	0.16		81.37	4.95	
	ACH	WT	6.50	0.18	0.792	16.14	4.89	0.029
		KO	6.62	0.37		36.11	6.86	
	SNP	WT	7.36	0.10	0.006	1.40	2.94	0.615
		KO	7.75	0.07		3.04	1.51	
Renal	PE	WT	5.89	0.33	0.879	78.75	10.43	0.995
		KO	5.95	0.19		78.66	6.61	
	ACH	WT	6.05	0.27	0.553	36.36	7.96	0.655
		KO	6.29	0.28		41.15	7.06	
	SNP	WT	7.07	0.12	0.412	12.09	3.47	0.506
		KO	6.85	0.19		16.35	5.05	

Table 5.3 Differences in vascular reactivity between *Gpr81*$^{-/-}$ and *Gpr81*$^{+/+}$ mice after AZ'5538 incubation

All vessels incubated with AZ'5538 (30 µM for 15 minutes) prior to dose response curves.EC/IC$_{50}$ is expressed as -log[Molar conc] and E/I$_{max}$ as a percentage of the KPSS response for each drug. n=6 for all. Statistically significant (P<0.05) values are given in red. Statistics calculated from non-linear regressions formed using an extra sun-of-square F test.

With the aim to identify differences between the WT and *Gpr81*$^{-/-}$ mouse renal artery vasoconstriction by AZ'5538, increasing doses of the GPR81 agonist were applied to the arteries. Although there were no differences in the overall genotype effect when analysing by two-way ANOVA, there was a significant different in the interaction of the dose response curves (Figure 5.12, ANOVA genotype P=0.263, concentration P<0.0001 and interaction P=0.008). There was a trend towards a difference in EC_{50} values with the KO renal arteries requiring a higher dose of AZ'5538 to reach the same vasoconstriction as WT arteries (Table 5.4). Due to large variation in the contraction at the highest dose of AZ'5538 (30 µM), there is also no significant difference in E_{max} between genotypes. To get a full dose response curve for these vessels, a higher dose of AZ'5538 is required however, as shown in Figure 5.1, doses above 30 µM effect the viability of vessels and any results seen may actually be due to damage of the vessels.

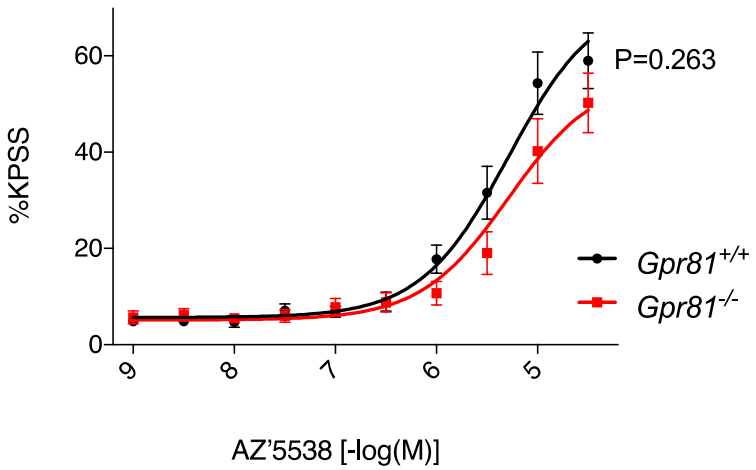

Figure 5.13 Vasoconstriction in renal arteries from *Gpr81*$^{-/-}$ and *Gpr81*$^{+/+}$ mice caused by AZ'5538

Renal arteries from *Gpr81* WT and null mice treated with increasing concentrations of AZ'5538 (n=10-11 from 6 mice). Data plotted as a percentage of the maximum constriction from 125 mM KCl and a non-linear regression formed. All data was analysed by two-way ANOVA where the P value given is the effect of the genotype.

		-LogEC$_{50}$	SD	P value	E$_{max}$	SD	P value
AZ'5538	WT	5.42	0.12	0.059	67.72	4.68	0.630
	KO	5.07	0.16		63.54	7.59	

Table 5.4 EC$_{50}$ and E$_{max}$ for AZ'5538 on renal arteries in *Gpr81*$^{-/-}$ and *Gpr81*$^{+/+}$ mice

EC$_{50}$ is expressed as -log[Molar conc] and E$_{max}$ as a percentage of the KPSS response for AZ'5538. N=10-11 from 6 mice. Statistics calculated from non-linear regressions formed using an extra sun-of-square F test.

5.3 Discussion

In this chapter, I assessed the effect of GPR81 activation and genetic deletion on *ex vivo* arterial reactivity. The main findings were; a) AZ'5538 induced contraction which was partly dependent on ETRA, b) genetic deletion of *Gpr81* altered the response to ACH, renal arteries had a lower maximal vasodilation while mesenteric arteries responded quicker to lower doses, c) importantly, the majority of direct vascular actions of AZ'5538 appear to be off target since they were also observed in *Gpr81* null mice.

5.3.1 GPR81 mediated arterial reactivity

The literature on lactate (the endogenous ligand of GPR81) causing direct vasoactive effects is brief however there are some suggestions of a vasoactive role for lactate and GPR81 *ex vivo*, which I aimed to explore. On aortic segments from basal tone, L-lactate (10 nM - 1 mM) had no effect[169]. Physiological plasma levels of lactate around 0.5-2mM, rising to 10-30mM during intense exercise or prolonged hypoxia[30,31,85] with the EC_{50} of the receptor to lactate being ~5 mM[31]. It could be that the concentration of lactate used in this study was not high enough to elicit a response however this is consistent with our findings in aortae with AZ'5538 as no effect was seen. Interestingly, a study using isolated rat mesenteric arteries which were preconstricted showed relaxation with increasing concentrations of L-lactate[170] which was seen in both renal and mesenteric arteries with AZ'5538, although this was not assessed in the *Gpr81*$^{-/-}$ animals to confirm specificity[170]. This study by McKinnon *et al.*, used a much higher concentration of lactate going up to 50 mM and showed significant relaxation from 6 mM. These vessels were preconstricted with noradrenaline prior to lactate administration however they saw no response to lactate if the vessels were preconstricted with 45 mM K^+. Here, vessels were all preconstricted with a lower concentration of K^+ (25 mM) and relaxation was seen with AZ'5538 treatment. It could be that the tension was too high in their study to allow lactate to cause relaxation or again this could be a non GPR81-mediated response which was seen with AZ'5538. The relaxation effect they saw here was not pH, endothelium or nitric oxide

dependant which supports our data of GPR81 being expressed in smooth muscle cells and this being a direct response. It is well documented that plasma lactate levels increase in states of hypoxia[85] and there is literature looking at the effect of oxygen deprivation on vascular tone *ex vivo* and *in vivo* but none of which have made the connection with lactate. In general, hypoxia causes vasoconstriction of the pulmonary arteries and vasodilation systemically[171] which is caused by responses in both endothelial and smooth muscle cells[172]. *Ex vivo*, hypoxia (partial oxygen pressure (PO_2) <5 mmHg) caused decreased vessel tone in rat mesenteric arteries after preconstriction with high K^+[173], the same way AZ'5538 did in both mouse mesenteric and renal arteries[171]. In this study by Otter *et al.*, the decrease in tone was coupled with decreased pH which could imply an increase in lactate due to hypoxic conditions.

As discussed in previous chapters, *in vitro* and *in vivo* it is known that circumstances where lactate levels are high (for example hypoxia or intense exercise), ET-1 levels are also increased[119,163]. Since a relationship was determined between GPR81 and ETRA, the aim was to prevent AZ'5538 mediated vasoconstriction by blocking the ETRA as it was possible to inhibit the blood pressure response seen *in vivo*. Using BQ-123 as in the *in vivo* studies, the effect of AZ'5538 on renal arteries was dampened by not prevented. As vasoconstriction was still seen with AZ'5538 in the *Gpr81*$^{-/-}$ mouse, this may be why there is still an increase in tension even though ETRA is blocked.

Although it was not possible to determine the underlying mechanism of GPR81-mediated vasoconstriction using wire myography, there is a wealth of literature to support GPR81, ET-1 and vasoconstriction. It is well established in adipocytes that GPR81 functions to inhibit lipolysis through a G_i coupled pathway, lowering cAMP levels which downstream decreases PKA activity[31]. I have not yet shown this in vessels, but other studies support the concept. For example, in preconstricted mesenteric arteries exhibited vasodilation with

lactate administration[170]. This effect was blocked in the presence of a cAMP analogue (Rp stereoisomer of adenosine-3',5'-cyclic monophosphothioate) suggesting that the vascular effects of lactate are mediated through cAMP. A similar mechanism has been suggested *ex vivo* in mouse femoral arteries where increased cAMP using the phosphodiesterase inhibitor Cilostazol prevented vasoconstriction by ET-1[162], implying a connection between G_i pathway inactivation and ET-1. This study and others used *in vitro* models with smooth muscle cells to determine that ET-1 dependent calcium influx is inhibited by preventing the inactivation of cAMP which may be the cause of this smooth muscle ET-1 vasoconstriction[147,162]. Adenosine also functions in a G_i coupled manner and Hansen *et al.* has shown in isolated perfused mouse afferent arterioles of the kidney that lowering cAMP therefore decreasing PKA activity causes vasoconstriction[145]. This is of particularly interest as I have previously suggested GPR81 expression in the smooth muscle cells of afferent and efferent arterioles of the kidney where it may initiate a vasoactive response causing increase blood pressure and decreased renal blood flow. Finally, *ex vivo* studies using hypoxia have shown increased ET-1 and changes in vascular function. In rat mesenteric arteries, hypoxia increased ET-1 release causing vasoconstriction and suggesting an important role in local vascular tone in states of hypoxia[120]. In the same way, in porcine coronary arteries, it is suggested that the systemic vascular response to hypoxia of vasodilation is counteracted by the release of ET-1 causing vasoconstriction[121]. Although the underlying connection and mechanism between hypoxia, GPR81, ET-1 and vascular tone have not been fully elucidated it would seem there is a connection which the literature supports, and which needs to be further investigated.

5.3.2 Effect of *Gpr81* genetic deletion and vascular function

Many differences were seen between vessels from wildtype C57BL/6JCrl animals treated with AZ'5538 or vehicle, in particular in the responses to PE and ACH. To assess if these were due to GPR81 activation, incubation with

AZ’5538 was carried out in both genotypes. These differences were no longer presented suggesting this was an off-target effect of the agonist.

There were differences in vascular responses between arteries from *Gpr81*$^{+/+}$ and *Gpr81*$^{-/-}$ mice. Specifically, renal arteries from *Gpr81*$^{-/-}$ mice showed a reduction in their ability to vasodilate in response to ACH which resulted in a decreased maximal vasodilation. Mesenteric arteries from KO animals showed a leftward shift in the dose response curve and an increased -logIC_{50} meaning they are able to vasodilate at lower concentrations of ACH. These opposing findings could suggest changes to the endothelial cell in response to the deletion of *Gpr81*. There was also a significant increase in the -logIC_{50} in KO animals to SNP however the data was very variable. If this is a true finding, it would be interesting to analyse other resistance vessels throughout the *Gpr81*$^{-/-}$ mouse vasculature to assess if others have altered (either increased or decreased) ability to relax to a range of endothelium dependant and independent vasodilators.

5.3.3 Off target effects of AZ’5538 in wire myography

In chapter 3 I showed that AZ’5538 causes a range of cardiovascular and renal effects when IV infused into mice *in vivo*. These effects were GPR81-specific as the AZ’5538 had no action in *Gpr81*-null mice. Conversely, in this chapter, vasoconstriction was seen only in renal arteries, but this effect was present in the *Gpr81*$^{-/-}$ mice also. In the well of the myograph, there are off-target GPR81 independent mechanisms which are changing vascular tone by AZ’5538. There are still differences between genotypes, suggesting that some of the effect seen is GPR81 specific as there is an interaction difference between the dose response curves for the wildtype and knockout animals. An obvious cause for this change would be a pH change in the bath causing the change in vascular tone however the pH of the vehicle is always altered to that of the drug (around pH 5) and there was no effect of vehicle alone so that theory can be discounted.

AZ'5538 is a specific GPR81 drug created by AstraZeneca. The compound was designed and selected using a series of thorough *in vitro* and *in vivo* discovery steps to ensure specificity of the compound to GPR81[65]. These included high-throughput screening of forskolin-stimulated cAMP in GPR81 transfected cells, inhibition of lipolysis experiments in primary human and rat adipocytes, pharmacokinetic evaluation and assessment of lipolysis inhibition in anesthetised rats. The off-target effects in wire myography are surprising when you consider the rigorous selection process by AstraZeneca along with our data on *in vivo* specificity of the drug.

A way to assess the specificity of GPR81 mediated vasoconstriction could be the use of a different compound to activate the receptor. Other exogenous agonists for GPR81 do exist, these include 3-hydroxybenzoic acid (3-HBA) which targets both GPR81 and GPR109a while 3,5 dihydroxybenzoic acid (3,5-DHBA) is specific to GPR81[174], 3-chloro-5- hydroxybenzoic acid (CHBA) has also been identified as a specific GPR81[66]. For all of these compounds, there is currently no literature on blood pressure or vasoreactivity of these compounds however they have been implicated in altering lipid profiles by receptor activation both *in vivo* and *in vitro*[66,175]. Assessment of new agonists would also require repeating the *in vivo* experiments to confirm that all agonists of GPR81 cause these hypertensive effects as well as *ex vivo* analysis using wire myography to determine if all GPR81 agonists have off target effects in this setting.

The data suggests that there is something that differs *in vivo* in comparison to the well of myography to explain the effects in the knockout animals. This could potentially be caused by damage to the vessels endothelium when mounting the vessels, however, responses to ACH confirm this is not the case. An obvious element that is missing in the well of the myograph is the circulation. I have previously discussed the presence of GPR81 on immune cells[176] and this could be the missing link between *in vivo* and *ex vivo* here. It is possible to

isolate immune cells and use them in the myograph and this would be an important experiment to carry out in the future.

The literature and our data suggest that there is a role for GPR81 in direct vasoconstriction of vessels however more work needs to be done to understand the specific effects and the knockout mouse model will be useful in assessing specific GPR81 effects.

5.3.4 Summary of chapter findings

- AZ'5538 causes vasoconstriction in mouse renal arteries however this is not GPR81-specific.
- BQ-123 does not completely block vasoconstriction caused by AZ'5538.
- AZ'5538 also causes dose dependant vasodilation on mesenteric and renal arteries after preconstriction with K_+ which is not confirmed to be GPR81 specific.
- *Gpr81*$^{-/-}$ mice show opposing differences in ACH responses in different vessel types compared to wildtype. Mesenteric arteries respond at a lower dose while renal arteries have an impaired vasodilatation.

Chapter 6 - Discussion

The major findings of my PhD are as follows: that GPR81 is expressed in the vasculature, including the renal vasculature, of the mouse; that activation of the receptor *in vivo* causes a GPR81 specific rapid increase in blood pressure; reduction in blood flow to the kidneys and glomerular filtration rate. I further demonstrated that the blood pressure increase caused by GPR81 activation is ETRA dependent and causes an increase of ET-1 in the circulation.

6.1 Localisation of GPR81

The majority of studies focus on GPR81 expression in adipose tissue. The receptor is enriched here, and the effects of receptor activation are well defined. However, it is also present across a range of non-adipose tissues, with expression in the highly vascularised tissues of heart, skeletal muscle and kidney being ~10% of that in adipocytes[30]. My studies localised *Gpr81* expression in the mouse within the vascular smooth muscle of the aorta and renal arteries, the glomerular arterioles in the kidney cortex as well as within the medulla. To confirm smooth muscle localisation of the *Gpr81* RNA, it would be necessary to colocalise this expression with known markers, e.g. α-smooth muscle actin. I also have preliminary data from the Denby group in our centre who used fluorescence-activated cell sorting (FACS) on CD-1 adult mouse whole kidneys. They separated cell populations with antibodies for PDGFRβ for pericytes and fibroblasts, CD31 for endothelial cells, F4/80 for macrophages and lotus tetragonolobus lectin for tubular kidney cells. From the 4 cDNA samples made from each of these cell populations, I was able to perform qPCR for GPR81 and determine cell type expression in the healthy mice from their study. The results for this are shown in Figure 6.1. No *Gpr81* expression was found in the 4 tubular cell samples and only one for the F4/80-positive macrophage group. The cell population with the highest *Gpr81* expression was the PDGFRβ-positive pericyte/fibroblast group. There was one sample with some expression in endothelial CD31-positive cells with close to zero in the others. This is consistent with previous observations that *Gpr81* reporter expression does not co-localise with endothelial cell markers in the cerebral vasculature[42]. However, a study published in September 2019,

described high levels of GPR81 in cultured immortalised human umbilical vein endothelial cells[177]. Unfortunately, primary arterial vascular smooth muscle cells were not a cell population which were included in the FACS study; therefore, it is not possible to compare the relative expression levels between these and PDGFRβ-positive cells[177].

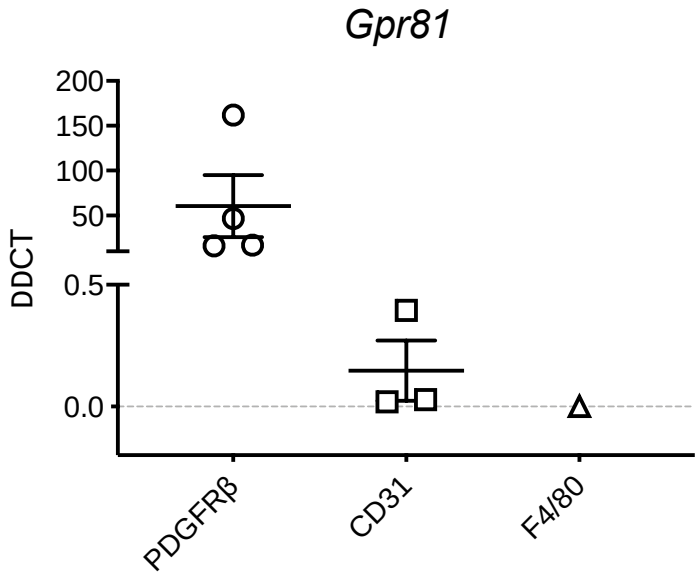

Figure 6.1 *Gpr81* expression in cell sorted kidney cells from wildtype healthy CD1 mice

Four whole kidneys from healthy adult male CD-1 mice were sorted using fluorescence-activated cell sorting (FACS) flow cytometry to separate out pericytes and fibroblasts (PDGFRβ), endothelial cells (CD31), macrophages (F4/80) and tubular cells (lotus tetragonolobus lectin). qPCR was carried out using the UPL system with primers for *Gpr81*. Four samples for each cell type were assayed and only those with positive values are shown here. Data are mean±SEM.

During the course of my PhD study, single-cell RNA sequencing has become more widely used and the sharing of large transcriptomic data more commonplace. I was thus able to examine transcriptome data from mice to analyse the cell type specific expression of *Gpr81* in a range of tissues. Firstly, the Kidney Cell Explorer[178] is an excellent resource for renal researchers to investigate nephric and ureteric gene expression (https://cello.shinyapps.io/kidneycellexplorer/). This database shows that highest levels of *Gpr81* (Hcar1) expression is grouped within the vascular and interstitial cell subsets. It is then possible to determine expression at specific

points through the nephron and collecting duct where *Gpr81* is only found at the very end of the collecting duct, within the cells of the deep inner medullar and renal pelvis. In my *in situ* hybridisation studies there was extensive staining for *Gpr81* within the medulla. Transcriptomic data confirming renal vascular expression is also promising as I found *Gpr81* RNA in renal arteries as well as what appears to be the afferent and efferent arterioles adjacent to glomeruli in the cortex. A second single-cell sequencing data set which is readily available has investigated the cell type expression of genes from vascular tissue in the brain and lungs of adult transgenic reporter mice[93]. Previous studies have reported expression of GPR81 in the brain vasculature, specifically in the pial fibroblast-like cells that line blood vessels and in pericyte-like cells along intracerebral microvessels[42]. This is supported by this sequencing data where in the brain, *Gpr81* expression is enriched in the fibroblast-like subsets as well as some expression seen in pericytes (Figure 6.2 (A)). There is also a range of expression levels throughout the subsets of both vascular smooth muscle and endothelial cells. The expression profile for *Gpr81* in the lung vasculature is quite different (Figure 6.2 (B)). A relatively high level of expression is found in pericyte cells with a broad expression profile throughout endothelial subsets. No expression is seen in the vascular smooth muscle cells of the lungs. This is of particular interest since in states of hypoxia, where an increase in lactate production is seen, pulmonary vessels tend to vasoconstrict while the peripheral vasculature shows opposing effects and vasodilation is usually seen[179]. Overall, these data suggest that *Gpr81* is present in both pericytes and endothelial cells, a finding which I did not replicate using RNAscope. As previously stated, co-localisation studies are essential for determining the cell specific location of *Gpr81* in the kidney and renal vasculature. None of the data shown has analysed the expression of GPR81 at a protein level and therefore may not give a clear idea of the location of the active receptor. To achieve this, in depth antibody validation would need to be carried out to determine specificity prior to analysis. It is worth noting that my AZ collaborators indicated that commercially available antibodies were

unselective, providing positive results in tissue from KO mice (K Wallenius, personal communication).

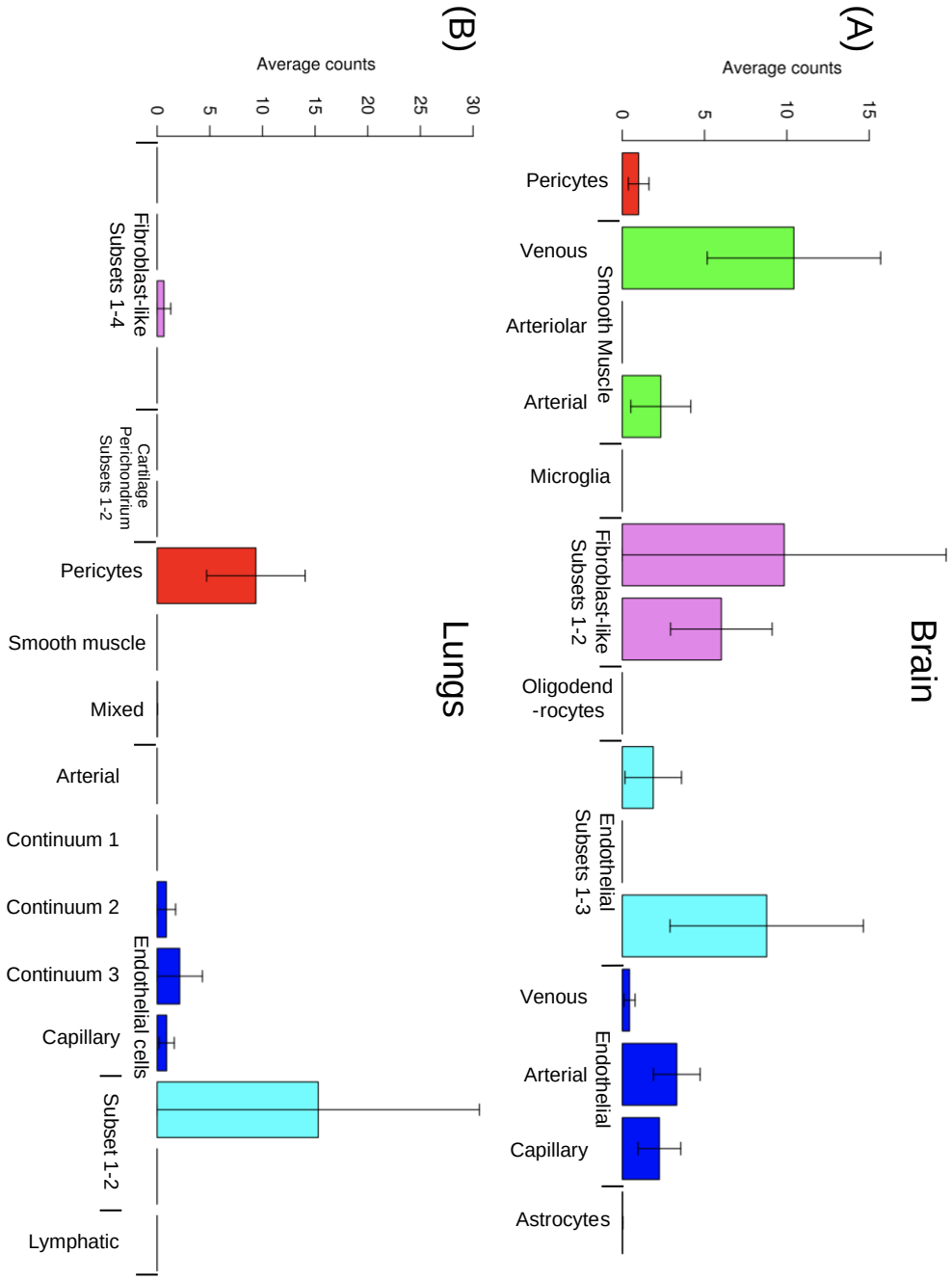

Figure 6.2 *Gpr81* expression from single-cell RNA sequencing of vascular and vessel-associated cell types of the mouse brain and lungs

Figures adapted from the online database from the single-cell RNA sequencing experiment by He *et al*.[93,180] http://betsholtzlab.org/VascularSingleCells/database.html. The brain and lungs from adult transgenic reporter mice were sorted into 15 and 17 different cell types or subtypes respectively prior to sequencing. Average counts for Gpr81 are shown here for all cell subtypes analysed.

6.2 Mechanism of GPR81 vasoactivity

The expression profile suggests GPR81 is involved in vascular and microvascular function, as described for other GPCRs with metabolic intermediates. For example, niacin, which activates GPR109a, reduces the production of reactive oxygen species by arterial endothelial cells[138] and also promotes vasodilation by stimulating prostaglandin production[139]. Succinate activation of GPR91, which like GPR81 is coupled to G_i, acutely increases BP in rats[142] and has direct effects on arterial contractility[143]. For lactate/GPR81, however, functional data are limited. Increasing lactate concentration in the brain, either through exercise or by exogenous administration, promotes angiogenesis[42]. This effect is GPR81-dependent since lactate-induced angiogenesis does not occur in knockout mice. Lactate also vasoconstricts rat retinal microvessels[92] but it is not known whether this is GPR81-mediated or relates to other actions of lactate on cell membrane transporters[92]. Infusion of very high concentrations of lactate increases BP in rats[89] but this most likely reflects the sympathoexcitation induced by panic, rather than activation of GPR81 in blood vessels[92]. I have shown that *in vivo* GPR81 activation causes a rapid increase in BP, a reduction in blood flow to the kidneys, decreased GFR and no change in tubular reabsorption. I have also shown that the blood pressure effects of GPR81 activation are dependent on ETRA. Receptor activation of ETRA in the kidneys by ET-1 has directly comparable effects to GPR81 with vasoconstriction of both the afferent and efferent arterioles confirmed as well as decreased glomerular filtration and decreased blood flow to the kidney through ETRA[181].

The cellular mechanism underpinning GPR81-mediated vasoconstriction via ETRA is not known. In adipocytes, GPR81 couples to Gi, downregulating cAMP production and protein kinase A signaling[141]. Activation of Gi pathways in vascular smooth muscle cells, by GPCR kinase 5 for example, lowers intracellular cAMP, enhances vasoconstriction and causes sustained hypertension[144]. Similarly, activation of A1 receptors by adenosine constricts the renal afferent arteriole by a Gi-mediated cascade which activates

phospholipase C[145]. Reciprocally, agents that increase cAMP promote arterial vasorelaxation[147,148]. However, my data suggests the vasomotor effects of GPR81 activation are indirect, mediated by ETRA vasoconstriction. The mechanism by which this occurs is dependent on the cell type where GPR81 is activated and where ET-1 is being released from. The majority of ET-1 is produced and released from endothelial cells. In response to an external stimulus, which act to either increases intracellular calcium or cAMP levels[150], ET-1 is released from Weibel-Palade bodies and activates ETRA on VSM cells. ET-1 is also synthesised and secreted from VSMC where it is able to alter vascular responsiveness[111,112,182]. It is possible that activation of GPR81 in VSMC promotes ET-1 production within the same cell as an inverse relationship between intracellular cAMP and myocyte ET-1 production is established[160,161,162]. However, the rates at which VSMC can produce ET-1 are around 1,800 times lower than that of endothelial cells in isolated aortae[113] suggesting that this is insufficient to cause such a rapid and pronounced BP response. Another option is that GPR81 is activated on endothelial cells and causes direct release of ET-1 from Weible-Palade bodies, however, as previously mentioned, these storage vesicles degranulate and release their contents in response to increased intracellular cAMP[183] where as GPR81 activation decreases cAMP levels. The most probable cellular mechanism, given the increase in plasma ET-1, is that GPR81 in smooth muscle communicates with the endothelial cell to enhance release of ET-1 by the constitutive pathway[101]. A strategy to further understand this would be to utilise conditional ETRA knock out mice, be that on endothelial and smooth muscle cells and repeat the experiments carried out here.

There is a range of data that states that lactate and hypoxia cause vasodilation, in particular on vessels which are already constricted[90–92]. The mechanism by which lactate or hypoxia causes vasodilation has been shown to be independent of endothelial cell presense[90], suggesting a differing pathway to that of GPR81 mediated vasoconstriction. It has been hypothesised that lactate, via GPR81, may serve to constrict blood vessels

when energy supplies are ample but in response to local metabolic need can switch to vasodilation once stores are restricted. I suggest that these are by two different intracellular mechanisms, one which involves ET-1 release from endothelial cells and the other by a currently unknown pathway.

6.3 GPR81 as a therapeutic target

It is well known that renal ischemia reperfusion injury (IRI) increases internal extracellular lactate concentrations[184]. A unilateral model of IRI with contralateral nephrectomy was carried out in adult male *Gpr81*$^{-/-}$ mice and wildtype littermates by my collaborators as AstraZeneca and I was provided with a proportion of frozen kidney to assess whether global genetic deletion of the receptor was protective. I selected a panel of transcriptional markers to capture cardinal features of IRI, demonstrating the anticipated increase in KIM-1, col1a1, TNFα and F4/80 expression in wild-type mice. In contrast, *Gpr81*$^{-/-}$ mice demonstrate renoprotection, with significantly lower induction of the markers of tubular injury, fibrosis and inflammation (Figure 6.3). It is possible that increased lactate in IRI binds to GPR81 causing increased renal vasoconstriction which induces damage, therefore preventing this injury may have beneficial effects in kidney injury.

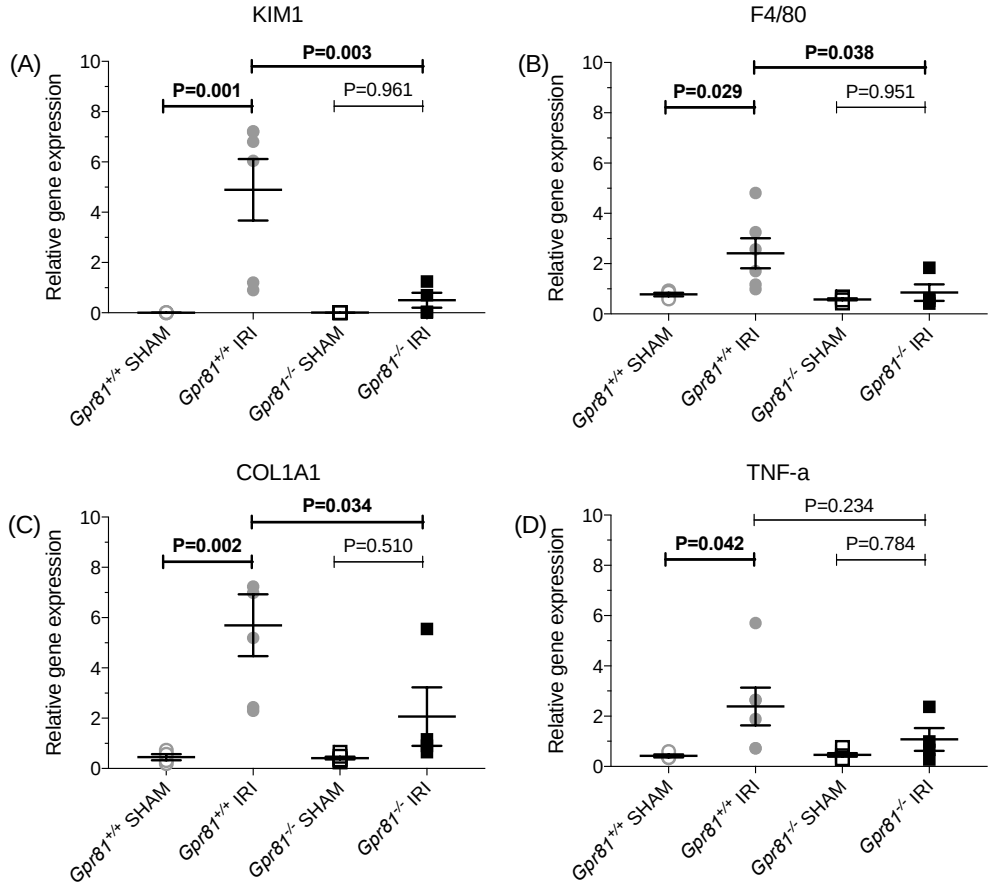

Figure 6.3 *Gpr81*$^{-/-}$ mice are protected from renal ischaemia reperfusion injury

Male adult *Gpr81*$^{-/-}$ mice and wildtype littermates underwent sham surgery or left renal IRI for 27 minutes with a contralateral right kidney nephrectomy. After 7 days, mice were culled and tissues collected. Gene expression was measured in cDNA from left kidneys by qPCR which was all normalised to housekeeper gene *Hprt*. Data are mean±SEM, n=4-6 and statically analysis was carried out using one-way ANOVA with multiple comparisons.

Similar beneficial outcomes are reported in cerebral ischaemic injury: overexpression of GPR81 amplifies sensitivity to ischaemic injury in a neuronal cell line; 3-hydroxy-butyrate, which antagonises GPR81, prevents lactate-induced injury in primary cultured neurons and is neuroprotective in mice exposed to cerebral artery occulsion[72]. My study does not establish the mechanism of renoprotection in *Gpr81*$^{-/-}$ mice. Based on my data, a plausible hypothesis is that deletion of the receptor prevents sustained vasoconstriction following injury. Certainly, renal IRI has a strong haemodynamic component[185] and strategies preventing sustained vasoconstriction may offer beneficial vascular support in the post-injury phase[186]. The Home Office project licence

under which these studies were performed did not include the use of the IRI model and therefore extensive investigation into the mechanisms behind this protection were not possible during my PhD. However, I have established that GPR81 mediated vasoconstriction acts in an ETRA dependent manner and therefore blockade of this pathway should have similar results to GPR81 knock out. In fact, it has been previously shown that unilateral IRI in CD-1 mice causes an increase in ET-1 protein and mRNA expression alongside an increase in ETRA (but not ETRB) mRNA levels[184]. Gene deletion of ET-1 from vascular endothelial cells has been shown to significantly protect from a range of renal injury parameters in a bilateral mouse model of IRI[187]. ETRA has been targeted as a potential therapy in AKI using renal injury models. Specific ETRA antagonist BQ-123 in a rat model of kidney transplantation showed reduced renal reperfusion injury with less tubular and glomerular injury compared to controls. In the same way, a similar antagonist, Atrasentan, in a mouse model of unilateral IRI showed reduced microvascular injury and prevented renal mass reduction. As these drugs are already used by clinicians and are reasonably well tolerated, targeting ETRA directly rather than via GPR81, which I would expect to have similar outcomes, is a more promising therapeutic strategy[185].

The off target pressor effects of GPR81 activation mean that this is no longer a plausible target for the treatment of dyslipidemias and AstraZeneca have therefore closed their project on this. I believe the future of cardiorenal GPR81 research is in the potential protective role of gene deletion or antagonism in a range of renal or cardiac injury settings along with a more advanced understanding of the interactions with the endothelin system.

In summary, my PhD studies have indicated that GPR81 activation regulates macro- and microvascular perfusion within the kidney, dependent on ET-1 signalling by ETRA. The physiological requirement for such a system is not clear since this would vasoconstrict regions of high anaerobic cellular metabolism. Earlier work associating exercise-induced accumulation of

extracellular lactate in skeletal muscle with the release of ET-1 into the circulation[163] provides some insight. Here it was proposed that ET-1 release helped to maintain systemic BP during exercise[163]. My studies suggest a mechanistic link and it may be that GPR81 activation constrains and regulates flow into relatively ischemic areas of the kidney, militating against hyperaemic damage. When ischemia is sustained, blockade of the GPR81 system or ETRA directly, could be therapeutically tractable to offer vascular support and reduce renal injury.

References

1 Kearney PM, Whelton M, Reynolds K, Muntner P, Whelton PK, He J. Global burden of hypertension: Analysis of worldwide data. *Lancet*. 2005. doi:10.1016/S0140-6736(05)70151-3.

2 Udani S, Lazich I, Bakris GL. Epidemiology of hypertensive kidney disease. Nat. Rev. Nephrol. 2011. doi:10.1038/nrneph.2010.154.

3 Kokubo Y, Matsumoto C. Hypertension is a risk factor for several types of heart disease: Review of prospective studies. In: *Advances in Experimental Medicine and Biology*. 2017 doi:10.1007/5584_2016_99.

4 Yusuf S, Joseph P, Rangarajan S et al. Modifiable risk factors, cardiovascular disease, and mortality in 155 722 individuals from 21 high-income, middle-income, and low-income countries (PURE): a prospective cohort study. *Lancet*. 2019. doi:10.1016/s0140-6736(19)32008-2.

5 Guyton AC, Coleman TG, Cowley AW, Scheel KW, Manning RD, Norman RA. Arterial pressure regulation. Overriding dominance of the kidneys in long-term regulation and in hypertension. *Am J Med*. 1972. doi:10.1016/0002-9343(72)90050-2.

6 Pao AC. Update on the Guytonian view of hypertension. Curr. Opin. Nephrol. Hypertens. 2014. doi:10.1097/01.mnh.0000450777.17698.8e.

7 Ivy JR, Bailey MA. Pressure natriuresis and the renal control of arterial blood pressure. J. Physiol. 2014. doi:10.1113/jphysiol.2014.271676.

8 Pires SLS, Barrès C, Sassard J, Julien C. Renal blood flow dynamics and arterial pressure lability in the conscious rat. *Hypertension*. 2001. doi:10.1161/01.HYP.38.1.147.

9 Cupples WA, Novak P, Novak V, Salevsky FC. Spontaneous blood pressure fluctuations and renal blood flow dynamics. *Am J Physiol*. 1996.

10 Gordon Betts J, Young KA, Wise JA et al. *Anatomy and Physiology*. 1st ed. OpenStax: Houston, Texas, 2013.

11 Bidani AK, Griffin KA, Williamson G, Wang X, Loutzenhiser R. Protective

importance of the myogenic response in the renal circulation. Hypertension. 2009. doi:10.1161/HYPERTENSIONAHA.109.133777.

12 Hill MA, Davis MJ, Meininger GA, Potocnik SJ, Murphy T V. Arteriolar myogenic signalling mechanisms: Implications for local vascular function. In: *Clinical Hemorheology and Microcirculation*. 2006.

13 Holstein-Rathlou NH, Wagner AJ, Marsh DJ. Tubuloglomerular feedback dynamics and renal blood flow autoregulation in rats. *Am J Physiol - Ren Fluid Electrolyte Physiol*. 1991.

14 Persson AEG, Lai EY, Gao X, Carlström M, Patzak A. Interactions between adenosine, angiotensin II and nitric oxide on the afferent arteriole influence sensitivity of the tubuloglomerular feedback. Front. Physiol. 2013. doi:10.3389/fphys.2013.00187.

15 Mattson DL, Lu S, Roman RJ, Cowley AW. Relationship between renal perfusion pressure and blood flow in different regions of the kidney. *Am J Physiol - Regul Integr Comp Physiol*. 1993.

16 Thurau K. Renal hemodynamics. *Am J Med*. 1964. doi:10.1016/0002-9343(64)90181-0.

17 Burke M, Pabbidi M, Farley J, Roman R. Molecular Mechanisms of Renal Blood Flow Autoregulation. *Curr Vasc Pharmacol*. 2014. doi:10.2174/15701611113116660149.

18 Schnermann J. Concurrent Activation of Multiple Vasoactive Signaling Pathways in Vasoconstriction Caused by Tubuloglomerular Feedback: A Quantitative Assessment. *Annu Rev Physiol*. 2015. doi:10.1146/annurev-physiol-021014-071829.

19 Guan Z, Inscho EW. Endothelin and the renal vasculature. In: *Endothelin in Renal Physiology and Disease*. 2011 doi:10.1159/000328720.

20 Inscho EW. Renal microvascular effects of P2 receptor stimulation. In: *Clinical and Experimental Pharmacology and Physiology*. 2001 doi:10.1046/j.1440-1681.2001.03450.x.

21 Vargas SL, Toma I, Jung JK, Meer EJ, Peti-Peterdi J. Activation of the succinate receptor GPR91 in macula densa cells causes renin release. *J Am Soc Nephrol*. 2009. doi:10.1681/ASN.2008070740.

22 De Castro Fonseca M, Aguiar CJ, Da Rocha Franco JA, Gingold RN, Leite MF. GPR91: Expanding the frontiers of Krebs cycle intermediates. Cell Commun. Signal. 2016. doi:10.1186/s12964-016-0126-1.

23 Lander ES, Linton LM, Birren B et al. Initial sequencing and analysis of the human genome. *Nature*. 2001. doi:10.1038/35057062.

24 Ahmed K, Tunaru S, Offermanns S. GPR109A, GPR109B and GPR81, a family of hydroxy-carboxylic acid receptors. *Trends Pharmacol Sci*. 2009;30(11):557–562.

25 Tunaru S, Lättig J, Kero J, Krause G, Offermanns S. Characterization of determinants of ligand binding to the nicotinic acid receptor GPR109A (HM74A/PUMA-G). *Mol Pharmacol*. 2005. doi:10.1124/mol.105.015750.

26 Tunaru S, Kero J, Schaub A et al. PUMA-G and HM74 are receptors for nicotinic acid and mediate its anti-lipolytic effect. *Nat Med*. 2003;9(3):352–355.

27 Taggart AKP, Kero J, Gan X et al. (D)-β-hydroxybutyrate inhibits adipocyte lipolysis via the nicotinic acid receptor PUMA-G. *J Biol Chem*. 2005. doi:10.1074/jbc.C500213200.

28 Ahmed K, Tunaru S, Langhans CD et al. Deorphanization of GPR109B as a receptor for the β-oxidation intermediate 3-OH-octanoic acid and its role in the regulation of lipolysis. *J Biol Chem*. 2009. doi:10.1074/jbc.M109.019455.

29 Costa CG, Dorland L, Holwerda U et al. Simultaneous analysis of plasma free fatty acids and their 3-hydroxy analogs in fatty acid β-oxidation disorders. *Clin Chem*. 1998.

30 Liu C, Wu J, Zhu J et al. Lactate inhibits lipolysis in fat cells through activation of an orphan G-protein-coupled receptor, GPR81. *J Biol Chem*. 2009;284(5):2811–2822.

31 Cai TQ, Ren N, Jin L et al. Role of GPR81 in lactate-mediated reduction of adipose lipolysis. *Biochem Biophys Res Commun*. 2008;377(3):987–991.

32 Ahmed K. Biological roles and therapeutic potential of hydroxy-carboxylic acid receptors. Front. Endocrinol. (Lausanne). 2011.

doi:10.3389/fendo.2011.00051.

33 Zellner C, Pullinger CR, Aouizerat BE et al. Variations in human HM74 (GPR109B) and HM74A (GPR109A) niacin receptors. *Hum Mutat*. 2005. doi:10.1002/humu.20121.

34 Soga T, Kamohara M, Takasaki J et al. Molecular identification of nicotinic acid receptor. *Biochem Biophys Res Commun*. 2003. doi:10.1016/S0006-291X(03)00342-5.

35 Wise A, Foord SM, Fraser NJ et al. Molecular identification of high and low affinity receptors for nicotinic acid. *J Biol Chem*. 2003. doi:10.1074/jbc.M210695200.

36 Yousefi S, Cooper PR, Mueck B, Potter SL, Jarai G. cDNA representational difference analysis of human neutrophils stimulated by GM-CSF. *Biochem Biophys Res Commun*. 2000. doi:10.1006/bbrc.2000.3678.

37 Irukayama-Tomobe Y, Tanaka H, Yokomizo T, Hashidate-Yoshida T, Yanagisawa M, Sakurai T. Aromatic D-amino acids act as chemoattractant factors for human leukocytes through a G protein-coupled receptor, GPR109B. *Proc Natl Acad Sci U S A*. 2009. doi:10.1073/pnas.0811844106.

38 Schaub A, Fütterer A, Pfeffer K. PUMA-G, an IFN-γ-inducible gene in macrophages is a novel member of the seven transmembrane spanning receptor superfamily. *Eur J Immunol*. 2001. doi:10.1002/1521-4141(200112)31:12<3714::AID-IMMU3714>3.0.CO;2-1.

39 Hoque R, Farooq A, Ghani A, Gorelick F, Mehal WZ. Lactate reduces liver and pancreatic injury in toll-like receptor- and inflammasome-mediated inflammation via gpr81-mediated suppression of innate immunity. *Gastroenterology*. 2014;146(7):1763–1774.

40 Thangaraju M, Cresci GA, Liu K et al. GPFM 09A is a G-protein-coupled receptor for the bacterial fermentation product butyrate and functions as a tumor suppressor in colon. *Cancer Res*. 2009. doi:10.1158/0008-5472.CAN-08-4466.

41 Bermudez Y, Benavente CA, Meyer RG, Coyle WR, Jacobson MK,

Jacobson EL. Nicotinic acid receptor abnormalities in human skin cancer: Implications for a role in epidermal differentiation. *PLoS One*. 2011. doi:10.1371/journal.pone.0020487.

42 Morland C, Andersson KA, Haugen ØP et al. Exercise induces cerebral VEGF and angiogenesis via the lactate receptor HCAR1. *Nat Commun*. 2017;8:15557.

43 Lauritzen KH, Morland C, Puchades M et al. Lactate receptor sites link neurotransmission, neurovascular coupling, and brain energy metabolism. *Cereb Cortex*. 2014;24(10):2784–2795.

44 Boyd AE, Giamber SR, Mager M, Lebovitz HE. Lactate inhibition of lipolysis in exercising man. *Metabolism*. 1974;23(6):531–542.

45 Achten J, Jeukendrup AE. Optimizing fat oxidation through exercise and diet. Nutrition. 2004;20(7–8):716–727.

46 Owen OE, Felig P, Morgan AP, Wahren J, Cahill GF. Liver and kidney metabolism during prolonged starvation. *J Clin Invest*. 1969. doi:10.1172/JCI106016.

47 Benyó Z, Gille A, Bennett CL, Clausen BE, Offermanns S. Nicotinic acid-induced flushing is mediated by activation of epidermal langerhans cells. *Mol Pharmacol*. 2006. doi:10.1124/mol.106.030833.

48 Ranganathan P, Shanmugam A, Swafford D et al. GPR81, a Cell-Surface Receptor for Lactate, Regulates Intestinal Homeostasis and Protects Mice from Experimental Colitis. *J Immunol*. 2018. doi:10.4049/jimmunol.1700604.

49 Lim EL, Hollingsworth KG, Smith FE, Thelwall PE, Taylor R. Inhibition of lipolysis in Type 2 diabetes normalizes glucose disposal without change in muscle glycogen synthesis rates. *Clin Sci (Lond)*. 2011;121(4):169–77.

50 Karpe F, Dickmann JR, Frayn KN. Fatty acids, obesity, and insulin resistance: Time for a reevaluation. Diabetes. 2011;60(10):2441–2449.

51 Mittendorfer B. Origins of metabolic complications in obesity: adipose tissue and free fatty acid trafficking. *Curr Opin Clin Nutr Metab Care*. 2011;14(6):535–41.

52 Carlson LA. Nicotinic acid: The broad-spectrum lipid drug. A 50th anniversary review. J. Intern. Med. 2005. doi:10.1111/j.1365-2796.2005.01528.x.

53 Offermanns S. The nicotinic acid receptor GPR109A (HM74A or PUMA-G) as a new therapeutic target. Trends Pharmacol. Sci. 2006. doi:10.1016/j.tips.2006.05.008.

54 Taylor AJ, Sullenberger LE, Lee HJ, Lee JK, Grace KA. Arterial Biology for the Investigation of the Treatment Effects of Reducing cholesterol (ARBITER) 2: A double-blind, placebo-controlled study of extended-release niacin on atherosclerosis progression in secondary prevention patients treated with statins. *Circulation*. 2004. doi:10.1161/01.CIR.0000148955.19792.8D.

55 Brown BG, Zhao XQ, Chait A et al. Simvastatin and niacin, antioxidant vitamins, or the combination for the prevention of coronary disease. *N Engl J Med*. 2001. doi:10.1056/NEJMoa011090.

56 Lukasova M, Malaval C, Gille A, Kero J, Offermanns S. Nicotinic acid inhibits progression of atherosclerosis in mice through its receptor GPR109A expressed by immune cells. *J Clin Invest*. 2011. doi:10.1172/JCI41651.

57 Kamanna VS, Ganji SH, Kashyap ML. The mechanism and mitigation of niacin-induced flushing. Int. J. Clin. Pract. 2009. doi:10.1111/j.1742-1241.2009.02099.x.

58 Capuzzi DM, Guyton JR, Morgan JM et al. Efficacy and safety of an extended-release niacin (Niaspan): A long- term study. In: *American Journal of Cardiology*. 1998 doi:10.1016/S0002-9149(98)00731-0.

59 Boatman PD, Richman JG, Semple G. Nicotinic acid receptor agonists. J. Med. Chem. 2008. doi:10.1021/jm800896z.

60 Semple G, Skinner PJ, Gharbaoui T et al. Nicotinic Acid Receptor , G-Protein Coupled Receptor 109a , with Antilipolytic but No Vasodilatory Activity in Mice. *J Med Chem*. 2008.

61 Walters RW, Shukla AK, Kovacs JJ et al. β-Arrestin1 mediates nicotinic acid-induced flushing, but not its antilipolytic effect, in mice. *J Clin Invest*.

2009. doi:10.1172/JCI36806.

62 Semple G, Skinner PJ, Cherrier MC et al. 1-Alkyl-benzotriazole-5-carboxylic acids are highly selective agonists of the human orphan G-protein-coupled receptor GPR109b. *J Med Chem*. 2006. doi:10.1021/jm051099t.

63 Skinner PJ, Webb PJ, Sage CR et al. 5-N,N-Disubstituted 5-aminopyrazole-3-carboxylic acids are highly potent agonists of GPR109b. *Bioorganic Med Chem Lett*. 2009. doi:10.1016/j.bmcl.2009.05.108.

64 Sakurai T, Davenport R, Stafford S et al. Identification of a novel GPR81-selective agonist that suppresses lipolysis in mice without cutaneous flushing. *Eur J Pharmacol*. 2014. doi:10.1016/j.ejphar.2014.01.029.

65 Wallenius K, Thalén P, Björkman J et al. Involvement of the metabolic sensor GPR81 in cardiovascular control. *JCI Insight*. 2017;2(19):1–18.

66 Dvorak CA, Liu C, Shelton J et al. Identification of hydroxybenzoic acids as selective lactate receptor (GPR81) agonists with antilipolytic effects. *ACS Med Chem Lett*. 2012;3(8):637–639.

67 Tang H, Lu JYL, Zheng X, Yang Y, Reagan JD. The psoriasis drug monomethylfumarate is a potent nicotinic acid receptor agonist. *Biochem Biophys Res Commun*. 2008. doi:10.1016/j.bbrc.2008.08.041.

68 Reich K, Thaci D, Mrowietz U, Kamps A, Neureither M, Luger T. Efficacy and safety of fumaric acid esters in the long-term treatment of psoriasis - A retrospective study. *J Ger Soc Dermatology*. 2009;7(7):603–611.

69 Offermanns S, Schwaninger M. Nutritional or pharmacological activation of HCA2 ameliorates neuroinflammation. Trends Mol. Med. 2015. doi:10.1016/j.molmed.2015.02.002.

70 Castillo X, Rosafio K, Wyss MT et al. A probable dual mode of action for both L- and D-lactate neuroprotection in cerebral ischemia. *J Cereb Blood Flow Metab*. 2015;30(April):1–9.

71 Berthet C, Lei H, Thevenet J, Gruetter R, Magistretti PJ, Hirt L. Neuroprotective role of lactate after cerebral ischemia. *J Cereb Blood Flow Metab*. 2009;29(11):1780–1789.

72 Shen Z, Jiang L, Yuan Y et al. Inhibition of G Protein-Coupled Receptor 81 (GPR81) Protects Against Ischemic Brain Injury. *CNS Neurosci Ther*. 2015;21(3):271–279.

73 Roland CL, Arumugam T, Deng D et al. Cell surface lactate receptor GPR81 is crucial for cancer cell survival. *Cancer Res*. 2014;74(18):5301–5310.

74 Lee YJ, Shin KJ, Park S-A et al. G-protein-coupled receptor 81 promotes a malignant phenotype in breast cancer through angiogenic factor secretion. *Oncotarget*. 2016;7(43):70898–70911.

75 Consoli A, Nurjhan N, Reilly JJ, Bier DM, Gerich JE. Contribution of liver and skeletal muscle to alanine and lactate metabolism in humans. *Am J Physiol - Endocrinol Metab*. 1990.

76 Adeva-Andany M, López-Ojén M, Funcasta-Calderón R et al. Comprehensive review on lactate metabolism in human health. Mitochondrion. 2014. doi:10.1016/j.mito.2014.05.007.

77 Le A, Cooper CR, Gouw AM et al. Inhibition of lactate dehydrogenase A induces oxidative stress and inhibits tumor progression. *Proc Natl Acad Sci U S A*. 2010. doi:10.1073/pnas.0914433107.

78 Connor H, Woods HF, Ledingham JGG, Murray JD. A model of Z,(+)-lactate metabolism in normal man. *Ann Nutr Metab*. 1982. doi:10.1159/000176571.

79 Bricker DK, Taylor EB, Schell JC et al. A mitochondrial pyruvate carrier required for pyruvate uptake in yeast, Drosophila, and humans. *Science (80-)*. 2012. doi:10.1126/science.1218099.

80 Andersen LW, Mackenhauer J, Roberts JC, Berg KM, Cocchi MN, Donnino MW. Etiology and therapeutic approach to elevated lactate levels. Mayo Clin. Proc. 2013. doi:10.1016/j.mayocp.2013.06.012.

81 Baron DN. Clinical and Biochemical Aspects of Lactic Acidosis. *J Clin Pathol*. 1977. doi:10.1136/jcp.30.1.92-d.

82 Cerretelli P, Samaja M. Acid-base balance at exercise in normoxia and in chronic hypoxia. Revisiting the ‘lactate paradox’. Eur. J. Appl. Physiol. 2003. doi:10.1007/s00421-003-0928-x.

83 Van Den Nouland DPA, Brouwers MCGJ, Stassen PM. Prognostic value of plasma lactate levels in a retrospective cohort presenting at a university hospital emergency department. *BMJ Open*. 2017. doi:10.1136/bmjopen-2016-011450.

84 Park YJ, Kim DH, Kim SC et al. Serum lactate upon emergency department arrival as a predictor of 30-day in-hospital mortality in an unselected population. *PLoS One*. 2018. doi:10.1371/journal.pone.0190519.

85 Goodwin ML, Harris JE, Hernández A, Gladden LB. Blood lactate measurements and analysis during exercise: a guide for clinicians. *J Diabetes Sci Technol*. 2007;1(4):558–69.

86 Jeong JH, Chang JS, Jo YH. Intracellular glycolysis in brown adipose tissue is essential for optogenetically induced nonshivering thermogenesis in mice. *Sci Rep*. 2018. doi:10.1038/s41598-018-25265-3.

87 Kim HY, Han NR, Kim NR et al. Effect of fermented porcine placenta on physical fatigue in mice. *Exp Biol Med*. 2016. doi:10.1177/1535370216659945.

88 Chudalla R, Baerwalde S, Schneider G, Maassen N. Local and systemic effects on blood lactate concentration during exercise with small and large muscle groups. *Pflugers Arch*. 2006;452(6):690–7.

89 Wikander I, Roos T, Stakkestad A, Eriksson E. Sodium lactate elicits a rapid increase in blood pressure in wistar rats and spontaneously hypertensive rats effect of pretreatment with the antipanic drugs clomipramine and alprazolam. *Neuropsychopharmacology*. 1995;12(3):269–272.

90 McKinnon W, Aaronson PI, Knock G, Graves J, Poston L. Mechanism of lactate-induced relaxation of isolated rat mesenteric resistance arteries. *J Physiol*. 1996;490 (Pt 3:783–792.

91 Skov Jensen P, Metz Mariendal Pedersen S, Aalkjaer C, Bek T. The vasodilating effects of insulin and lactate are increased in precapillary arterioles in the porcine retina ex vivo. *Acta Ophthalmol*. 2016.

doi:10.1111/aos.13025.

92 Yamanishi S, Katsumura K, Kobayashi T, Puro DG. Extracellular lactate as a dynamic vasoactive signal in the rat retinal microvasculature. *Am J Physiol Hear Circ Physiol*. 2006;290(3):H925-34.

93 He L, Vanlandewijck M, Mäe MA et al. Data descriptor: Single-cell RNA sequencing of mouse brain and lung vascular and vessel-associated cell types. *Sci Data*. 2018. doi:10.1038/sdata.2018.160.

94 Strandberg TE, Pitkala K. What is the most important component of blood pressure: systolic, diastolic or pulse pressure? *Curr Opin Nephrol Hypertens*. 2003;12(3):293–7.

95 Yanagisawa M, Kurihara H, Kimura S et al. A novel potent vasoconstrictor peptide produced by vascular endothelial cells. *Nature*. 1988. doi:10.1038/332411a0.

96 Inoue A, Yanagisawa M, Takuwa Y, Mitsui Y, Kobayashi M, Masaki T. The human preproendothelin-1 gene. Complete nucleotide sequence and regulation of expression. *J Biol Chem*. 1989.

97 Sakurai T, Yanagisawa M, Takuwat Y et al. Cloning of a cDNA encoding a non-isopeptide-selective subtype of the endothelin receptor. *Nature*. 1990. doi:10.1038/348732a0.

98 Turner AJ, Murphy LJ. Molecular pharmacology of endothelin converting enzymes. Biochem. Pharmacol. 1996. doi:10.1016/0006-2952(95)02036-5.

99 Takahashi M, Matsushita Y, Iijima Y, Tanzawa K. Purification and characterization of endothelin-converting enzyme from rat lung. *J Biol Chem*. 1993.

100 Haynes WG, Webb DJ. Contribution of endogenous generation of endothelin-1 to basal vascular tone. *Lancet*. 1994. doi:10.1016/S0140-6736(94)92827-4.

101 Davenport AP, Hyndman KA, Dhaun N et al. Endothelin. *Pharmacol Rev*. 2016;68(2):357–418.

102 Russell FD, Davenport AP. Secretory pathways in endothelin synthesis. Br. J. Pharmacol. 1999. doi:10.1038/sj.bjp.0702315.

103 Russell FD, Skepper JN, Davenport AP. Detection of endothelin receptors in human coronary artery vascular smooth muscle cells but not endothelial cells by using electron microscope autoradiography. *J Cardiovasc Pharmacol*. 1997. doi:10.1097/00005344-199706000-00017.

104 Bouallegue A, Bou Daou G, Srivastava A. Endothelin-1-Induced Signaling Pathways in Vascular Smooth Muscle Cells. *Curr Vasc Pharmacol*. 2006. doi:10.2174/157016107779317161.

105 Wright CE, Fozard JR. Regional vasodilation is a prominent feature of the haemodynamic response to endothelin in anaesthetized, spontaneously hypertensive rats. *Eur J Pharmacol*. 1988. doi:10.1016/0014-2999(88)90425-6.

106 Schinelli S. Pharmacology and Physiopathology of the Brain Endothelin System: An Overview. *Curr Med Chem*. 2006. doi:10.2174/092986706776055652.

107 Johnström P, Fryer TD, Richards HK et al. Positron emission tomography using 18F-labelled endothelin-1 reveals prevention of binding to cardiac receptors owing to tissue-specific clearance by ET B receptors in vivo. *Br J Pharmacol*. 2005. doi:10.1038/sj.bjp.0706064.

108 Angus JA, Wright CE. Role of endothelin-1 clearance in the haemodynamic responses to endothelin-1 in the pulmonary and hindquarter vasculature of anaesthetised rats. *Eur J Pharmacol*. 2019. doi:10.1016/j.ejphar.2019.05.009.

109 Fukuroda T, Fujikawa T, Ozaki S, Ishikawa K, Yano M, Nishikibe M. Clearance of circulating endothelin-1 by etb receptors in rats. *Biochem Biophys Res Commun*. 1994. doi:10.1006/bbrc.1994.1395.

110 Guruli G, Pflug BR, Pecher S, Makarenkova V, Shurin MR, Nelson JB. Function and survival of dendritic cells depend on endothelin-1 and endothelin receptor autocrine loops. *Blood*. 2004. doi:10.1182/blood-2003-10-3559.

111 Russo D, Minutolo R, Clienti C et al. Endothelin-1 released by vascular smooth muscle cells enhances vascular responsiveness of rat

mesenteric arterial bed exposed to high perfusion flow. *Am J Hypertens*. 1999. doi:10.1016/S0895-7061(99)00085-0.

112 Woods M, Mitchell JA, Wood EG et al. Endothelin-1 is induced by cytokines in human vascular smooth muscle cells: Evidence for intracellular endothelin-converting enzyme. *Mol Pharmacol*. 1999.

113 Kanse S, Takahashi K, Warren J et al. Production of endothelin by vascular smooth muscle cells. *J Cardiovasc Pharmacol*. 1991;17(Suppl 7):S113-6.

114 Shinagawa S, Okazaki T, Ikeda M et al. T cells upon activation promote endothelin 1 production in monocytes via IFN-γ and TNF-α. *Sci Rep*. 2017. doi:10.1038/s41598-017-14202-5.

115 Wahl JR, Goetsch NJ, Young HJ et al. Murine macrophages produce endothelin-1 after microbial stimulation. *Exp Biol Med*. 2005. doi:10.1177/153537020523000907.

116 Paradis A, Xiao D, Zhou J, Zhang L. Endothelin-1 promotes cardiomyocyte terminal differentiation in the developing heart via heightened DNA methylation. *Int J Med Sci*. 2014. doi:10.7150/ijms.7802.

117 Thomas PB, Liu ECK, Webb ML, Mukherjee R, Hebbar L, Spinale FG. Exogenous effects and endogenous production of endothelin in cardiac myocytes: Potential significance in heart failure. *Am J Physiol - Hear Circ Physiol*. 1996.

118 Yamashita K, Discher DJ, Hu J, Bishopric NH, Webster KA. Molecular regulation of the endothelin-1 gene by hypoxia. Contributions of hypoxia-inducible factor-1, activator protein-1, GATA-2, and p300/CBP. *J Biol Chem*. 2001;276(16):12645–12653.

119 Hieda HS, Gomez-Sanchez CE. Hypoxia increases endothelin release in bovine endothelial cells in culture, but epinephrine, norepinephrine, serotonin, histamine and angiotensin II do not. *Life Sci*. 1990;47(3):247–251.

120 Rakugi H, Tabuchi Y, Nakamaru M et al. Evidence for endothelin-1 release from resistance vessels of rats in response to hypoxia. *Biochem*

Biophys Res Commun. 1990;169(3):973–977.

121 Hedegaard ER, Stankevicius E, Simonsen U, Fröbert O. Non-endothelial endothelin counteracts hypoxic vasodilation in porcine large coronary arteries. *BMC Physiol*. 2011;11(1). doi:10.1186/1472-6793-11-8.

122 Lee DC, Sohn HA, Park ZY et al. A lactate-induced response to hypoxia. *Cell*. 2015;161(3):595–609.

123 Evans RG, Madden AC, Oliver JJ, Lewis T V. Effects of ETA- and ETB-receptor antagonists on regional kidney blood flow, and responses to intravenous endothelin-1, in anaesthetized rabbits. *J Hypertens*. 2001. doi:10.1097/00004872-200110000-00013.

124 Brooks DP, DePalma PD, Pullen M, Nambi P. Characterization of canine renal endothelin receptor subtypes and their function. *J Pharmacol Exp Ther*. 1994.

125 Wellings RP, Corder R, Warner TD, Cristol J -P, Thiemermann C, Vane JR. Evidence from receptor antagonists of an important role for ETB receptor-mediated vasoconstrictor effects of endothelin-1 in the rat kidney. *Br J Pharmacol*. 1994. doi:10.1111/j.1476-5381.1994.tb14767.x.

126 Agapitov A V., Haynes WG. Role of endothelin in cardiovascular disease. JRAAS - J. Renin-Angiotensin-Aldosterone Syst. 2002. doi:10.3317/jraas.2002.001.

127 Cohen H, Chahine C, Hui A, Mukherji R. Bosentan therapy for pulmonary arterial hypertension. Am. J. Heal. Pharm. 2004.

128 Ihara M, Noguchi K, Saeki T et al. Biological profiles of highly potent novel endothelin antagonists selective for the ETA receptor. *Life Sci*. 1992. doi:10.1016/0024-3205(92)90331-I.

129 Ishikawa K, Ihara M, Noguchi K et al. Biochemical and pharmacological profile of a potent and selective endothelin B-receptor antagonist, BQ-788. *Proc Natl Acad Sci U S A*. 1994. doi:10.1073/pnas.91.11.4892.

130 Truett GE, Heeger P, Mynatt RL, Truett AA, Walker JA, Warman ML. Preparation of PCR-quality mouse genomic dna with hot sodium hydroxide and tris (HotSHOT). *Biotechniques*. 2000;29(1):52–54.

131 Wang F, Flanagan J, Su N et al. RNAscope: A novel in situ RNA analysis platform for formalin-fixed, paraffin-embedded tissues. *J Mol Diagnostics*. 2012. doi:10.1016/j.jmoldx.2011.08.002.

132 Bankhead P, Loughrey MB, Fernández JA et al. QuPath: Open source software for digital pathology image analysis. *Sci Rep*. 2017. doi:10.1038/s41598-017-17204-5.

133 Schindelin J, Arganda-Carreras I, Frise E et al. Fiji: An open-source platform for biological-image analysis. Nat. Methods. 2012. doi:10.1038/nmeth.2019.

134 Nagase T, Aoki T, Oka T, Fukuchi Y, Ouchi Y. ET-1 induced bronchoconstriction is mediated via ET(B) receptor in mice. *J Appl Physiol*. 1997. doi:10.1152/jappl.1997.83.1.46.

135 Jones N. *Novel vascular functions of the lactate receptor GPR81 - MscR mini project 2*. 2016.

136 Sakurai T, Davenport R, Stafford S et al. Identification of a novel GPR81-selective agonist that suppresses lipolysis in mice without cutaneous flushing. *Eur J Pharmacol*. 2014;727(1):1–7.

137 Culshaw GJ, Costello HM, Binnie D et al. Impaired pressure natriuresis and non-dipping blood pressure in rats with early type 1 diabetes mellitus. *J Physiol*. 2018;597(3):767–780.

138 Ganji SH, Qin S, Zhang L, Kamanna VS, Kashyap ML. Niacin inhibits vascular oxidative stress, redox-sensitive genes, and monocyte adhesion to human aortic endothelial cells. *Atherosclerosis*. 2009. doi:10.1016/j.atherosclerosis.2008.04.044.

139 Carballo-Jane E, Gerckens LS, Luell S et al. Comparison of rat and dog models of vasodilatation and lipolysis for the calculation of a therapeutic index for GPR109A agonists. *J Pharmacol Toxicol Methods*. 2007. doi:10.1016/j.vascn.2007.05.007.

140 Madaan A, Chaudhari P, Nadeau-Vallée M et al. Müller Cell–Localized GPR81 (HCA1) Regulates Inner Retinal Vasculature via Norrin/Wnt Pathways. *Am J Pathol*. 2019;189(6). doi:10.1016/j.ajpath.2019.05.016.

141 Sun S, Li H, Chen J, Qian Q. Lactic Acid: No Longer an Inert and End-

Product of Glycolysis. *Physiology*. 2017. doi:10.1152/physiol.00016.2017.

142 He W, Miao FJP, Lin DCH et al. Citric acid cycle intermediates as ligands for orphan G-protein-coupled receptors. *Nature*. 2004. doi:10.1038/nature02488.

143 Leite LN, Gonzaga NA, Simplicio JA et al. Pharmacological characterization of the mechanisms underlying the vascular effects of succinate. *Eur J Pharmacol*. 2016. doi:10.1016/j.ejphar.2016.07.045.

144 Keys JR, Zhou RH, Harris DM, Druckman CA, Eckhart AD. Vascular smooth muscle overexpression of G protein-coupled receptor kinase 5 elevates blood pressure, which segregates with sex and is dependent on G i-mediated signaling. *Circulation*. 2005. doi:10.1161/CIRCULATIONAHA.104.531657.

145 Hansen PB, Castrop H, Briggs J, Schnermann J. Adenosine induces vasoconstriction through Gi-dependent activation of phospholipase C in isolated perfused afferent arterioles of mice. *J Am Soc Nephrol*. 2003. doi:10.1097/01.ASN.0000086474.80845.25.

146 Moratinos J, Reverte M. Effects of catecholamines on plasma potassium: the role of alpha- and beta-adrenoceptors. *Fundam Clin Pharmacol*. 1993. doi:10.1111/j.1472-8206.1993.tb00228.x.

147 Nishimura J, van Breemen C. Direct regulation of smooth muscle contractile elements by second messengers. *Biochem Biophys Res Commun*. 1989. doi:10.1016/0006-291X(89)92311-5.

148 Karsten AJ, Derouet H, Ziegler M, Eckert RE. Involvement of cyclic nucleotides in renal artery smooth muscle relaxation. *Urol Res*. 2003. doi:10.1007/s00240-002-0281-2.

149 Ristic B, Bhutia YD, Ganapathy V. Cell-surface G-protein-coupled receptors for tumor-associated metabolites: A direct link to mitochondrial dysfunction in cancer. Biochim. Biophys. Acta - Rev. Cancer. 2017. doi:10.1016/j.bbcan.2017.05.003.

150 Rondaij MG, Bierings R, Kragt A, Van Mourik JA, Voorberg J. Dynamics and plasticity of Weibel-Palade bodies in endothelial cells. Arterioscler.

Thromb. Vasc. Biol. 2006. doi:10.1161/01.ATV.0000209501.56852.6c.

151 Valentijn KM, Sadler JE, Valentijn JA, Voorberg J, Eikenboom J. Functional architecture of Weibel-Palade bodies. Blood. 2011. doi:10.1182/blood-2010-09-267492.

152 Fyhrquist F, Saijonmaa O, Metsärinne K, Tikkanen I, Rosenlöf K, Tikkanen T. Raised plasma endothelin-I concentration following cold pressor test. *Biochem Biophys Res Commun*. 1990. doi:10.1016/0006-291X(90)91456-3.

153 Macarthur H, Warner TD, Wood EG, Corder R, Vane JR. Endothelin-1 release from endothelial cells in culture is elevated both acutely and chronically by short periods of mechanical stretch. *Biochem Biophys Res Commun*. 1994. doi:10.1006/bbrc.1994.1462.

154 Russell FD, Skepper JN, Davenport AP. Human endothelial cell storage granules: A novel intracellular site for isoforms of the endothelin-converting enzyme. *Circ Res*. 1998. doi:10.1161/01.RES.83.3.314.

155 Carew MA, Paleolog EM, Pearson JD. The roles of protein kinase C and intracellular Ca2+ in the secretion of von Willebrand factor from human vascular endothelial cells. *Biochem J*. 1992. doi:10.1042/bj2860631.

156 van Mourik JA, de Wit TR, Voorberg J. Bioenesis and exocytosis of Weibel-Palade bodies. *Histochem Cell Biol*. 2002. doi:10.1007/s00418-001-0368-9.

157 Loesberg C, Gonsalves MD, Zandbergen J et al. The effect of calcium on the secretion of factor VIII-related antigen by cultured human endothelial cells. *BBA - Mol Cell Res*. 1983. doi:10.1016/0167-4889(83)90039-3.

158 King AJ, Brenner BM, Anderson S. Endothelin: A potent renal and systemic vasoconstrictor peptide. *Am J Physiol - Ren Fluid Electrolyte Physiol*. 1989.

159 Loutzenhiser R, Epstein M, Hayashi K, Horton C. Direct visualization of effects of endothelin on the renal microvasculature. *Am J Physiol - Ren Fluid Electrolyte Physiol*. 1990.

160 Woods M, Wood EG, Mitchell JA, Warner TD. Cyclic AMP regulates

cytokine stimulation of endothelin-1 release in human vascular smooth muscle cells. *J Cardiovasc Pharmacol*. 2000. doi:10.1097/00005344-200008000-00017.

161 Wort SJ, Mitchell JA, Woods M, Evans TW, Warner TD. The prostacyclin-mimetic cicaprost inhibits endogenous endothelin-1 release from human pulmonary artery smooth muscle cells. *J Cardiovasc Pharmacol*. 2000. doi:10.1097/00005344-200036001-00084.

162 Kawanabe Y, Takahashi M, Jin X et al. Cilostazol Prevents Endothelin-Induced Smooth Muscle Constriction and Proliferation. *PLoS One*. 2012. doi:10.1371/journal.pone.0044476.

163 Barrett-O'Keefe Z, Ives SJ, Trinity JD et al. Taming the "sleeping giant": the role of endothelin-1 in the regulation of skeletal muscle blood flow and arterial blood pressure during exercise. *Am J Physiol Circ Physiol*. 2012. doi:10.1152/ajpheart.00603.2012.

164 Hameroff SR, Otto CW, Kanel J, Weinstein PR, Blitt CD. Acute cardiovascular effects of dimethylsulfoxide. *Crit Care Med*. 1981. doi:10.1097/00003246-198112000-00011.

165 Regard JB, Sato IT, Coughlin SR. Anatomical Profiling of G Protein-Coupled Receptor Expression. *Cell*. 2008. doi:10.1016/j.cell.2008.08.040.

166 Harland SP, Kuc RE, Pickard JD, Davenport AP. Characterization of endothelin receptors in human brain cortex, gliomas, and meningiomas. *J Cardiovasc Pharmacol*. 1995.

167 Silldorff EP, Yang S, Pallone TL. Prostaglandin E2 abrogates endothelin-induced vasoconstriction in renal outer medullary descending vasa recta of the rat. *J Clin Invest*. 1995. doi:10.1172/JCI117976.

168 Falloon BJ, Stephens N, Tulip JR, Heagerty AM. Comparison of small artery sensitivity and morphology in pressurized and wire-mounted preparations. *Am J Physiol - Hear Circ Physiol*. 1995;268(2):H670–H678.

169 Maenhaut N, Boydens C, Van de Voorde J. Hypoxia enhances the

relaxing influence of perivascular adipose tissue in isolated mice aorta. *Eur J Pharmacol*. 2010;641(2–3):207–212.

170 McKinnon W, Aaronson PI, Knock G, Graves J, Poston L. Mechanism of lactate-induced relaxation of isolated rat mesenteric resistance arteries. *J Physiol*. 1996. doi:10.1113/jphysiol.1996.sp021186.

171 Waypa GB, Schumacker PT. Hypoxia-induced changes in pulmonary and systemic vascular resistance: Where is the O2 sensor? Respir. Physiol. Neurobiol. 2010. doi:10.1016/j.resp.2010.08.007.

172 Chan CK, Vanhoutte PM. Hypoxia, vascular smooth muscles and endothelium. *Acta Pharm Sin B*. 2013. doi:10.1016/j.apsb.2012.12.007.

173 Otter D, Austin C. Mechanisms of hypoxic vasodilatation of isolated rat mesenteric arteries: A comparison with metabolic inhibition. *J Physiol*. 1999;516(1):249–259.

174 Liu C, Kuei C, Zhu J et al. 3,5-Dihydroxybenzoic Acid, a Specific Agonist for Hydroxycarboxylic Acid 1, Inhibits Lipolysis in Adipocytes. *J Pharmacol Exp Ther*. 2012. doi:10.1124/jpet.112.192799.

175 Juurlink BHJ, Azouz HJ, Aldalati AMZ, Altinawi BMH, Ganguly P. Hydroxybenzoic acid isomers and the cardiovascular system. Nutr. J. 2014;13(1). doi:10.1186/1475-2891-13-63.

176 Errea A, Cayet D, Marchetti P et al. Lactate inhibits the pro-inflammatory response and metabolic reprogramming in Murine macrophages in a GPR81-independent manner. *PLoS One*. 2016. doi:10.1371/journal.pone.0164098.

177 Sun Z, Han Y, Song S, Chen T, Han Y, Liu Y. Activation of GPR81 by lactate inhibits oscillatory shear stress-induced endothelial inflammation by activating the expression of KLF2. *IUBMB Life*. 2019. doi:10.1002/iub.2151.

178 Ransick A, Lindström NO, Liu J et al. Single Cell Profiling Reveals Sex, Lineage and Regional Diversity in the Mouse Kidney. *bioRxiv*. 2019. doi:10.1101/673335.

179 Michiels C. Physiological and pathological responses to hypoxia. Am. J. Pathol. 2004. doi:10.1016/S0002-9440(10)63747-9.

180 Vanlandewijck M, He L, Mäe MA et al. A molecular atlas of cell types and zonation in the brain vasculature. *Nature*. 2018. doi:10.1038/nature25739.

181 López-Farré A, Montañés I, Millás I, López-Novoa JM. Effect of endothelin on renal function in rats. *Eur J Pharmacol*. 1989. doi:10.1016/0014-2999(89)90417-2.

182 Haug C, Voisard R, Lenich A et al. Increased endothelin release by cultured human smooth muscle cells from atherosclerotic coronary arteries. *Cardiovasc Res*. 1996;31:807–13.

183 Brandherm I, Disse J, Zeuschner D, Gerke V. cAMP-induced secretion of endothelial von Willebrand factor is regulated by a phosphorylation/dephosphorylation switch in annexin A2. *Blood*. 2013. doi:10.1182/blood-2012-12-475251.

184 Zager R a, Johnson ACM, Andress D, Becker K. Progressive endothelin-1 gene activation initiates chronic/end-stage renal disease following experimental ischemic/reperfusion injury. *Kidney Int*. 2013;84(4):703–12.

185 Bonventre J, Yang L. Cellular pathophysiology of ischemic acute kidney injury. *J Clin Invest*. 2011;121(11):4210–4221.

186 Matejovic M, Ince C, Chawla LS et al. Renal Hemodynamics in AKI: In Search of New Treatment Targets. *J Am Soc Nephrol*. 2016. doi:10.1681/ASN.2015030234.

187 Arfian N, Emoto N, Vignon-Zellweger N, Nakayama K, Yagi K, Hirata K ichi. ET-1 deletion from endothelial cells protects the kidney during the extension phase of ischemia/reperfusion injury. *Biochem Biophys Res Commun*. 2012;425(2):443–449.